UNIVERSITY OF BIRMINGHAM

THE USE AND PRODUCTION OF NATURAL ANTIOXIDANTS FOR FOOD APPLICATIONS

JOHN NOON

A thesis submitted to

The University of Birmingham

For the degree of

DOCTOR OF PHILOSOPHY

School of Chemical Engineering

College of Engineering and Physical Sciences

University of Birmingham

2020

UNIVERSITY OF
BIRMINGHAM

University of Birmingham Research Archive

e-theses repository

This unpublished thesis/dissertation is copyright of the author and/or third parties. The intellectual property rights of the author or third parties in respect of this work are as defined by The Copyright Designs and Patents Act 1988 or as modified by any successor legislation.

Any use made of information contained in this thesis/dissertation must be in accordance with that legislation and must be properly acknowledged. Further distribution or reproduction in any format is prohibited without the permission of the copyright holder.

Thesis abstract

Antioxidant compounds are ubiquitous throughout the natural world where their properties are used to combat potentially damaging oxidative reactions which occur within living organisms. These antioxidant compounds can be extracted from their natural sources (including fruits, vegetables, spices, herbs, and grains) and incorporated into consumer goods to utilise their antioxidant properties for a specific purpose. A key focus of this thesis was to improve the efficacy of natural antioxidants in terms of, firstly, their ability to combat lipid oxidation (LO) in oil-in-water (O/W) food emulsions, and secondly, in their capacity to provide additional health benefits within food or pharmaceutical products. Therefore, this thesis investigated a specific use of antioxidants, which was in their ability to combat LO in a range of O/W emulsion formulations, in addition to the investigation of a novel antioxidant nanonisation technique which could be used to help improve the bioavailability of antioxidant compounds when incorporated into food or pharmaceutical products.

The use of natural antioxidants to combat LO in O/W emulsions served as the primary research focus of this thesis. The motivation for this work predominantly stemmed from high consumer demand for the sole use of natural, 'clean label' ingredients in food products coupled with the increased use of highly oxidisable unsaturated fats in O/W food emulsions which, due to their structure, are already highly susceptible to LO. Initial research into this area assessed the behaviour and efficacy of several natural antioxidant compounds (namely, quercetin, curcumin, rutin hydrate and ascorbic acid) in their ability to combat LO in a range of different O/W emulsion environments. This work developed into the assessment of one particular antioxidant, rutin hydrate (RH), in its ability to act as a Pickering emulsifier and offer dual-purpose functionality through providing O/W

emulsions with both physical and oxidative stability. Research showed that emulsion environment was paramount in determining the efficacy of natural antioxidants at combatting LO. Furthermore, RH particles were found to be capable of physically stabilising O/W emulsions, however, the ability of these particles to provide oxidative stability in emulsions was found to be limited by their inability to form a continuous and effective barrier at the oil-water interface.

The secondary focus of this thesis was on the production of antioxidant nanoparticles through the development of a novel microwave-assisted antisolvent precipitation (MAP) technique to help overcome limited bioavailability issues which many natural antioxidants possess. Through use of the MAP technique, curcumin and silymarin antioxidant compounds were successfully nanonised and transformed from exhibiting crystalline structures to more amorphous structures; this is known to enhance dissolution velocity which is key in the bioavailability enhancement of many antioxidant compounds.

Acknowledgements

I would firstly like to thank my academic supervisors, Professor Ian Norton, and Dr Tom Mills for providing me with this opportunity in addition to their invaluable support and advice throughout the course of my time in Birmingham. I would also like to express thanks to Dr Aditya Nayak, whose mentorship and guidance, particularly at the start of my PhD, was paramount in my development as a doctoral researcher.

I do of course have to thank all my colleagues, both past and present, in the food microstructure group. I feel this research group has always been blessed with a lovely group of people and I have truly enjoyed my time spent with you all, both inside and outside of the department.

Most of all, I would like to give special thanks to my amazing family, and in particular my parents, Gary and Carole, whose belief in me, and unwavering support throughout life has been fundamental to all of my achievements. For a debt that could never be repaid, thank you.

Table of contents

List of Figures

List of Tables

CHAPTER 1: INTRODUCTION

1.1 Project background

The addition of antioxidants can add tremendous benefits to food and pharmaceutical products. One key benefit for which their use is already commonplace is in the fight against lipid oxidation (LO) in food products. As a chemical process, LO can result in changes to the taste, texture and appearance of fat (lipid) containing food products in addition to loss of nutritional value and reduced shelf-life (McClements and Decker, 2000). Hence it is largely an unwanted phenomenon in food and is a particular problem within oil-in-water (O/W) food emulsions (which are commonly encountered on the supermarket shelves in products such as milk, mayonnaise, soups, sauces and various processed foods) due to the high surface areas generated between oil and water phases through emulsification which serves to greatly accelerate the process of oxidation (Waraho et al., 2011).

Furthermore, LO in food products such as emulsions is increasingly becoming a larger concern for the food industry for two key reasons. Firstly, there exists long-standing health advice, particularly throughout the western world, that people generally need to decrease their consumption of saturated fats (Vieira et al., 2015) and replace this intake with healthier, unsaturated fats. Unfortunately however, unsaturated fats are far more susceptible to LO due to the reduced bond dissociation energies harboured within these lipid molecules compared to saturated ones (Domínguez et al., 2019) and hence suffer from a shorter shelf-life. Therefore, it is necessary to provide novel solutions to overcome this issue, to enable both the reduction of saturated fats in foods whilst ensuring long shelf-life and enable healthier eating for consumers. Secondly, at present, the food industry is also largely focused on the replacement of synthetic, and often highly effective antioxidants with natural alternatives (Caleja et al., 2017) due to safety concerns

(Alagarsamy et al., 2014) and consumer acceptance surrounding artificial ingredients (Waraho et al., 2011). Therefore people are increasingly demanding the sole usage of natural ingredients in food products (Wunsch, 2019) and are turned away when artificial ingredients are used; in a recent report in the UK for example, 36% of adults believed that foods containing artificial ingredients cannot be healthy (Price, 2020). Therefore, this thesis specifically investigates the use of natural antioxidants for combatting LO within O/W emulsions.

Another key benefit of natural antioxidants is in their incorporation into food or pharmaceutical products to make use of their antioxidant activity to exert a specific health benefit. Natural antioxidants have been proven to exhibit a vast array of potential health benefits due to their possession of anti-cancer, anti-inflammatory, anti-bacterial, anti-viral and anti-aging properties among many others (Xu et al., 2017). Unfortunately however, the major issue with many natural antioxidants, and numerous other natural bioactive compounds in their use for food or pharmaceutical applications is that they possess poor oral bioavailability, and are therefore inefficiently utilised within the body upon their consumption. This is often found when natural antioxidants possess a low aqueous solubility (as the human body is largely comprised of water) and is an issue which can be overcome through particle size reduction via nanonisation. Through nanonisation, the dissolution velocity of a compound can be dramatically enhanced which is a key factor in the bioavailability enhancement of many compounds. Development of novel, and effective nanonisation techniques could also benefit the pharmaceutical industry, in which as of 2017, over 90% of drug compounds in development were deemed to be poorly soluble in aqueous environments (Svagan et al., 2017). Therefore, this thesis also focuses

on the development of a scalable, and novel nanonisation technique to produce antioxidant nanoparticles.

1.2 Aims and objectives

- Provide fundamental understanding of antioxidant behaviour within a range of O/W emulsion environments through assessment of the efficacies of a range of natural antioxidants at combatting lipid oxidation in different emulsion formulations.
- Investigate the novelty of using natural antioxidant Pickering particles for providing O/W emulsions with both physical and oxidative stability to open-up the potential use of a new, dual-purpose, food microstructure for combatting lipid oxidation.
- Develop a novel and scalable nanonisation technique to help overcome the limited aqueous solubility issues associated with numerous natural antioxidant compounds and aid in enabling their increased usage for commercial applications.

1.3 Thesis layout

This thesis is comprised of 7 chapters which includes an introduction, a literature review, three experimental results chapters, a chapter on overall conclusions/future work recommendations and a list of references.

- Chapter 1 is an introduction providing the background information to the project, in addition to the aims, objectives and rationale for the research.
- Chapter 2 provides a review of the relevant literature for this thesis along with an explanation of the underlying science most pertinent to this research.
- Chapter 3 is the first chapter of experimental results and investigates the use of natural antioxidants to combat LO when added to O/W emulsions.

- Chapter 4 is the second experimental results chapter which assesses the use of antioxidant Pickering particles as a novel method for providing O/W emulsions with dual-purpose functionality.
- Chapter 5 is the final experimental results chapter which focuses on the development of a novel microwave-assisted antisolvent precipitation (MAP) technique for the nanonisation of antioxidant nanoparticles.
- Chapter 6 summarises the overall conclusions of the research and details suggestions for future work.
- Chapter 7 provides a list of all references cited in this thesis.

Chronologically, experimental work of Chapter 5 was carried out first, followed by the work in Chapter 3 and then Chapter 4. The layout chosen for this thesis was therefore non-chronological, and this was done as it provided the most coherent flow of ideas.

1.4 Publications

The research from each of the three experimental chapters has been published as three scientific research articles which are referenced below:

- Noon, J., Mills, T. B. & Norton, I. T. 2020. The use of natural antioxidants to combat lipid oxidation in O/W emulsions. Journal of Food Engineering, 281, 110006.
- Noon, J., Mills, T. B. & Norton, I. T. 2020. The use of antioxidant rutin hydrate Pickering particles to combat lipid oxidation in O/W emulsions. Journal of Food Engineering, 274, 109830.
- Aditya, N. P., Hamilton, I. E., Noon, J. & Norton, I. T. 2019. Microwave-Assisted Nanonization of Poorly Water-Soluble Curcumin. ACS Sustainable Chemistry & Engineering, 7, 9771-9781.

CHAPTER 2: LITERATURE REVIEW

2.1 Lipid oxidation within oil-in-water (O/W) emulsions

This thesis investigated a specific use of natural antioxidants in food systems. This specific use was in their ability to combat lipid oxidation (LO) within oil-in-water (O/W) emulsions. LO remains a major current issue in the food industry. Although in certain instances like in the case of cheese, a degree of LO can enhance the flavour profile and quality of food, it is generally an unwanted phenomenon which causes negative changes to food products (McClements, 2004). LO typically occurs at a greater rate in O/W emulsions compared to bulk oils; this finding is predominantly attributed to the substantial increase in interfacial area between the oil and water phases which inevitably comes from the creation of an emulsion (Jacobsen, 2016).

2.2 Emulsions

Emulsions are thermodynamically unstable systems consisting of two immiscible liquid phases dispersed within each other. The main types of emulsion configurations are either O/W or water-in-oil (W/O) depending on which phase is continuous and which is dispersed. Within the food industry, emulsions are commonplace, with familiar examples including milk, cream, mayonnaise, soups and sauces (Tatar et al., 2017).

Emulsions are usually produced through mixing two immiscible liquids under mechanical disruption (Schubert et al., 2009) (e.g. high shear mixing, high pressure homogenisation, microfluidization etc.); upon mixing of these phases, due to their immiscibility, phase separation will generally occur in the immediate aftermath as this minimises interfacial area (A) between the two phases and hence, is thermodynamically favourable, lowering the Gibbs free energy change (ΔG):

$$\Delta G = \gamma \Delta A - T\Delta S \qquad \textbf{(Equation 2-1)}$$

(Where ΔG = Gibbs free energy change, γ = interfacial tension, ΔA = change in interfacial area, T = temperature, ΔS = entropy of mixing).

It can also be seen from Equation 2-1 (Gibbs, 1873) that a reduction in interfacial tension (γ) can lower the Gibbs free energy change and this is typically achieved with use of an emulsifier. During emulsification, emulsifiers locate at the oil-water interface which typically results in reduced interfacial tension. Hence, emulsifiers are able to provide emulsions with kinetic stability and they are thus able to resist phase separation for prolonged periods of hours, days, months and years; although it is a thermodynamic certainty that eventually emulsion phases will separate. Thus, simple emulsions can essentially be divided into three regions: the dispersed phase, the continuous phase, and the interfacial layer. This thesis only investigates O/W emulsions and therefore this is the only emulsion system considered in this review.

2.3 Physical stability of O/W emulsions

2.3.1 Emulsion physical instability mechanisms

There are several major mechanisms of emulsion physical instability which are illustrated in Figure 2-1. All these instability mechanisms apart from phase inversion contribute to emulsion phase separation.

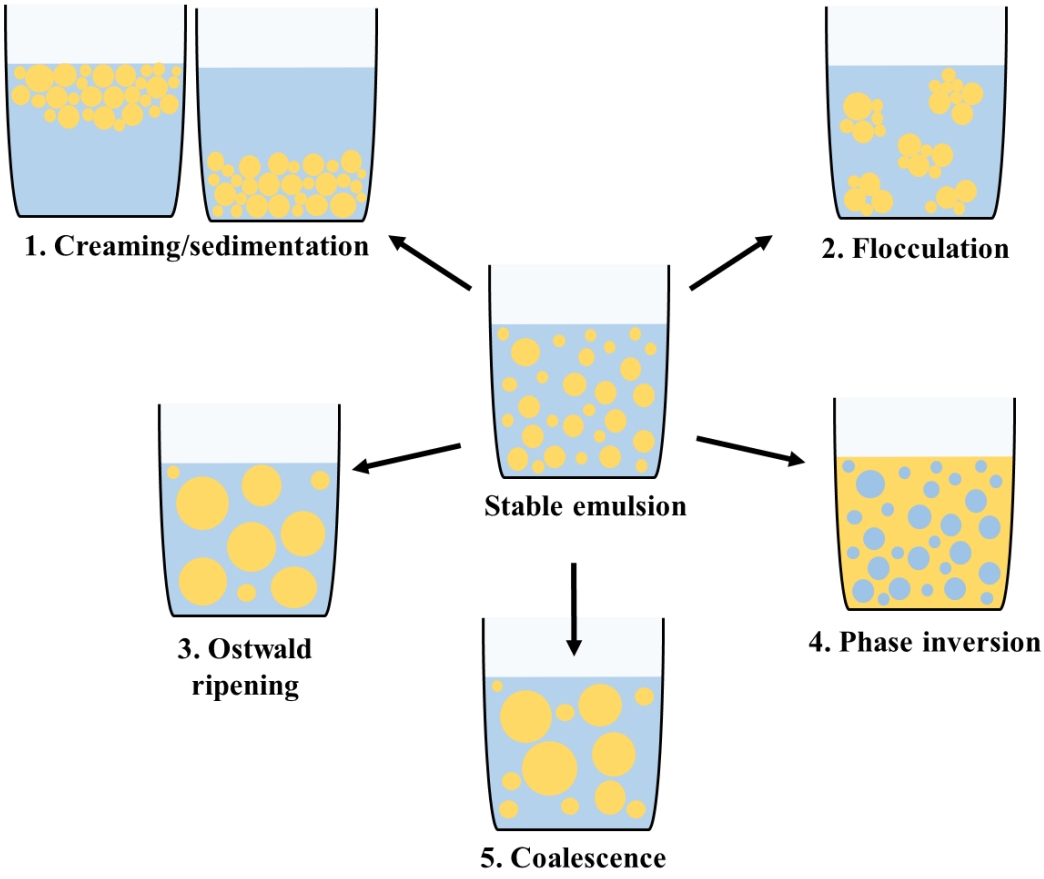

Figure 2-1: Physical instability mechanisms of emulsions.

1. **Creaming/sedimentation -** When gravitational or centrifugal forces outweigh the Brownian motion of oil droplets this will cause them to group together in a specific location. If the oil droplets have a density less than water (this is usually the case) they will group together at the top of an emulsion mixture and this is called creaming, whereas if the density of oil droplets are more than that of water then they will group at the bottom of the emulsion mixture in a process called sedimentation. Although creaming and sedimentation are considered reversible processes because they can be undone with gentle agitation/shaking; both processes increase contact time between oil droplets and therefore increase the likelihood of droplet coalescence and phase separation which are irreversible processes.

2. **Flocculation –** In flocculation, emulsion oil droplets form groups or 'flocs' throughout the emulsion mixture and stick to each other whilst remaining as separate droplets. This process occurs when the van der Waals forces of attraction between oil droplets outweigh repulsive forces. Due to a larger effective radius, flocculated droplets undergo creaming/sedimentation at a greater rate than individual droplets (Dickinson, 2009).

3. **Ostwald ripening** – This is the process by which larger oil droplets grow at the expense of smaller ones. This phenomenon arises due to the increased chemical potential of smaller oil droplets within water compared to larger ones as a result of their greater curvature (Ostwald, 1901), meaning that smaller oil droplets dissolve and diffuse into larger oil droplets. This process in accelerated with increasing solubility of the dispersed phase within the continuous phase and with increasing range of droplet sizes. This phenomenon is also witnessed in the case of solid particles suspended in aqueous media, such as nanosuspensions.

4. **Phase inversion** – In phase inversion the dispersed and continuous phases will invert, thereby changing an O/W emulsion to a W/O emulsion or *vice-versa*. This can occur because of changes in environment (such as increased dispersed phase concentration, temperature, pH etc.) or after prolonged periods of time.

5. **Coalescence** – Upon contact of oil droplets, the thin film positioned between them may rupture resulting in the merging, or coalescence of two separate oil droplets into one larger droplet resulting in an increase of average emulsion droplet size. If this

process is left unchecked, it can lead to complete separation between oil and water phases. This process can be hindered or prevented with selection of an appropriate emulsifier that provides either steric, electrostatic, or rheological action against coalescence (Pawar et al., 2011).

2.4 Emulsifiers

Emulsifiers are imperative for the formation of emulsions as they prevent or hinder the aforementioned instability mechanisms and consequently prevent phase separation for a period of time. Numerous emulsifiers are used in the food industry and these can broadly be split into three material groups: surfactants, molecular proteins, and Pickering particles.

2.4.1 Surfactants

Surfactants are amphiphilic molecules which consist of a hydrophilic head, and a hydrophobic tail. As such, these molecules can locate at the oil-water interface within emulsions, thereby reducing the interfacial tension between phases and lowering the energy required for emulsion formation. Once surfactant molecules have been adsorbed, they provide steric or electrostatic repulsion at the oil-water interface to stabilise an emulsion (Katepalli, 2014). A plethora of surfactants exist which can be characterised by their hydrophile-lipophile balance (HLB) number (which determines a surfactants affinity for the aqueous or oil phase) or surfactant head charge status which can either be anionic, cationic, non-ionic or zwitterionic. Particularly at high concentrations, surfactants form micellar structures within the continuous phase of emulsions to minimise contact between their hydrophilic/hydrophobic regions and the corresponding continuous phase medium (either water or oil).

2.4.2 Molecular proteins

Molecular proteins are the most commonly used emulsifiers to stabilise food emulsions (Güell et al., 2017). Molecular proteins function in much the same way as surfactants as they are amphiphilic molecules which adsorb at the oil-water interface within emulsions to lower interfacial tension, facilitate droplet break-up, and stabilise an emulsion either sterically, electrostatically or rheologically. However, their typically bulkier size compared to surfactants means that their diffusion to the oil-water interface is generally slower and this can hinder their emulsifying properties. This bulkier size of proteins also results in a thicker interfacial layer of around 1-15nm compared to 0.5-1nm for surfactants (Jacobsen, 2016) around oil droplets which can serve as a strong viscoelastic barrier to help prevent droplet coalescence. The polyelectrolyte structure of molecular proteins allows them to also electrostatically stabilise emulsion droplets in the same way as charged surfactant molecules.

2.4.3 Pickering particles

Solid particle emulsifiers, known as Pickering particles differ from conventional, molecular emulsifiers as they do not typically stabilise emulsions through a reduction in interfacial tension, but rather are able to sterically stabilise emulsions through situating at the oil-water interface and preventing droplet coalescence. Therefore, the major difference between Pickering particles and conventional emulsifiers is that the former uses solid particles whereas the latter uses molecular surfactants for emulsion stabilisation. The most widely encountered Pickering particles for the stabilisation of food emulsions are currently derived from proteins (de Folter et al., 2012), fats (Zafeiri et al., 2020) and starches (Lu et al., 2018).

A pre-requisite for particles to accumulate at the oil-water interface is that they must not be soluble in either the continuous or dispersed phase. Once at the interface, the contact angle (θ) at which particles orientate themselves towards the aqueous or oil phase is dependent on their wettability:

$$\cos\theta = \frac{\gamma_{p/o} - \gamma_{p/w}}{\gamma_{o/w}} \qquad \textbf{(Equation 2-2)}$$

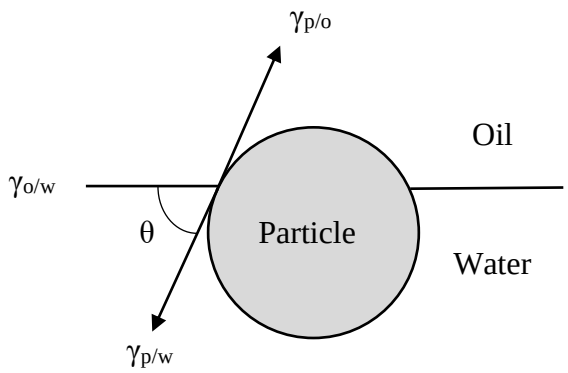

Figure 2-2: Pickering particle contact angle.

(Where $\gamma_{P/O,}$ $\gamma_{P/W,}$ $\gamma_{O/W,}$ is the interfacial tension between the particle-oil, particle-water and oil-water phase respectively).

If the contact angle is less than 90°, then the particles are hydrophilic and preferentially wetted by the aqueous phase, conversely, if the contact angle is greater than 90° the particles are hydrophobic and preferentially wetted by the oil phase (Young, 1805). The contact angle of a Pickering particle is analogous to the hydrophilic-lipophilic (HLB) value encountered with surfactants and this will largely determine their emulsifying capacity for a particular emulsion formulation.

Once particles become adsorbed at the interface, their free energy of desorption (ΔG_D) is:

$$\Delta G_D = \pi r^2 \gamma_{o/w}(1 - \cos\theta)^2 \qquad \textbf{(Equation 2-3)}$$

It can therefore be seen that particle size (radius) (r) is the most important factor in ensuring that particles do not desorb from the surface. Due to their comparatively enormous size compared with surfactants, particles, even as small as 10nm, are said to be irreversibly adsorbed as the binding energy of particles dwarfs thermal energy fluctuations which acts to remove particles from the oil-water interface (French et al., 2016).

Although the emulsifying capacity of Pickering particles was discovered over a century ago in 1903 (Pickering, 1907, Ramsden and Gotch, 1904), Pickering emulsions are an area of major current interest due to their ability to resist droplet coalescence and reduce toxicity issues compared to conventional emulsifiers (Yang et al., 2017b).

2.5 Lipid oxidation mechanism in O/W emulsions

There are several mechanisms through which lipid oxidation (LO) can occur such as auto-oxidation, photo-oxidation, and enzymatic-oxidation; however among these auto-oxidation is believed to be the most prevalent within O/W emulsions (McClements and Decker, 2000). Auto-oxidation is defined as the spontaneous reaction between lipids and molecular oxygen via a free-radical chain reaction (Shahidi and Zhong, 2010). As a process auto-oxidation can be divided into three distinct phases of (1) initiation, (2) propagation and (3) termination (Ahmed et al., 2016):

Initiation: A hydrogen atom (H) is extracted from a double bonded carbon atom of a lipid (L) in response to a trigger (initiator) such as heat or a transition metal acting as a catalyst.

$$LH \xrightarrow{initiator} L^{\cdot} + H^{\cdot} \quad \textbf{(Equation 2-4)}$$

Propagation: Alkyl radicals ($L^{\cdot}$) react with oxygen to form peroxyl radicals ($LOO^{\cdot}$), which in turn abstract a hydrogen atom from other lipid molecules leading to the production of lipid hydroperoxides (LOOH) and more alkyl radicals. Lipid hydroperoxides are primary oxidation products and their relatively poor stability means that they undergo decomposition into a range of secondary oxidation products including ketones, aldehydes and alcohols which are predominantly responsible for the generation of off-flavours in foods due to LO.

$$L^{\cdot} + O_2 \rightarrow LOO^{\cdot} \quad \textbf{(Equation 2-5)}$$

$$LOO^{\cdot} + LH \rightarrow LOOH + L^{\cdot} \quad \textbf{(Equation 2-6)}$$

Termination: Two radical species react together to form non-radical compounds, thus ending the propagation process.

$$L^{\cdot} + L^{\cdot} \rightarrow LL \quad \textbf{(Equation 2-7)}$$

$$L^{\cdot} + LOO^{\cdot} \rightarrow LOOL \quad \textbf{(Equation 2-8)}$$

$$LOO^{\cdot} + LOO^{\cdot} \rightarrow LOOL + O_2 \quad \textbf{(Equation 2-9)}$$

Within O/W emulsions however, due to the high surface area available between oil droplets and prooxidants in the aqueous phase, it is believed that the most responsible pathway for the promotion of LO is the decomposition of lipid hydroperoxides into highly reactive alkoxyl (LO·) and peroxyl (LOO·) radicals via prooxidant transition metals (McClements and Decker, 2000), for example:

$$Fe^{2+} + LOOH \rightarrow Fe^{3+} + LO^{\cdot} + OH^{-} \quad \textbf{(Equation 2-10)}$$

$$Fe^{3+} + LOOH \rightarrow Fe^{2+} + LOO^{\cdot} + H^{+} \quad \textbf{(Equation 2-11)}$$

Formed alkoxyl and peroxyl radicals will react with unsaturated lipids thus creating more radicals and further propagation reactions:

$$LO^{\cdot} + LH \rightarrow LOH + L^{\cdot} \quad \textbf{(Equation 2-12)}$$

$$LOO^{\cdot} + LH \rightarrow LOOH + L^{\cdot} \quad \textbf{(Equation 2-13)}$$

Alkoxyl radicals (LO·) can also undergo beta-scission to form an array of secondary oxidation products such as ketones, hydrocarbons, aldehydes and alcohols (McClements and Decker, 2000) which means the presence of prooxidants such as iron is of particular importance in the formation of secondary oxidation products and off-flavours in food.

Transition metals (M) also promote lipid oxidation and generate highly reactive and toxic (Winterbourn, 1995) hydroxyl radicals (·OH) via the Fenton reaction in which they react

with hydrogen peroxide (HOOH). Evidently, LO is a complex process with a myriad of associated and interlinked reactions.

$$M^{n-1} + HOOH \rightarrow M^{n} + OH^{-} + \cdot OH \qquad \textbf{(Equation 2-14)}$$

2.6 Antioxidant mechanisms to combat lipid oxidation in food

The use of antioxidants to combat chemical food spoilage (as opposed to microbial or physical spoilage) has been practised since ancient times in countries such as India where they found, through experimentation, that the addition of antioxidant spices (such as turmeric and ginger) to foods prolonged their shelf-life and combatted spoilage (Shahidi, 2015). Today, synthetic antioxidants such as butylated hydroxytoluene (BHT), butylated hydroxyanisole (BHA), tert-butylhydroquinone (TBHQ) and propyl gallate (PG) are used throughout the food industry due to their ability to effectively combat LO (Alamed et al., 2009, Prasad et al., 2015, Shahidi, 2000). However, the use of natural antioxidants such as flavonoids instead of these can remove toxicity issues and make food products 'clean-label' (Symonowicz and Kolanek, 2012) which boosts consumer acceptance and is a major reason for the recent increase in their interest (Glodde et al., 2018).

Antioxidants can combat LO through a variety of mechanisms. Moreover, some antioxidants possess the ability to act through multiple mechanisms simultaneously whereas others rely largely on one particular mechanism for their antioxidant activity.

2.6.1 Free radical scavenging

Free radical scavenging by an antioxidant (AO) is due to its ability to donate an electron from within its structure to that of free-radical, thus ending an auto-oxidised chain

reaction. This leads to the generation of an antioxidant radical which is typically far more stable than lipid radicals (Equation 2-15) and this, in the case of numerous antioxidants that contain an aromatic ring structure, is due to the resonance delocalisation of electrons within this structure (Lü et al., 2010).

$$LOO^{\cdot} + AO \rightarrow LOOH + AO^{\cdot} \qquad \textbf{(Equation 2-15)}$$

The ability of antioxidants to scavenge free radicals is determined by their reduction potential; any antioxidant with a lower reduction potential than that of a free radical is able to donate a hydrogen atom (Akoh and B. Min, 2002). For example, the reduction potential (E°) of a peroxyl radical (LOO·) is ~1000mv, therefore it can accept a hydrogen atom from ascorbic acid (E°= 330mv) or quercetin (E°= 330mv) radicals (Choe and Min, 2009). The ability of antioxidants to donate hydrogen atoms is largely determined by the number of hydroxyl (OH) groups they possess as the bond dissociation energy for this particular moiety, and consequently the reduction potential, is relatively low. Essentially, the lower the bond dissociation energy a compound possesses, the greater ease with which it can donate a hydrogen atom and hence, the more effective its free-radical scavenging ability.

The dissociation energy of an OH bond is also dependent on its positioning within a molecule. For example. one study investigating the positioning of OH groups in phenolic compounds found them to possess greater antioxidant potency in the *ortho* rather than *para* or *meta* positions due to the ability of molecules in the *ortho* position to form intramolecular hydrogen bonds, thus enhancing the stability of their radical form (Bendary et al., 2013).

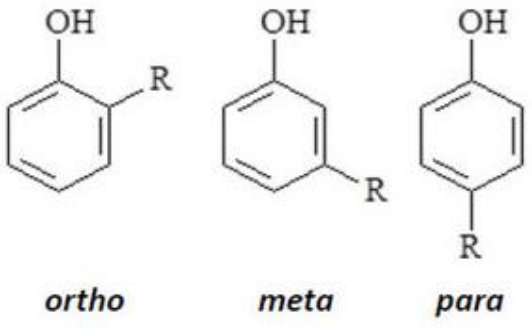

Figure 2-3: Different positions of the OH group on a phenolic compound (Mu'azu et al., 2017).

Various methods exist to quantify the free radical scavenging ability of antioxidants, and among these methods the 1,1-diphenyl-2-picrylhydrazyl (DPPH) assay appears to be one of the most popular due to its simplicity and sensitivity. DPPH exists in a radical form which is violet in colour (absorbing visible light at 517nm) and stable due to the delocalisation of a spare electron over its structure (Gangwar et al., 2014). When an antioxidant hydrogen-donor reacts with the DPPH radical it transfers an electron (in the form of a hydrogen atom) to yield a DPPH-H molecule which is yellow in colour. Therefore, through measurement of light absorbance it is possible to quantify the amount of DPPH scavenging activity which has taken place and thus, this gives a measure of the radical scavenging potential of antioxidants.

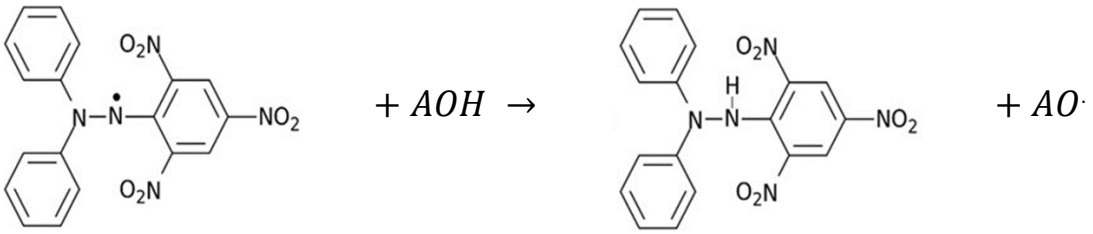

DPPH radical (violet) DPPH-H (yellow)

Figure 2-4: Reaction mechanism for DPPH assay (where AO = antioxidant, H = hydrogen atom and · = radical).

2.6.2 Chelation of metals

Metals are major prooxidants in foods; it is believed the main reason for the rapid oxidation of red and processed meat is due to their high iron content (Van Hecke et al., 2017). Therefore, the chelation of metals is often a highly effective mechanism for combatting LO when caused through auto-oxidation. Metals act as catalysts for LO reactions, lowering the activation energy, and accelerating the process. Metal chelating antioxidants perform by reducing the redox potential of prooxidant metals (Fouegue Tamafo et al., 2017); this is typically achieved through either the prevention of redox cycling, precipitation of metal complexes or simply through prevention of contact between prooxidant metals and oxidation-labile species (Graf and Eaton, 1990). It has also been noted that the free-radical scavenging efficacy of antioxidants can be increased via their complexation with metals (Kostyuk et al., 2001), a finding which was suggested to be due the attainment of an additional free-radical scavenging metal which functioned through electron transfer. Metal chelators need to be in their ionised form to perform their role, hence their behaviour is highly pH dependent (Aaneby, 2012).

Ethylenediaminetetraacetic acid (EDTA) is a common synthetic food additive used for its excellent metal chelation activity. Like most chelating agents, EDTA is water-soluble (Choe and Min, 2009) and this hinders its effectiveness in bulk oils. Many natural antioxidants however possess a highly non-polar nature, which enhances their effectiveness in bulk oils and potentially in high oil phase volume emulsions due to favourable partitioning behaviour.

Many different techniques exist to measure the metal chelating activity of antioxidants, however for the assessment of antioxidant efficacy within an O/W emulsion environment, the Ferrozine assay is highly suitable. This is because within the environment of an O/W emulsion, ferrous iron is generally believed to be the most potent prooxidant metal as studies have shown that when specific proteins known to bind with ferrous iron (transferrin and lactoferrin) are added to emulsions there is a tremendous decrease in LO (Huang et al., 1999). Ferrozine is a molecule which binds strongly with ferrous iron (Berker et al., 2010), forming a magenta coloured complex which absorbs light at 562nm. Therefore, this assay works through mixing a ferrous iron chelating antioxidant with a known quantity of ferrous iron, after allowing the antioxidant to bind with the ferrous iron for a period of time, the Ferrozine is added which effectively ‘mops’ up the remaining unbound ferrous iron. Measuring this light absorbance at 562nm at this stage thus allows for a quantification of the amount of ferrous iron the antioxidant was able to chelate, thereby giving a measure of its metal chelating activity.

2.6.3 Singlet oxygen quenching

The ground state of oxygen, and the most abundant type of oxygen on earth is oxygen in its triplet state. Singlet oxygen differs from triplet oxygen in its electron arrangement

making it a highly reactive, non-radical prooxidant compound (Min and Boff, 2002). Unlike triplet oxygen which only reacts with radical species, singlet oxygen can react directly with electron-rich double bonds found in unsaturated lipids in addition to lipid hydroperoxides.

Singlet oxygen is predominantly formed through the absorbance of light by photo-sensitizers including chlorophyll and flavins which interact with triplet oxygen (Sibuea et al., 2018) to form singlet oxygen . Therefore, one way to eliminate this prooxidant would be to package foods to prevent exposure to light or remove oxygen, however, where this is not possible quenching compounds can be used (Johnson and Decker, 2015). Quenching can be either physical or chemical. In physical quenching, a quenching molecule (Q) transfers energy or charge to singlet oxygen thus returning it to the ground state (Choe and Min, 2009); in energy transfer the quenching molecule is excited to the triplet state but readily loses its energy to the surroundings and returns to its original state (Ramel et al., 2012):

$$^1O_2 + Q \rightarrow {}^3O_2 + {}^3Q \qquad \textbf{(Equation 2-16)}$$

$$^3Q \rightarrow {}^1Q \text{ (energy transfer)} \qquad \textbf{(Equation 2-17)}$$

Charge transfer typically occurs when quenching molecules possess strong electron-donating potentials. In this case, quenchers donate electrons to electron-deficient singlet oxygen molecules forming a charged intermediate which undergoes intersystem crossing to change to the triplet state before finally dissociating into a triplet oxygen and quencher molecule.

$$^1O_2 + Q \rightarrow [^-O_2 \text{ --- } Q^+]^{\,1} \rightarrow [^-O_2 \text{ --- } Q^+]^{\,3} \rightarrow {}^3O_2 + Q \qquad \textbf{(Equation 2-18)}$$

(charge transfer)

In chemical quenching, the quencher is oxidised and typically consumed, leading to the formation of oxygen in the triplet state (Ramel et al., 2012).

Carotenoid molecules, such as β-carotene and lycopene, are known to be effective singlet oxygen quenchers (Terao et al., 2011) and this is mainly due to their possession of multiple conjugated double bonds which facilitate quenching through energy transfer, however phenolic compounds can also quench singlet oxygen (Choe and Min, 2009).

2.7 Other factors influencing lipid oxidation in O/W emulsions

2.7.1 Lipid phase

One of the main reasons LO remains such a major challenge in the food industry is due to the relentless drive for the removal of saturated fats (lipids) where possible and their potential replacement with healthier, unsaturated fats. Although this may be advantageous in one aspect, the incorporation of fats of a higher degree of unsaturation makes them more susceptible to LO. This is due to the extraction of hydrogen atoms from lipids becoming easier when they are attached to electron-rich double-bonded carbon atoms (Ghnimi et al., 2017, Johnson and Decker, 2015). Therefore, polyunsaturated fats are particularly susceptible as they contain multiple double bonds and methylene bridges which are highly oxidisable (Shahidi and Zhong, 2010). However, it is not only the degree of unsaturation of the lipid phase; one study found that the positioning of double bonds within the structure of lipid molecules impacted upon their oxidative stability (Miyashita

et al., 1995) which was due to these ease with which they could be attacked by prooxidants. Furthermore, emulsions containing fatty acids in the lipid phase have been shown to suffer poorer oxidative stability (Mistry and Min, 1987), and this was likely due to the surface-active nature of these fatty acids enabling their migration to the oil-water interface where they could impart a negative charge to emulsion droplets resulting in the attraction of positively charged prooxidants.

2.7.2 Prooxidants

Transition metals are the most important prooxidants typically found in emulsions in terms of the impact they have on LO and due to their solubility profile, these predominantly locate in the aqueous phase. Water-soluble prooxidants are of particular importance in O/W emulsions due to the large surface area oil droplets possess in contact with the aqueous phase. Metals are found in relatively high quantities in crude sunflower oil (Brevedan et al., 2000), they are also present in drinking water and can be introduced to emulsions during emulsification or through packaging operations. Furthermore, even trace quantities of metals have been shown to have significant impact on LO (Mozuraityte et al., 2016), so it is imperative to control the effect that these prooxidants have.

Even ‘antioxidants’ can act as prooxidants under certain conditions. One recent study found that in W/O emulsions, ascorbic acid acted as an antioxidant at relatively low concentrations (5ppm) and as a prooxidant under higher concentrations (100ppm) (Rege et al., 2015). This was attributed to a shift in equilibrium in the disproportionation reaction of ascorbyl radical anions (formed after ascorbic acid reacts with radical compounds) to favour the formation of non-radical products when using lower ascorbic acid concentrations; thereby enhancing oxidative stability. Polyphenols are also widely

reported to display dual antioxidant and prooxidant behaviour (Osborn and Akoh, 2003, Zhou, 2012) which is particularly prevalent in the presence of transition metals such as Fe^{3+} and Cu^{2+} which can be reduced by polyphenols yielding more potent Fe^{2+} and Cu^{+} prooxidant ions (Eghbaliferiz and Iranshahi, 2016). Ultimately, the antioxidant or prooxidant nature of a compound is highly dependent on its environment so the behaviour of a compound added to combat LO must always be fully understood within a specific formulation.

2.7.3 Oil-water interfacial properties

It is well established that LO is accelerated by free-radical reactions which predominantly take place at the oil-water interface (McClements and Decker, 2000) and it therefore makes sense that interfacial properties are crucially important in determining the rate of LO. Oxidation is mainly prevalent at the oil-water interface due to the increased lipid contact with prooxidants/oxygen, in addition to the migration of more polar (and more oxidisable) lipid components (such as hydroperoxides) away from the core of oil droplets towards the interface where they can react (Akoh and B. Min, 2002).

The major interfacial properties affecting LO are the structure and thickness of the oil-water interface, as well as its surface charge; and these are largely determined through the selection of a particular emulsifier (Jacobsen, 2016). In O/W emulsions these emulsifiers will typically be either surfactants (such as polysorbates and spans), molecular proteins (such as casein or whey proteins) or Pickering particles (such as fat crystals or starch/protein particles). These emulsifiers can vary tremendously in their size, structure and charge as is illustrated in Figure 2-5.

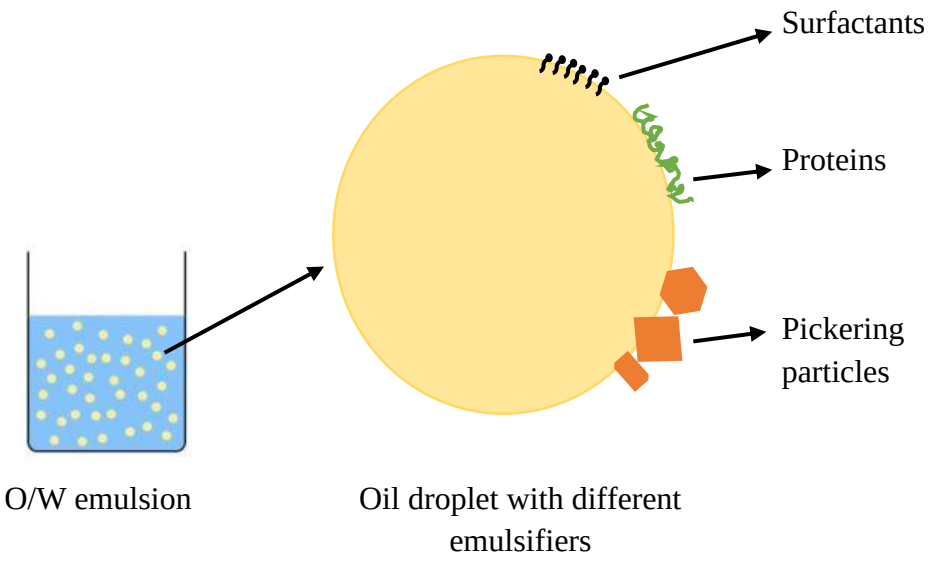

Figure 2-5: Schematic diagram of an emulsion droplet showing different types of emulsifiers (not to scale).

2.7.3.1 Structure and thickness of the oil-water interface

A tight, thick, and continuous interfacial layer of emulsifiers can serve as a physical barrier to protect the lipid phase of O/W emulsions from prooxidants located in the aqueous phase. This is an example of a non-conventional antioxidant mechanism. Protein emulsifiers generally form thicker interfacial layers of around 15nm, compared to 1nm for surfactants (Berton-Carabin et al., 2014) which is part of the reason why a number of studies have found that proteins possess superior oxidative stability to surfactants (Lamothe et al., 2019, Zhu et al., 2018) when used to stabilise emulsions. Through comparison of different proteins, one study suggested that casein stabilised emulsions possessed superior oxidative stability to whey or soy protein emulsions due to their greater hydrophobicity allowing it to form a thicker interfacial barrier (Hu et al., 2003b). On the contrary however, another study (Berton-Carabin et al., 2012) found that protein stabilised emulsions generally possessed lower oxidative stability than tween emulsions, and acknowledged that this is in contradiction of widely reported beliefs that a thicker

interfacial barrier results in enhanced oxidative stability. This contradiction was explained by noting that previous studies concluding that molecular protein emulsifiers were able to combat LO more effectively than surfactants used high emulsifier concentrations and did not account for unadsorbed emulsifiers; in the case of proteins, although these would serve as less effective antioxidants in the bulk aqueous phase (compared to when situated at the oil-water interface), they would still be able to interact with prooxidants and exert a significant antioxidant effect this way.

There are limited studies on the use of Pickering particles to combat LO, however these can typically range from 20-1000nm in size and are therefore substantially larger than surfactants or molecular proteins. One study compared two Pickering emulsifiers, microcrystalline cellulose (MCC) and modified starch (MS) and found that MCC was better able to combat LO than MS; this finding was partially attributed to the larger size of MCC particles and hence, the thicker interfacial barrier which it provided (Kargar et al., 2012). Another recent study compared lipid Pickering particles to conventional protein emulsifiers in their ability to protect sunflower oil emulsions against LO; the authors concluded that these lipid particles, and indeed Pickering particles in general, are likely unable to provide an effective physical barrier to oxidative attack due to their lack of homogeneity which creates gaps at the interface where prooxidants can attack (Schröder et al., 2019). Hence, although Pickering particles may form a very thick interfacial barrier, their effectiveness may be limited due to an inability to form a more continuous and substantial barrier unlike proteins and surfactants.

2.7.3.2 Interfacial charge

The interfacial charge of oil droplets is paramount in determining their oxidative stability. Charged prooxidant compounds such as transition metals as well as antioxidants (which may be present naturally or added to an emulsion) can dwell in the aqueous phase of emulsions and be either attracted to or repelled from the oil-water interface depending on interfacial charge (McClements and Decker, 2018).

One study found that in the case of salmon O/W emulsions, negatively charged sodium dodecyl sulphate (SDS) stabilised emulsions were more susceptible to lipid oxidation than non-ionic Brij stabilised emulsions which was attributed to SDS emulsions attracting positively charged transition metals to the surface of oil droplets (Mei et al., 1999). However, interestingly it was also noted that when antioxidant galloyl derivatives of differing charge status' (positive, neutral and negative) were added to emulsions with differently charged interfaces, it was not found that oppositely charged antioxidants (relative to the interfacial charge) were more effective. It was hypothesised this was because eventhough antioxidants may harbour an opposite charge to the interface, due to the emulsifier present, they may still not be able to partition through the interfacial barrier to the droplet surface where they can be more effective. Another study found that when decreasing the pH of whey protein isolate (WPI) stabilised emulsions from pH 7 to pH 3 there was increased oxidative stability (Donnelly et al., 1998). This finding was attributed to a shift from negative WPI emulsion surface charge at pH 7 to a positive one at pH 3 which acted to repel positively charged prooxidants.

2.7.4 Droplet size

As previously noted, LO predominantly occurs at the oil-water interface within O/W emulsions. Therefore, it would be logical to predict that with decreasing oil droplet size (assuming the same total oil volume), there will be an increased rate of LO as the interfacial surface area is increased. With increased interfacial surface area, there are more sites for LO reactions to occur and increased contact between the oil phase and aqueous phase in which prooxidants (such as transition metals) exist.

However, with that said, there are contradictory findings surrounding the impact of droplet size in the literature, with many studies finding that droplet size does significantly impact on lipid oxidation (Gohtani et al., 1999, Lee et al., 2011, Lethuaut et al., 2002), whereas others found there to be no significant impact of droplet size for their studied systems (Osborn and Akoh, 2004, Roozen et al., 1994). Authors from one review argued that in emulsions where there was a limited quantity of LO reactants, such as hydroperoxides, then these would all be present at the oil-water interface (due to their more hydrophilic nature compared with other constituents of the oil phase) regardless of droplet size within a certain range, and hence altering droplet size would not accelerate LO as this was not a limiting factor (McClements and Decker, 2000). Therefore, it is imperative to elucidate the impact of droplet size on LO for a particular system when investigating oxidative stability; if this is not understood, one may change an emulsion formulation parameter, such as the use of different surfactants, and then wrongly conclude that differences in oxidative stability were due to interfacial properties rather than simply the different droplet sizes attained through use of different surfactants.

2.7.5 Oil phase volume

Altering the total oil phase volume will impact on oxidative stability in several ways. The oil phase volume will impact upon the average oil droplet size produced during emulsification with larger oil phase volumes producing larger droplet sizes (which as mentioned earlier could impact on oxidation kinetics). One study sought to remove the impact droplet size had upon oxidation kinetics with different emulsion oil phase volumes by normalising the measured quantities of oxidation products by the total interfacial area of formulated emulsions; it was concluded in this case that droplet size had no significant effects on oxidation and that increasing oil phase volumes resulted in a reduction of the aqueous phase quantity in which prooxidants inhabited which led to increased oxidative stability (Kargar et al., 2011a). Another study also found greater oxidative stability of fish oil O/W emulsions with increasing oil phase volume, however this finding was instead attributed to the suppression of creaming with higher oil phase volumes meaning that fewer oil droplets were in contact with the air which provided better protection from oxidative attack (Sun and Gunasekaran, 2009). It should also be noted that although the literature suggests providing greater oil phase volumes enhances oxidative stability, it will of course also provide more lipids which can be oxidised, and decrease the distance separating oil droplets allowing reactants on one droplet to more easily react with those on a neighbouring droplet (Berton-Carabin et al., 2014).

2.7.6 Antioxidant synergism and antagonism

Antioxidant synergism is where the combined activity of multiple antioxidants is greater than the sum of their individual activities, and for antagonism the combined activity is reduced. Due to the complexity and variety of LO mechanisms which take place within food, it would be logical to expect that combining antioxidants which themselves utilise

different antioxidant mechanisms would be able to target multiple oxidation reaction schemes and thus prevent LO more effectively (Sonam and Guleria, 2017). For example, combination of one potent free-radical scavenging compound with a strong metal chelator can invoke a synergistic effect in which the chelator combats metal-catalysed oxidation thus inhibiting the production of free radicals, meaning that the concentration of the scavenging compound remains higher throughout LO and the process occurs at a reduced rate (Akoh and B. Min, 2002). However one study in which ascorbic acid was combined with various tocopherols showed only an additive effect between these antioxidants, which was potentially due to the similarity of antioxidant mechanisms between the combined compounds (Im et al., 2014). The authors hypothesised that synergism may have been observed with these combined compounds in a more complex environment such as if these antioxidants were present within a fruit, vegetable, or the bloodstream.

Furthermore, antioxidants may show synergism/antagonism through regeneration. This was exemplified in one study which found that combining green tea polyphenols with ascorbic acid and alpha-tocopherol led to synergistic action to prevent LO in linoleic acid; this was attributed to the regeneration of alpha-tocopherol by green tea polyphenols, and the subsequent regeneration of the green tea polyphenols by ascorbic acid (Dai et al., 2008). Regeneration occurs as a result of differing reduction potentials of various radical scavengers. Through combined action, a less potent antioxidant can ‘sacrifice’ itself by reacting with a radical which would otherwise react with the more potent antioxidant to create a synergistic antioxidant effect (Choe and Min, 2009).

2.7.7 Temperature

The open shelf-life of food decreases exponentially with increasing temperature (Frankel, 2012), and temperature is usually the most important single factor in determining the rate of LO in food. Strong correlations between increasing temperature and increased rate of LO in food products have been reported in many studies (Ito et al., 2019, Liu et al., 2019, Lu et al., 2014). Although avoidance of high temperatures would often be an effective solution to combatting LO, this is not possible for many food products which either need to undergo processing at higher temperatures (e.g. during heat treatment, emulsification, or mixing) or cannot be stored at low temperatures as it causes unwanted effects such as solidification of oil or turbidity (Johnson and Decker, 2015). Therefore, alternate solutions to adjustment of temperature are frequently required to combat LO.

2.7.8 Light

Light can promote lipid oxidation through photo-oxidation but also acts as an efficient initiator through auto-oxidation (Baigrie, 2003). Through photo-oxidation, LO is initiated through interaction of light with naturally occurring photo-sensitisers in food such as chlorophylls and flavins (Correddu et al., 2015). Hence, for assessment of LO the amount of light exposure to samples should be carefully controlled.

2.8 Measurement of lipid oxidation

Lipid oxidation comprises a complex and vast series of chain reactions which form a plethora of different reaction products depending on the extent of oxidation or the mechanism involved (Barriuso et al., 2013). It is therefore not surprising that there are an array of different measurement techniques available to characterise this process. It is strongly advised that at least two separate LO measurement techniques are employed to

obtain a meaningful quantification of this process. Shahidi and Zhong noted that there are essentially five categories of measurement techniques which can be characterised depending on what they measure, these are: (1) oxygen absorption, (2) initial substrate loss, (3) generation of free radicals, (4) generation of primary oxidation products and (5) generation of secondary oxidation products (Shahidi and Zhong, 2015). In addition, within each of these categories there are multiple different ways of measuring a particular metric, for example, the quantity of oxygen absorption can be measured in different ways. Therefore, for the purpose of this review, only the most commonly encountered measurement techniques will be discussed.

2.8.1 Headspace oxygen content (Oxidograph)

As LO occurs to an emulsion within a closed container, the oxygen pressure drops, and this pressure drop can be correlated to the extent of oxidation. As oxygen is essential for LO to occur this technique provides a direct way of measuring the process; this method is also able to quantify initiation and radical information which are difficult to measure in other ways. However, this technique does not reflect *absolute* oxidation. Absolute oxidation would measure solely oxidation of molecules at the oil-water interface, but oxygen is also consumed through its diffusion into the sample, through oxidation in the bulk phase or even through microbial growth; any stirring/agitation can strongly influence oxygen diffusion kinetics making it difficult to obtain reproducible results. Furthermore, pressure drop changes can be related to release of volatile oxidation products other than oxygen making this method non-specific (Schaich, 2016).

2.8.2 Primary oxidation products

2.8.2.1 Hydroperoxides

Hydroperoxides are amongst the most commonly measured LO products (Xia and Budge, 2017), as these are the major primary products of LO which later decompose to a number of secondary oxidation products. Quantification of hydroperoxides is carried out via peroxide value methods, two of which appear commonplace in the literature:

- **Iodometric titration method:** Potassium iodide is reacted with hydroperoxide to form iodine, which is then titrated against sodium thiosulphate in the presence of a starch indicator to quantify the amount of iodine, and therefore in theory, hydroperoxides which have been generated. These reactions are displayed in Equation 2-19 and Equation 2-20. This method has an advantage of being easy to set up, however it can produce incorrect results due to iodine being both absorbed by unsaturated bonds and, potentially generated directly from potassium iodide reacting with oxygen present in the measurement sample (Semb, 2012); meaning that the measurement of iodine is non-specific to hydroperoxides. Furthermore this method is known to be labour intensive, time consuming, and requires many different solvents (Deyrieux et al., 2018).

$$LOOH + 2KI + 2H^+ \rightarrow LOH + 2K^+ + H_2O + I_2 \qquad \textbf{(Equation 2-19)}$$

(Iodide to iodine oxidation)

$$I_2 + 2Na_2S_2O_3 \rightarrow 2NaI + Na_2S_4O_6$$ **(Equation 2-20)**

(Iodine titration)

- **Ferric thiocyanate method:** Ferrous iron is reacted with hydroperoxide to form ferric iron. Ferrous iron is also oxidised through reaction with any alkoxyl radicals present in the sample. After formation of ferric iron, this is reacted with thiocyanate to form a red-violet ferric thiocyanate complex. These reactions are shown in Equation 2-21, Equation 2-22, and Equation 2-23. With this method, any ferric iron present in the reaction prior to testing will generate erroneous results (MerckMillipore, 2019), furthermore, the presence of air whilst performing this method leads to the production of large peroxide values, however this is not an issue when only comparative results within the same study are required (Chapman and Mackay, 1949). By contrast to the iodometric titration method, the ferric thiocyanate method is less sensitive to erroneous readings as a result of oxidation of ferrous iron by the ambient air than are corresponding iodide solutions (Mihaljević et al., 1996). Furthermore this method is less time consuming, and only requires a small sample size, therefore this method was used to quantify hydroperoxides and is from herein referred to as the 'peroxide value' method within the experimental sections of this study.

$$Fe^{2+} + LOOH \rightarrow Fe^{3+} + LO^{\cdot} + OH^{-}$$ **(Equation 2-21)**

(Oxidation of ferrous iron by hydroperoxides)

$$LO^{\cdot} + Fe^{2+} + H^{+} \rightarrow LOH + Fe^{3+}$$ **(Equation 2-22)**

(Oxidation of ferrous iron by alkoxyl radicals)

$$Fe^{3+} + 5SCN^{-} \rightarrow Fe(SCN)_5^{2-}$$ **(Equation 2-23)**

(Complexation of ferric iron with thiocyanate forming ferric thiocyanate)

2.8.2.2 Conjugated dienes/trienes

Production of hydroperoxides through LO is usually accompanied with the formation of double bonds in the form of conjugated dienes/trienes as this helps stabilise newly formed radical structures (Barriuso et al., 2013). Thus these are also primary products of oxidation and have been extensively measured throughout research to quantify the extent of primary oxidation (Mei et al., 1998, Pazos et al., 2005, Zunino and Zygadlo, 2004). Measurement is typically carried out through adding an emulsion/oil to a suitable solvent and measuring the spectrophotometric UV absorbance at around 235nm (dienes) or 270nm (trienes). Hence this method is fast and simple, however, one major limitation is that it cannot be used to measure oxidation of monounsaturated lipids such as oleic acids as these do not yield conjugated dienes/trienes upon formation of hydroperoxides (Xia and Budge, 2017).

2.8.3 Secondary oxidation products

There is far greater variety of secondary compared to primary oxidation products. Secondary products include aldehydes, ketones, alcohols, epoxides, and many others.

2.8.3.1 Thiobarbituric acid reactive substances (TBARS) assay

The TBARS assay is utilised in determination of malondialdehyde (MDA), which is one of the most common secondary oxidation products. As is schematically displayed in Figure 2-6, MDA forms an adduct between two thiobarbituric acid (TBA) molecules to create a pink coloured complex which absorbs visible light at around 535nm and thus can be quantified (Dasgupta and Klein, 2014). TBARS is a fast and simple method to quantify LO, however it is a non-specific assay to MDA as it reacts with other compounds and, in certain lipids with fewer than two double bonds such as oleic acid, MDA is not formed as a secondary oxidation product and thus this assay could not be used (Barriuso et al., 2013).

(TBA) (MDA) (TBA-MDA complex) (Water)

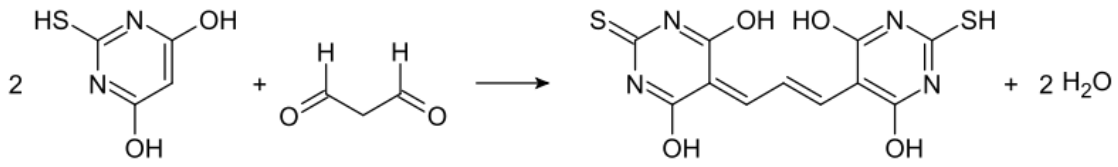

Figure 2-6: TBARS assay schematic diagram.

2.8.3.2 Para-anisidine (p-anisidine) assay

The p-anisidine assay quantifies the amounts of aldehydes, primarily 2-alkenals and 2,4-alkadienals (Yang and Boyle, 2016) which are formed following decomposition of hydroperoxides. In the presence of acetic acid, p-anisidine reacts with aldehydes to form a yellow coloured Schiff base (a chromophore) which is quantified through UV spectroscopy at 350nm. An example reaction with MDA is given in Figure 2-7. The p-anisidine assay has been found to correlate well with other LO measurement techniques including the peroxide value method, peroxide content and percent polymer assays

(Nuchi et al., 2009). A drawback of this technique is that although it reacts with all aldehydes, it reacts with certain aldehyde configurations more than others which can be an issue if assessing samples which are highly dissimilar.

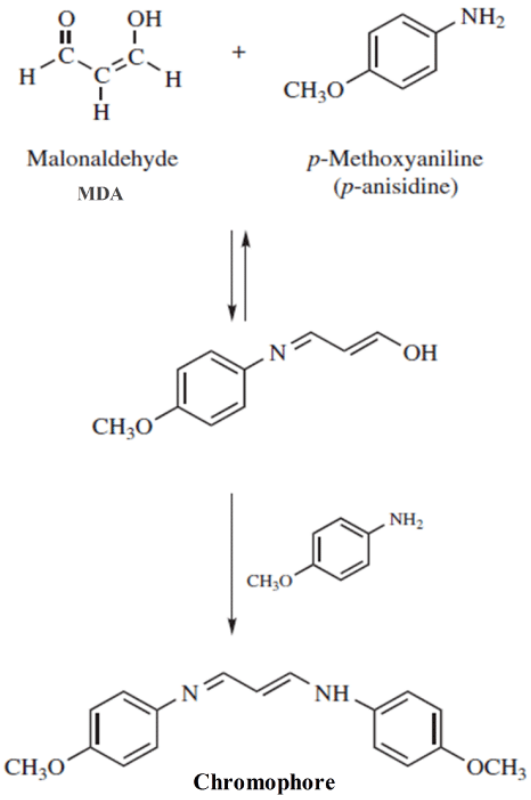

Figure 2-7: P-anisidine schematic showing reaction with MDA (Santos-Fandila et al., 2014).

2.9 Antioxidants used in this study

A brief detailing of natural antioxidants used in the experimental section of this thesis along with their molecular structure are given below.

- **Quercetin** is a flavonoid compound found in many plant-based foods such as capers, apples, leafy vegetables, and broccoli. Quercetin is known to exhibit antioxidant, anti-

cancer, anti-inflammatory, and anti-viral activity, in addition to combatting lipid oxidation (Aguirre et al., 2011).

- **Rutin hydrate** is the glycated form of quercetin, and consequently exhibits increased polarity and hydrophilicity in comparison. It can be found in similar foods to quercetin, with particularly high rutin hydrate concentrations found in capers, asparagus, and buckwheat.

- **Curcumin** is the principle active compound obtained from the root of the *Curcuma Longa* plant and has been used extensively throughout history in Ayurvedic medicine to treat illnesses ranging from the common cold, to cancer and HIV (Aditya et al., 2016). Curcumin possesses a vast range of pharmacological benefits including antioxidant, anticancer, anti-inflammatory, and antimicrobial action (Aftab and Vieira, 2010, Basniwal et al., 2014, Jurenka, 2009).

- **Silymarin** is an extract from the milk thistle plant and is a mixture of several polyphenols (silibinin, isosilibinin, silichristin and silidianin) of which silibinin is the principle active component. Silymarin has also been used extensively in medicine for thousands of years, particularly in the treatment of liver disease. Indeed, ancient Greeks and Romans have been known to use the leaves of the milk thistle plant to make tea in order to promote good liver health (Janos and Gabriella, 2012). Silymarin is a potent antioxidant, as well as showing anti-inflammatory and antifibrotic activity (Abenavoli et al., 2010).

- **Ascorbic acid** is vitamin C and therefore an essential component for normal bodily function. Unlike the other four antioxidants, ascorbic acid is not a polyphenol, and is soluble in water which greatly enhances its bioavailability *in vivo*. One of the essential roles of vitamin C is to safeguard components of cells from free-radical attack through its antioxidant properties (Beyer, 1994). Many plant-based foods are rich in ascorbic acid, such as citrus fruits.

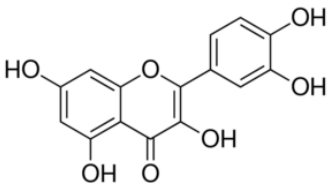

Quercetin

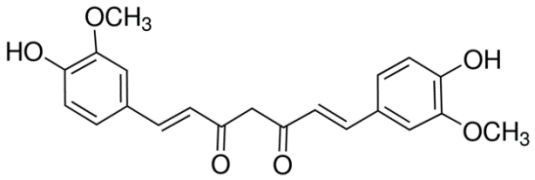

Curcumin

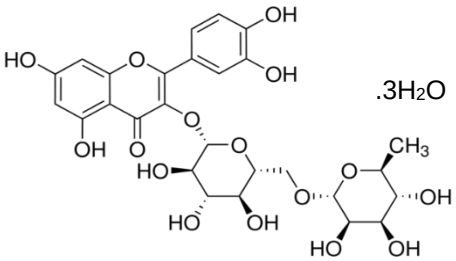

Rutin hydrate

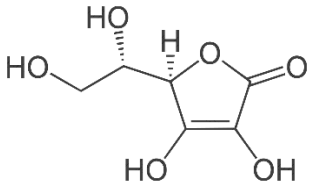

Ascorbic acid

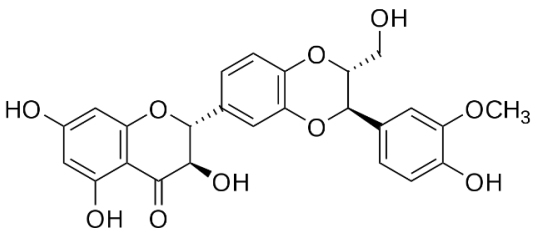

Silibinin (main component of silymarin)

Figure 2-8: Molecular structures of the five antioxidants used in this study.

2.10 Nanonisation of antioxidant compounds

2.10.1 Importance of nanonisation

A plethora of antioxidant and other bioactive compounds can be found throughout the natural world in both plant and animal products which possess the potential to provide numerous health benefits upon consumption. Natural antioxidants are predominantly polyphenolic compounds (Anwar et al., 2018) and numerous *in vitro* studies performed on this antioxidant class alone have shown their potential to impart health benefits through their ability to combat cancer, neurodegenerative and cardiovascular diseases, obesity, and type two diabetes (Cory et al., 2018). It is therefore desirable for humans to consume polyphenol-rich foods such as apples, berries and various spices as part of a balanced diet and even to extract such polyphenolic compounds from their natural sources and incorporate them into food products to produce 'functional foods'; these are foods which are able to provide health benefits in addition to basic nutrition (Hasler, 2002). Unfortunately however, many antioxidant polyphenols suffer from limited bioavailability upon consumption which is typically due to their low aqueous solubility, poor permeability across biological membranes or instability (leading to degradation) when they are passed through the alimentary canal or during storage (Oehlke et al., 2014).

Nanonisation of antioxidant compounds can help overcome low aqueous solubility issues, through increasing their dissolution velocity which can potentially lead to enhanced bioavailability. Overcoming this issue is not limited to the world of food, indeed, in the pharmaceutical industry for example over 40% of drugs with market approval and almost 90% of those currently in development contain bioactive ingredients which are poorly soluble in water (Kalepu and Nekkanti, 2015, Svagan et al., 2017). In general, before any bioactive compound can be absorbed across intestinal membranes and utilised within the

body, it must first be present in a dissolved form (Kumar and Singh, 2013) and as the human body is mainly comprised of water, aqueous solubility is paramount in determining the bioavailability of any compound.

Through nanonisation, there is typically a tremendous increase in surface area of a bioactive compound which enhances the dissolution velocity in accordance with the Noyes-Whitney equation (Noyes and Whitney, 1897):

$$\frac{dm}{dt} = \frac{DA}{d}(C_S - C) \qquad \textbf{(Equation 2-24)}$$

(Where dm/dt =compound dissolution rate, D= diffusion coefficient, A= surface area, d= thickness of the concentration gradient, C_S= concentration at the particle surface, C= bulk concentration).

Enhancement of dissolution velocity is of vital importance in addressing low solubility issues. Upon consumption of a particular bioactive compound, there is a finite transit time through the gastro-intestinal tract in which the compound can undergo dissolution and enter a viable form for its absorption, otherwise it will not be bioavailable and cannot be utilised (Aditya et al., 2016). Compounds with poor aqueous solubility will generally exhibit lower rates of dissolution and it is imperative to increase this to enable a bioavailability enhancement.

Nanonisation may also enhance a compound's apparent solubility. Apparent solubility differs from saturation solubility (normally termed simply 'solubility') in that saturation solubility is a thermodynamic property, referring to the equilibrium that develops when the amount of solid dissolving is equal to that of dissolved molecules precipitating when

the solid is in its thermodynamically favoured crystalline state (Mosharraf and Nystrom, 2003); whereas apparent solubility describes a compounds solubility when it is in a metastable state. Nanonisation can lead to the transformation of a crystalline structure to an amorphous one, which reduces crystal packing energy (Brough and Williams, 2013) and intermolecular forces holding a material together, thus increasing apparent solubility.

When approaching the nano-scale it is also widely reported that there is increased saturation solubility of a compound due to what is outlined in the Ostwald-Freundlich and Kelvin equations (Ostwald, 1900, Thomson, 1871). These equations state that as particle size is reduced, the curvature of a particle's liquid-solid interface increases, leading to increased interfacial energy and enhanced local solubility. However, it must be noted that this remains a controversial topic (Otto and de Villiers, 2009) with most studies concluding that particle size has no significant effect on saturation solubility (Murdande et al., 2015, Sun et al., 2012) which is perhaps because the major enhancement in saturation solubility is believed to occur only at particle sizes less than 10nm (Son et al., 2019).

In addition to bioavailability enhancement, certain antioxidants such as curcumin, silymarin, and rutin hydrate could be nanonised to give them a smaller size, a spherical shape and a greater degree of monodispersity to enable them to pack more tightly as Pickering particles at the oil-water interface within O/W emulsions. Smaller sized Pickering particles would be able to produce smaller droplet sizes when used in emulsions as Pickering particles generally need to be an order of magnitude smaller than the dispersed droplets themselves (Ngai and Bon, 2015); and a higher degree of Pickering particle monodispersity will ensure that a higher degree of oil droplet monodispersity

should follow. Droplet size and size distribution are both highly important in determining droplet stability as they influence the coalescence, flocculation, creaming as well as the Ostwald ripening of droplets themselves (Saifullah et al., 2016). In terms of providing oxidative stability, spherically shaped, smaller Pickering particles with a high degree of monodispersity could be able to form a more effective and continuous barrier at the oil-water interface and thus effectively safeguard oil droplets from oxidative attack.

2.10.2 Top-down vs. bottom-up nanonisation techniques

Numerous techniques exist for the formation of nanoparticles, and these can essentially be broken down as being either top-down or bottom-up fabrication methods (as are illustrated in Figure 2-9). Top-down processes focus on taking a bulk material and breaking it down into the nanometre range usually via a mechanical method such as grinding, milling or high-pressure homogenisation. Top-down processes are well established in industry and can provide high throughputs, but they have limitations in terms of high equipment and maintenance costs, in addition to the fact that it is difficult to produce nanoparticles of very small sizes (<100nm) with well-defined particle properties (Joye and McClements, 2013). In contrast, bottom-up processes are less established as an industrial technology (Sinha et al., 2013); these processes work through building up nanoparticles from an atomic or molecular level block by block via physical or chemical reactions. Key advantages of bottom-up methods over top-down processes for nanoparticle fabrication include:

- Significantly less energy input is required.
- Better control over nanoparticle properties such as size, shape, particle size distribution, and stability.

- They can be performed at low temperatures.
- Simple, relatively inexpensive equipment can typically be used, which makes certain bottom-up methods more easily scalable.

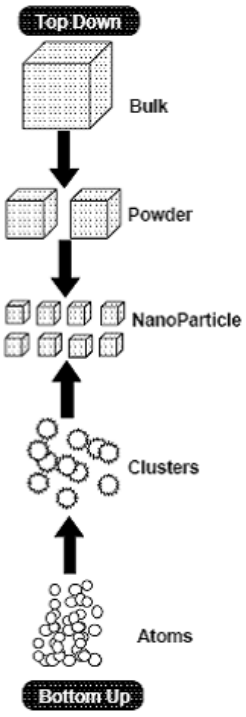

Figure 2-9: Top-down vs. bottom-up nanonisation techniques (Prayog, 2017).

2.10.3 Antisolvent precipitation

Antisolvent precipitation (AP) is one of the most well documented bottom-up techniques for nanoparticle fabrication and this is largely due to its simplicity, low cost (Sinha et al., 2013), and the fact that it represents a readily scalable technique with significantly less risk of contamination than typical top-down techniques. This is also why AP is already widely used in the pharmaceutical industry (Joye and McClements, 2013). Typically, in AP processes, a bioactive compound is dissolved in a solvent, which is then added to an antisolvent (in which the solvent is miscible) under intense mixing to achieve supersaturation of the solution followed by nucleation and particle growth.

The process of nanoparticle formation via AP processes can be understood using LaMer's seminal theory of nucleation and growth, which originally explained the synthesis of sulphur-sol nanoparticles (LaMer and Dinegar, 1950) but can be applied within the context of antisolvent precipitation processes. The LaMer theory detailed a mechanism for nanoparticle synthesis consisting of three distinct stages, which is outlined in Figure 2-10. Briefly, (1) the concentration of solute in a solvent-antisolvent mixture is increased and the mixture becomes increasingly supersaturated but there is no particle formation yet as the level of supersaturation has not reached the point at which nucleation is thermodynamically favourable (C_{min}), (2) the solute concentration exceeds C_{min}, consequently rapid (burst) nucleation occurs and the solute concentration decreases sharply, (3) the diffusible solute concentration drops below the critical concentration for nucleation and particles undergo growth but no further nucleation.

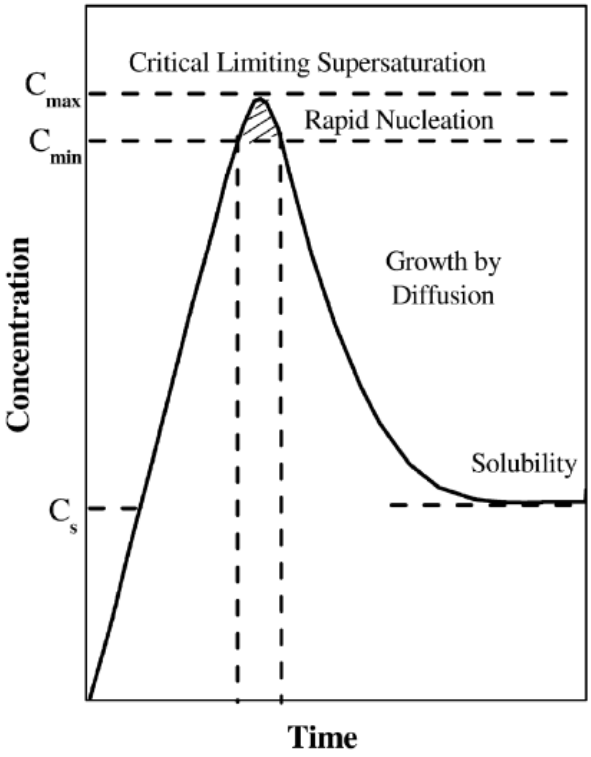

Figure 2-10: LaMer theory of nucleation and growth (Viswanatha et al., 2007).

Hence, according to the LaMer theory, to obtain smaller, more monodispersed nanoparticles, the solute concentration should be increased rapidly, to generate maximum supersaturation resulting in a shorter, burst nucleation event and ultimately the formation of a greater number of particles which will invariably be smaller in size. In addition, with generation of a burst nucleation event, it can be seen from the LaMer mechanism that the stages of nucleation and particle growth by diffusion are effectively separated, as the rate of nucleation is said to be infinite during a burst nucleation event in accordance with this theory; this helps generate nanoparticles of a greater degree of monodispersity. Nanoparticles of a higher degree of monodispersity will be more resistant to the effects of Ostwald ripening and will inherently be more stable.

To generate a high level of supersaturation capable of delivering a burst nucleation event, recent research into AP techniques has been largely focused on enhancing the solvent-antisolvent mixing step. Through effective mixing of solvent and antisolvent phases, a higher, more uniform level of supersaturation is generated which ultimately creates smaller nanoparticles. The most widely utilised AP mixing methods are discussed below.

2.10.3.1 Physical stirring

Physical stirring has been widely employed in research for the formation of bioactive nanoparticles in AP processes and this usually takes place through use of a magnetically stirred beaker. One study found that increasing the rate of magnetic stirring upon addition of solvent and antisolvent phases would result in a reduction of particle sizes due to the attainment of homogenous mixing in a shorter time (Kakran et al., 2012). However, another study found there was an optimum magnetic stirring speed above which, there would be an increase in the size of nanoparticles (Zu et al., 2014). This was likely because although higher mixing speeds generate greater supersaturation, they can also promote particle agglomeration and growth following nucleation due to high surface energies associated with nanoparticles.

2.10.3.2 Impinging jet mixing

Impinging jet mixing (IJM) entails the contacting of solvent and antisolvent streams with each other at a certain ratio and velocity within a mixing chamber. The high velocities of the streams ensures rapid mixing (Thorat and Dalvi, 2012). Conventional confined IJM units require roughly equal flowrates of the two contacting streams for more efficient mixing, this is a drawback as it limits the maximum achievable supersaturation level which can be reached. To overcome this drawback, a multi-inlet vortex mixer (MIVM) can be used in which there are four inlets and the liquid streams meet at an angle rather

than head on allowing for different volume ratios of solvent/antisolvent to be used. The MIVM is therefore able to achieve higher rates of supersaturation than the confined IJM's but confined IJM's are often still preferred as they are simpler to operate (MIVM's usually require programmable syringe pumps), easier to clean and cheaper (Han et al., 2012). A recent study successfully used IJM in continuous operation to produce caseinate coated zein nanoparticles (Ebert et al., 2017) which shows the potential of this technique for scale-up and commercialisation.

2.10.3.3 Supercritical antisolvent precipitation

In supercritical antisolvent precipitation (SAP), a compound is first dissolved in a solvent which is then contacted with a supercritical fluid (SCF) antisolvent. The solvent rapidly diffuses through the antisolvent consequently decreasing the solubility of the solute and causes precipitation. The precipitate is then washed and dried with the antisolvent (Sun, 2002). Carbon dioxide is the most common supercritical fluid used as it has near ambient critical temperature and relatively low critical pressure in addition to being relatively inexpensive and safe to use (Sinha et al., 2013).

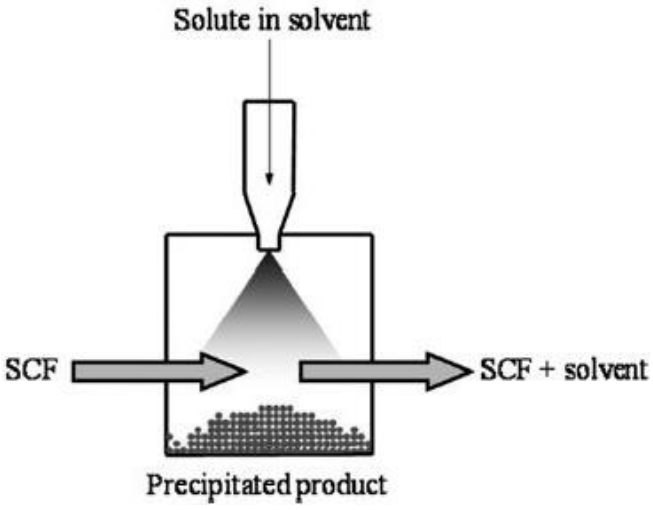

Figure 2-11: Typical setup of a supercritical antisolvent precipitation process (Chan and Kwok, 2011).

A major advantage of the SAP technique is the potential for the removal of the antisolvent via a simple pressure reduction of the gas phase (Reverchon, 1999), which removes the need for an extensive drying process following nanoparticle synthesis which can alter product properties. However, the use of a nozzle is a weak point in SAP, especially when dealing with solutions with a high solute concentration as this can cause nozzle blockages; with even a partially blocked nozzle the solution is likely to flow into the mixing chamber in uneven bursts which will cause non-uniform mixing and ultimately a large particle size distribution (PSD) (Shekunov et al., 2004). Non-uniform mixing and consequently a large PSD is also caused by localised mixing adjacent to the nozzle, and the nozzle flow causing a degree of recirculation (Shekunov et al., 2004). An additional drawback of SAP is that due to the slow solution feed rate through the nozzle, long periods of time are required for this process (Chan and Kwok, 2011). The SAP technique has been successfully utilised in one study to fabricate 325nm diameter curcumin nanoparticles (Zhao et al., 2015).

2.10.3.4 Sonoprecipitation

When a solvent containing a bioactive compound and antisolvent are added to a tank, high energy ultrasonic waves can be directed through the mixture via an ultrasonic probe causing the creation of bubbles which grow and grow until they reach a critical size at which point they burst. This process is known as cavitation and it creates localised conditions such as high temperatures and pressures which result in the generation of shockwaves (Guo et al., 2005). The rapid and violent nature of cavitation adds turbulence to the system and consequently promotes rapid mixing allowing for a high attainment of supersaturation to be generated leading to high nucleation rates and smaller particle sizes (Dhumal et al., 2008).

Sonication is also able to hinder the agglomeration process through shockwaves breaking apart larger particles (Guo et al., 2005). Furthermore, ultrasound ensures that the contact time between newly formed particles is reduced thus further preventing particle aggregation and agglomeration (Thorat and Dalvi, 2012). Additional benefits of sonoprecipitation are that only small, simple and relatively inexpensive equipment is required and that the process can be operated under ambient conditions (Li et al., 2003). By controlling parameters such as sonication duration and intensity, the probe length/depth to which it is immersed (Sinha et al., 2013), and the solution volume, it is possible to tailor nanoparticle properties using sonoprecipitation.

The use of ultrasound-assisted AP techniques are well documented in scientific papers (Dhumal et al., 2008, Jiang et al., 2012, Liu et al., 2010, Luque de Castro and Priego-Capote, 2007). In the preparation of amorphous cefuroxime axetil nanoparticles, one study found that sonoprecipitation created smaller particles with a narrower size

distribution, greater dissolution rates and higher bioavailability than those prepared using AP techniques without ultrasound (Dhumal et al., 2008). This was attributed to the particles amorphisation and increased surface area after sonoprecipitation was carried out. However, the violent nature of ultrasound mixing may damage sensitive compounds, and the potential damage caused to bioactive compounds must be assessed whenever using sonication. Recent studies have combined supercritical AP techniques with ultrasound with promising results (Jia et al., 2015, Kakran et al., 2013). One of these studies shown that the combined use of ultrasound with SAS to produce curcumin particles improved the mixing between the liquid solution and the supercritical fluid, leading to a higher degree of supersaturation which reduced curcumin's degree of crystallinity and generated a low PSD (Jia et al., 2015).

2.10.4 Other factors influencing nanoparticle properties in antisolvent precipitation

Besides mixing, there are many variables affecting nanoparticle properties in AP techniques. All these variables must be considered and understood before embarking on any precipitation technique. Figure 2-12 illustrates the numerous factors which enable the production of nanoparticles with a reduced particle size and narrow size distribution. Some of the most important factors are discussed in this section.

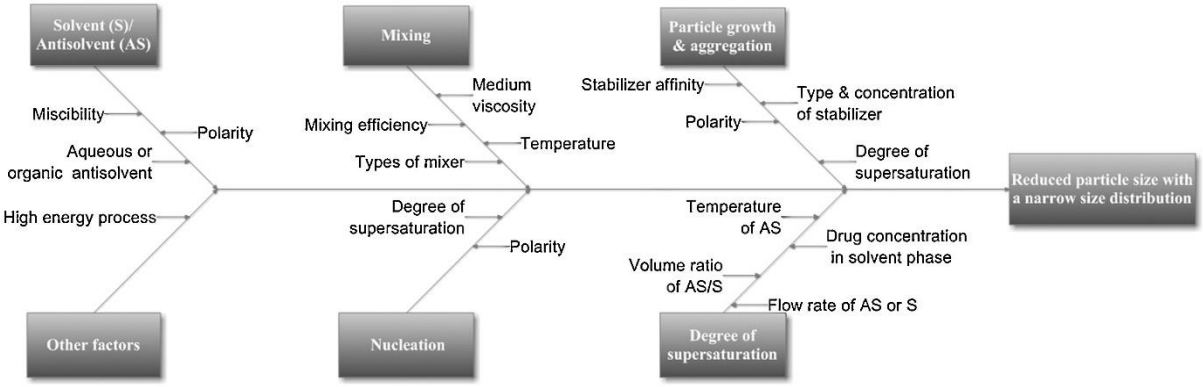

Figure 2-12: Fish-bone diagram illustrating the different parameters affecting fabricated nanoparticle properties in antisolvent precipitation processes (Sinha et al., 2013).

2.10.4.1 Selection of solvent and antisolvent

The selection of an appropriate solvent and antisolvent is crucial for obtaining highly monodispersed nanoparticles with a small size. Essentially, a solvent should be selected in which a solute compound has high solubility, and then an antisolvent should be chosen in which the solvent is highly miscible, yet the solute compound is completely immiscible within.

2.10.4.2 Rate and order of solvent and antisolvent addition

Both the rate and order of solvent to antisolvent addition will affect the rate and degree of supersaturation and, ultimately the particle sizes and morphologies. It is generally observed that by increasing the rate of addition of antisolvent to solvent, smaller particles are formed. This is because increasing the addition rate will effectively enhance mixing velocity by increasing the Reynolds number, which causes more rapid and uniform supersaturation (Sinha et al., 2013). As there is typically less solvent than antisolvent volume, addition of antisolvent to solvent can enhance the immediate mixing efficiency between these two phases.

2.10.4.3 Solvent-antisolvent ratio

A greater amount of antisolvent in the solvent-antisolvent (SAS) mixture will generally increase the level of supersaturation (producing smaller particles). With decreasing SAS ratios, the level of supersaturation generated generally increases due to the swift change in solute solubility in the solvent-antisolvent mixture compared to the solvent. It should be noted that if the SAS ratio is changed solely through increasing the level of antisolvent, this may not lead to the attainment of smaller particles. This is because, although the solute is not soluble in the antisolvent, it is also not completely insoluble and therefore when large amounts of antisolvent are present some of the solute will solubilise in this phase. It is also believed that a greater antisolvent-solvent ratio will hinder crystal growth (and hence aid in the production of smaller particles) as this increases the diffusional distance between solute molecules (Brock, 2004).

Furthermore, one study reported that the impact of decreasing the SAS ratio becomes less and less with further reduction and the minimum size of particles obtained through a reduction in SAS ratio will approach a critical value (Zhao et al., 2009). This is due to the rate of supersaturation increase decreasing with decreased SAS ratio's (i.e. a SAS ratio decrease from 1:5 to 1:10 will have greater impact on supersaturation than a reduction of 1:10 to 1:20). Therefore, decreasing SAS ratios will only decrease particle size up until a point, beyond which other parameters will need to be adjusted to invoke a further reduction.

2.10.4.4 Solute concentration

The solute concentration is another parameter for which an optimum amount exists due to opposing effects. On one hand, increasing solute concentration will increase supersaturation as there will be more poorly soluble solute in the antisolvent, hence this

will increase supersaturation and hence, the nucleation rate. However, increasing solute concentration will also increase the frequency of collisions between particles which will lead to particle growth, and hence, larger particles (Joye and McClements, 2013). Furthermore, higher solute concentrations can also cause an increase in the solution viscosity which is again believed to have two opposing effects. Firstly, an increased viscosity will hinder mixing between solvent and antisolvent phases and this will create non-uniform supersaturation, slower nucleation rates and increased particle agglomeration (Sinha et al., 2013) which will ultimately cause both increased particle size and particle size distribution. However, the increased viscosity will also decrease the collision frequency by slowing down particle movements which aids in the attainment of smaller particles. The opposing effects of drug concentration were illustrated in a recent study into the formation of lutein ester nanoparticles through AP which found that there was an optimum solute concentration to use due to the aforementioned reasons (Wu et al., 2019).

2.10.4.5 Temperature

Nucleation rate is inversely proportional to temperature, and generally, higher temperatures promote the formation of larger particles and a wide PSD. At lower temperatures, solute solubility generally decreases which causes increased supersaturation, greater nucleation rate and consequently, smaller particles (Patel, 2013). Higher temperatures also result in lower viscosities, which will have the same effect as those previously discussed.

2.10.4.6 Use of stabilisers

Surfactants and protein stabilisers are used in AP to lower interfacial tension which increases the nucleation rate thus leading to the generation of smaller particles. Stabilisers

are also able to coat the surface of newly formed nanoparticles and are thereby able to inhibit particle growth and maintain a smaller average particle size as was described in a recent study into the formation of paracetamol nanosuspensions (Shariare et al., 2018). Whether the stabiliser is in the solvent or antisolvent phase is also important. As there is typically less solvent than antisolvent, stabiliser dissolution in the solvent phase typically aids in the production of smaller particles as the stabiliser will not have to travel as far, or cross the solvent-antisolvent interface to adsorb at the nanoparticle surface which was demonstrated in a past study (Matteucci et al., 2006).

CHAPTER 3: THE USE OF NATURAL ANTIOXIDANTS TO COMBAT LIPID OXIDATION IN O/W EMULSIONS

Data and discussions from within this chapter have been published in:

Noon, J., Mills, T. B. & Norton, I. T. 2020. The use of natural antioxidants to combat lipid oxidation in O/W emulsions. Journal of Food Engineering, 281, 110006.

3.1 Abstract

This research investigated the efficacy of four natural antioxidants (quercetin, curcumin, rutin hydrate and ascorbic acid) in their ability to combat lipid oxidation (LO) within different oil-in-water (O/W) emulsion environments. The free radical scavenging and metal chelating ability of the four antioxidants were first assessed through 2,2-diphenyl-1-picrylhydrazyl (DPPH) and Ferrozine assays respectively and these were used to help explain the efficacy of each antioxidant in particular emulsion environments. Generally, in emulsions with no added iron, compounds that exhibited the greatest levels of DPPH and Ferrozine inhibition provided the best oxidative stability. In the presence of added iron, antioxidant effectiveness reduced dramatically and, in some cases, resulted in prooxidant activity. It was concluded that the antioxidant metal chelating mechanism of antioxidants in emulsions with added iron was largely insignificant compared to the prooxidant effect gained by these compounds through their interaction with iron. The most non-polar compounds, namely curcumin and quercetin, provided peroxide value (PV) reductions of 65% and 74% respectively in 5% oil phase volume emulsions compared to just 28% and 43% PV reductions in 40% oil phase volume emulsions; thus providing more evidence of the widely reported ‘polar paradox’ theory. Combinations of ascorbic acid with quercetin or curcumin resulted in antioxidant synergism, whereas other antioxidant combinations led only to additive or antagonistic effects. This research builds on the understanding of the fundamental behaviour of natural antioxidants within different emulsion formulations.

3.2 Introduction

The addition of highly potent, natural antioxidants provides a potential solution to the modern-day challenges posed by LO within O/W food emulsions. Consequently, there has been increased recent research into their use for combatting LO (Ghorbani Gorji et al., 2019, Glodde et al., 2018, Zahid et al., 2018). However, there has yet been limited research into the fundamental understanding of the behaviour of natural antioxidants in many different O/W emulsion environments (e.g. differing antioxidant/prooxidant concentrations, oil phase volumes, choice of emulsifiers, antioxidant combinations etc.). This chapter of work was produced to both gain understanding and build knowledge in this area though assessment of four antioxidants found widespread in nature, namely, quercetin, curcumin, rutin hydrate and ascorbic acid.

3.3 Materials and methods

3.3.1 Materials

Distilled water was used as the continuous phase within emulsions, this was obtained by pumping water through a reverse osmosis unit followed by a milli-Q water system prior to usage. Consumer grade sunflower oil was used as the dispersed phase in emulsions; a large batch of this oil was purchased from a local Aldi supermarket to avoid batch-to-batch composition variations. Polysorbate 20 was obtained from Acros organics. Quercetin (≥ 95%), curcumin (≥ 80%), rutin hydrate (≥ 94%), L-ascorbic acid (≥ 99%), Ferrozine (≥ 97%) and para-anisidine (99%) were all obtained from Sigma Aldrich. Sodium dodecyl sulphate (> 99%), iron (II) sulphate heptahydrate (≥ 98%), ammonium thiocyanate (≥ 97.5%), 2,4-decadienal aldehyde (85%), anhydrous barium chloride (≥ 97%), hydrochloric acid (37%), and glacial acetic acid (≥ 99.7%) were all provided by Fisher Scientific. Mirenat-D (69.3% ethyl lauryl arginate, 30.7% maltodextrin) cationic

surfactant was provided by Vedeqsa. Isooctane (> 98%) was provided by VWR international. Cumene hydroperoxide (80%) was provided by Scientific Laboratory Supplies Ltd.

3.3.2 Antioxidant activities

3.3.2.1 DPPH assay

The 1,1-diphenyl-2-picryl hydrazyl (DPPH) assay was taken from a previous study (Olugbami et al., 2015). This assay was used to determine the free radical scavenging activity of antioxidant compounds and was discussed in Section 2.6.1. In terms of the methodology, briefly, 1ml of 0.1mg/ml DPPH solution was added to 1.5ml of antioxidant solutions dissolved in ethanol at concentrations ranging from 0-80µg/ml. This mixture was shaken and then stored in the dark at room temperature for 20 minutes followed by UV absorbance measurement at 517nm using a UV spectrophotometer.

$$\text{DPPH inhibition (\%)} = 100 \times \frac{A_{control} - A_{sample}}{A_{control}} \qquad \textbf{(Equation 3-1)}$$

(Where A_{sample} and $A_{control}$ are the UV absorbance's of the samples with and without antioxidants respectively).

3.3.2.2 Ferrozine assay

The Ferrozine assay was a modified version taken from a previous study (Dinis et al., 1994). This assay was used to determine the ferrous iron chelation activity of antioxidant compounds and was discussed in Section 2.6.2. 10µl of 4mM ferrous sulphate solution was added to 2ml of ethanol solutions containing antioxidant concentrations of 0-4mg/ml. This mixture was shaken and left for 3 minutes. Then 10µl of 20mM Ferrozine solution

was added, the mixture was shaken and left for 10 minutes in the dark at room temperature followed by UV absorbance measurement at 562nm using a UV spectrophotometer.

$$\text{Ferrozine inhibition (\%)} = 100 \times \frac{A_{control} - A_{sample}}{A_{control}} \quad \textbf{(Equation 3-2)}$$

(Where A_{sample} and $A_{control}$ are the absorbance of the samples with and without antioxidants respectively).

3.3.3 Emulsion formulation

1% (w/w) emulsifier (either polysorbate 20, sodium dodecyl sulphate or Mirenat-D) was added to distilled water and stirred until dissolved at room temperature to form the aqueous phase of the emulsion. The desired amount of sunflower oil (either 5, 10, 20 or 40% (w/w)) was then added to this to make up a total emulsion weight of 100g. This mixture was emulsified through use of a Silverson L5M high shear mixer fitted using a fine emulsion screen, 57mm diameter head, and homogenisation speed of 7000rpm for 5 minutes. 25g of homogenously dispersed emulsion was then poured into individual sample pots to which the desired mass of antioxidants (either 1.0, 0.4, or 0.1mg dissolved in 1ml ethanol) and/or iron sulphate heptahydrate (to a concentration of either 0.02 or 0.1mM) were added if required. These 25g samples were used throughout the duration of the LO study (7 days). All emulsions were formulated at native pH.

3.3.4 Size measurement

The Sauter mean diameter (D [3,2]) of emulsified oil droplets was measured using a Mastersizer 2000. It was ensured that the Mastersizer was measuring >77% laser light transmittance prior to its operation. The stirring speed for all size measurements was

selected at 1300rpm and sample was added via pipetting until laser obscuration reached a value of 5%. A refractive index value of sunflower oil (1.47) was selected for all emulsions.

3.3.5 Zeta potential measurements

Zeta potential measurements were carried out using a Malvern Zetasizer Nano ZS at 25°C. Malvern folded capillary zeta cells (DTS1070) were used to house the samples.

3.3.6 Partition coefficient

The partitioning behaviour of antioxidants between distilled water and octanol was assessed. For this assessment, 5mg of antioxidant was added to a mixture of 10ml distilled water and 10ml of octanol. This mixture was shaken at a moderate speed for 24 hours after which time the mixture was left to separate and equilibrate for 4 hours. Then, samples were carefully extracted separately from the water and octanol phases and centrifuged at 4000rpm for 30 minutes. Following this, antioxidant-containing water and octanol phases were diluted appropriately with ethanol and UV absorbance measurements were performed to quantify their concentrations in each phase. The partition coefficient (P) of each antioxidant compound was calculated as shown below in Equation 3-3 (where C_O and C_W are the antioxidant concentrations within the octanol and water phases respectively). Quercetin, curcumin, rutin hydrate and ascorbic acid samples underwent UV absorbance measurement at 374, 423, 361, and 282nm, respectively. Standard curves of all antioxidant compounds were produced to verify this method, all of which displayed a linear relationship between antioxidant concentration and UV absorbance within the ranges encountered in this study.

$$P = \log\left(\frac{C_O}{C_W}\right)$$ **(Equation 3-3)**

3.3.7 Lipid oxidation study

The levels of primary and secondary oxidation products generated throughout a 7-day period were measured. Hydroperoxides served as the primary oxidation product, the quantity of which was measured via the peroxide value method. Secondary oxidation products were measured by the para-anisidine (p-anisidine) method which predominantly measured the quantity of unsaturated aldehydes. Emulsions were stored at 40°C throughout the experiment to accelerate the lipid oxidation process.

3.3.7.1 Peroxide value (PV) method

The PV method was a modified version taken from a previous study (Shantha and Decker, 1994). Briefly, emulsions were gently shaken to form a homogenous mixture. Then 100µl of emulsion sample was taken and added to 1.5ml of isooctane/propan-2-ol mixture (3:1 v/v). This mixture was vortexed for 10s intervals, 3 times in order to extract the hydroperoxides into the solvent phase and then the mixture was centrifuged at 4000rpm for 20 minutes. Post centrifugation, 200µl of the upper solvent layer was taken and added to 2.8ml of methanol/butan-1-ol (2:1 v/v) mixture along with 15µl of 0.072M ferrous iron solution and 15µl of 3.94M ammonium thiocyanate solution. Ferrous iron solution was obtained from the supernatant of a mixture of 25ml $BaCl_2$ solution (0.132M $BaCl_2$ in 0.4M HCL) and 25ml of 0.144M $FeSO_4$ solution. These samples were then placed in the dark for 20 minutes prior to absorbance measurement using a spectrophotometer at a wavelength of 510nm.

To quantify the amount of hydroperoxides within emulsion samples, a standard curve (shown in Figure 3-1) was produced using cumene hydroperoxide (CH). For this, a 21Mm CH solution in isooctane/propan-2-ol (3:1 v/v) was centrifuged at 4000rpm for 20 minutes. The supernatant was taken and diluted into several known concentrations. These different concentrations of CH then underwent the same method as emulsion samples for measurement of their light absorbance. The relationship was found to be linear among all PV's encountered in this study.

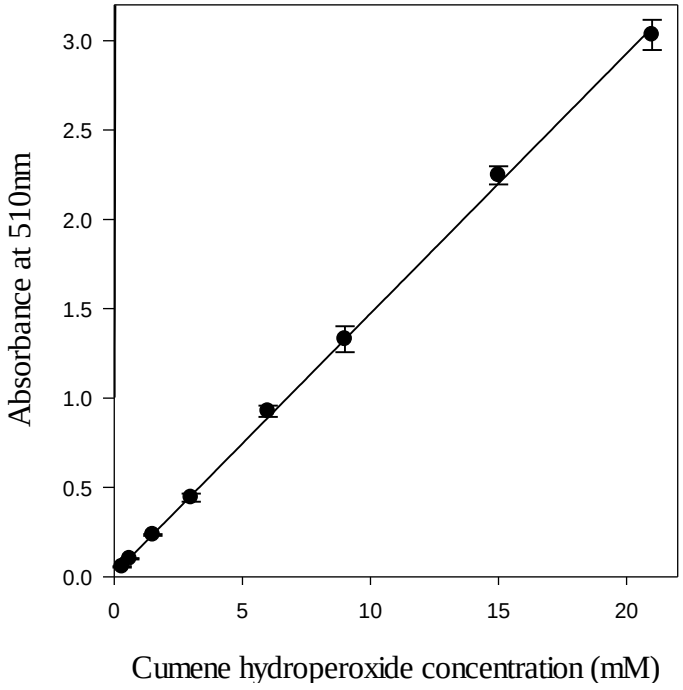

Figure 3-1: Cumene hydroperoxide standard curve.

3.3.7.2 P-anisidine value (AV) method

The AV method was a modified version taken from a previous study (O'Dwyer et al., 2013). Briefly, emulsions were gently shaken to form a homogenous mixture. Then 2ml emulsion samples were taken and added to 2ml of ethanol. Ethanol was used to help break-up the interfacial layer and allow for more effective extraction of secondary

oxidation products to the solvent phase upon vortex mixing. 8ml of isooctane was then added to this mixture and the sample was vortexed for 10s intervals, 3 times in order to extract the secondary oxidation products into the solvent phase and then the mixture was centrifuged at 4000rpm for 20 minutes. The absorbance of the supernatant was then measured at a wavelength of 350nm using the spectrophotometer to give the A_1 value. Then, 5ml of the supernatant was mixed with 1ml of p-anisidine solution (2.5mg/ml p-anisidine solution in glacial acetic acid). After keeping the samples in the dark for 10 minutes, the absorbance was measured at 350nm using the spectrophotometer to give the A_2 value.

$$AV = 25(1.2A_1 - A_2) \quad \textbf{(Equation 3-4)}$$

A standard curve (shown in Figure 3-2) using 2, 4-decadienal aldehyde (DA) was used to verify the accuracy of this method. To obtain the standard curve, a 1mM solution of DA in isooctane was prepared and suitable dilutions were made up. These dilutions then underwent the same method as emulsion samples for measurement of UV-absorbance. The relationship was found to be linear among all AV's encountered in this study.

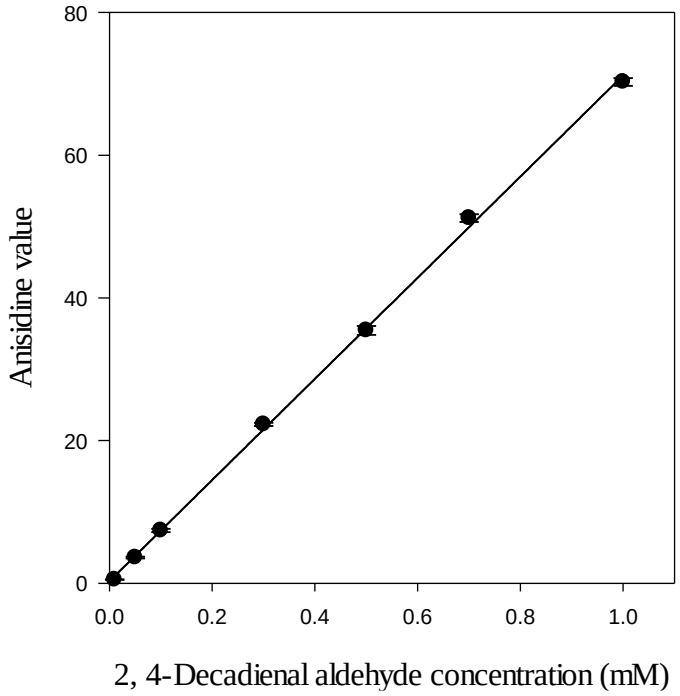

Figure 3-2: 2, 4-Decadienal aldehyde standard curve.

3.3.8 Antioxidant combinations

Four different antioxidant combinations were investigated to assess potential synergistic or antagonistic effects on LO, these were, quercetin-rutin hydrate (Q +RH), quercetin-ascorbic acid (Q+AA), curcumin-rutin hydrate (C+RH) and curcumin-ascorbic acid (C+AA). These specific combinations were chosen as AA has very different properties to Q or C, therefore it was hypothesised these different properties could generate antioxidant synergies in the form of Q+AA and C+AA. Whereas, in the case of Q+RH and C+RH it was hypothesised that because these compounds shared similar properties, synergism would not be as profound.

Antioxidants were always added in equal measure to a total of 1mg antioxidant mass (500µg of each antioxidant dissolved in 1ml of ethanol) which was then added to 25g of emulsion sample (formulated as described previously). Experimental values ('Exp')

obtained were compared with additive values (‘Add’) predicted if antioxidants did not hinder or complement each other but instead displayed a solely additive antioxidant effect. For this study only, PV’s and AV’s were given as cumulative values over a 7-day period (measurements were taken on the same days as previous experiments and then added together). This was performed to enable greater clarity of any synergistic or antagonistic interactions which occurred between antioxidant compounds. Single factor ANOVA was used to assess statistical difference between measurements, a probability value of < 0.05 was deemed as significant and when this was the case, a post hoc t-Test was performed to assess between which specific measurements this significant difference occurred.

3.3.9 Statistical analysis

All experiments were carried out in triplicate, with error reported as plus/minus a single standard deviation unless otherwise stated. Any additional statistical analysis is detailed within individual methodology descriptions.

3.4 Results and discussion

3.4.1 Antioxidant activities

The antioxidant activity of ascorbic acid as well as polyphenols including quercetin, curcumin and rutin hydrate is believed to stem predominantly from their ability to free radical scavenge and chelate prooxidant metals (van Acker et al., 1998). Therefore, initial experiments were performed to quantify the free radical scavenging and metal (ferrous iron) chelating ability of these compounds using DPPH and Ferrozine assays, respectively. The Ferrozine assay assessed each compounds ability to chelate ferrous metal ions which are one of the most prevalent and prooxidant metals found in food products (Waraho et al., 2011). To assess the antioxidant activities of these compounds, it is useful to consider their chemical structures, shown in Figure 3-3.

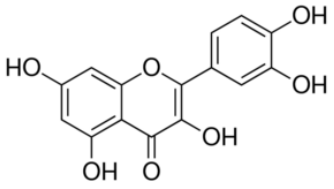

Quercetin

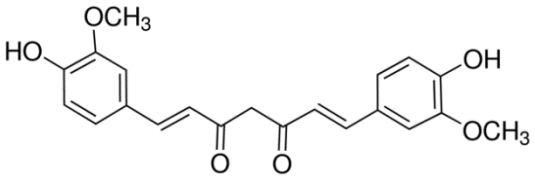

Curcumin

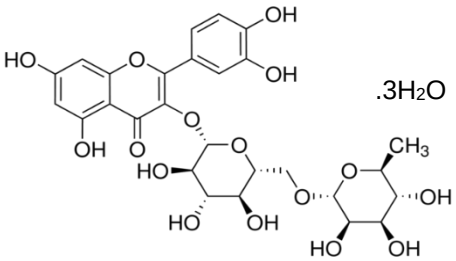

Rutin hydrate

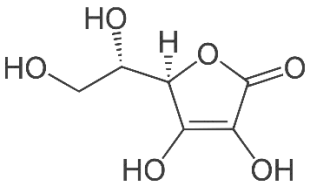

Ascorbic acid

Figure 3-3: Chemical structures of investigated compounds.

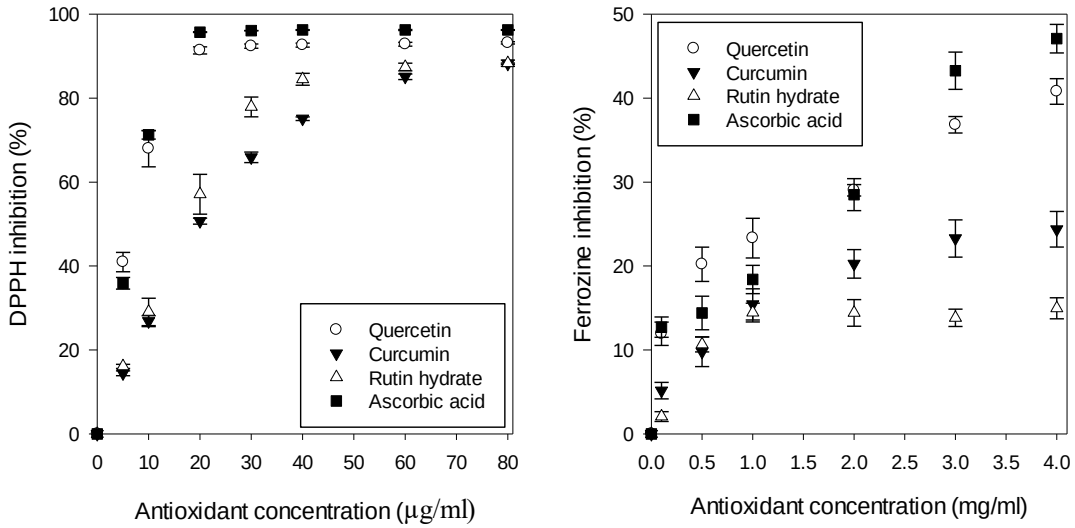

Figure 3-4: Antioxidant activities of investigated compounds.

As shown in Figure 3-4, in terms of DPPH inhibition, curcumin was found to be the least effective as it required the highest concentration to reach an end value of inhibition which was the joint lowest value along with rutin hydrate (88%). This makes sense considering that radical scavenging ability is dependent on the ability of these compounds to donate hydrogen atoms (Ammar et al., 2009) which is especially related to the number of hydroxyl groups they possess and, to a lesser extent other moieties such as methyl groups (Pekkarinen et al., 1999). As shown in Figure 3-3, curcumin possesses the lowest number of hydroxyl (OH) groups, and consequently it exhibited poor DPPH scavenging ability. Rutin hydrate is the glycated form of quercetin, and it is believed that the added rutinose dissacharide group of rutin (compared to quercetin) serves to block hydroxyl groups present on the flavonoid backbone structure from donating hydrogen atoms which reduces its free-radical scavenging potential (de Araújo et al., 2013). This explains why rutin hydrate displayed poorer DPPH inhibition compared to quercetin. Quercetin and ascorbic acid were found to be the best DPPH inhibitors overall with ascorbic acid

showing a greater maximum inhibition than quercetin which was also found in another recent study (Rahim et al., 2017). The smaller size of ascorbic acid molecules compared to quercetin could enhance their mobility and thereby allow for easier donation of hydrogen atoms and thus be the reason for its superior level of DPPH inhibition.

All four antioxidants studied, possessed multiple hydroxyl groups along with carbonyl moieties, which meant they each possessed several sites for metal chelation (Leopoldini et al., 2006). Rutin hydrate exhibited the lowest ferrous iron chelation activity, which was found to be significantly lower than the closely structurally related quercetin; a finding which was echoed in another recent study (Yi et al., 2017). Rutin hydrate possesses one less chelating site than quercetin due to the replacement of a hydroxyl group with a rutinose dissacharide group (C. Hider et al., 2001). In addition to reducing free radical scavenging activity, the presence of the rutinose group is responsible for lowering metal chelation activity through blocking access to hydroxyl groups through which chelation could occur (Jo et al., 2009). Curcumin is understood to possess three possible chelation sites, two of them being hydroxyl groups situated on either end of the molecule, and one being the di-ketone moiety in the centre of the molecule (Daniel et al., 2004). Again however, the greater number of hydroxyl groups on quercetin and ascorbic acid molecules are most likely the reason why these molecules exhibited the greatest level of Ferrozine inhibition.

3.4.2 Antioxidant concentration

The concentration of ‘antioxidant’ compounds is known to be an important factor in determining whether they possess antioxidant or prooxidant activity (Zhou and Elias, 2013). However, all four compounds in this study enhanced oxidative stability in 1%

(w/w) P20 emulsions and their ability to do so was found to be only aided with increasing concentration up to the maximum value examined. This can be seen in Figure 3-5 which shows that P20 emulsion samples exhibited consistently lower PV's and/or AV's when antioxidants were added compared to control samples (P20) in which they were not.

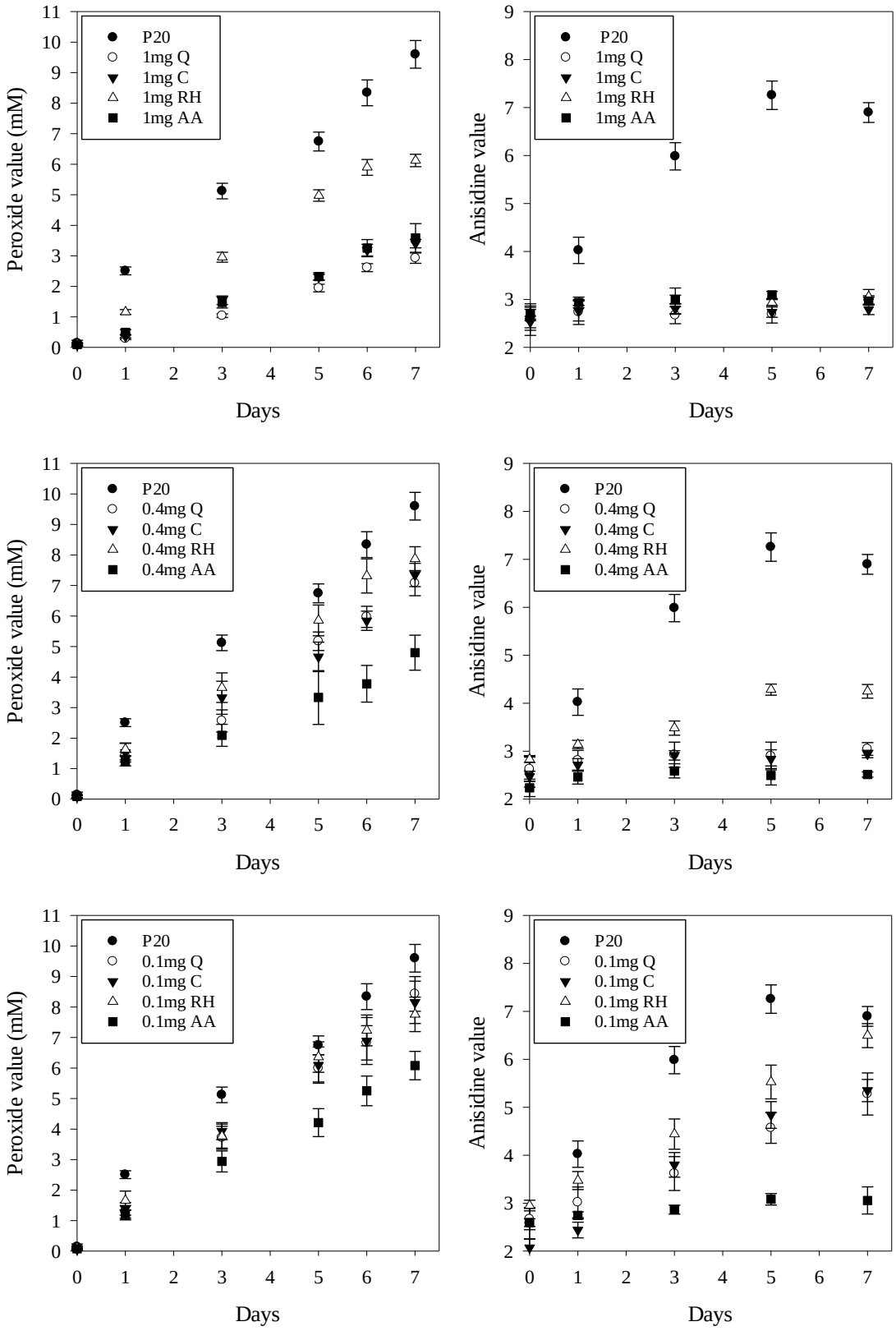

Figure 3-5: Oxidative stabilities of 1% (w/w) P20 emulsions under varying antioxidant concentrations. Where Q = quercetin, C = curcumin, RH = rutin hydrate, and AA = ascorbic acid.

The results in Figure 3-5 correlate well with earlier results in Figure 3-4. Ascorbic acid was found to be the most potent antioxidant as this was able to provide greatest oxidative stability when used at lower concentrations (added antioxidant masses of 0.4mg and 0.1mg) compared to the other compounds which makes sense as this compound was found to be the most potent of the four investigated in terms of its DPPH and Ferrozine inhibition. Interestingly, although curcumin was found to cause significantly lower DPPH and Ferrozine inhibition than quercetin it still exhibited near-identical levels of PV's and AV's compared to quercetin at all tested antioxidant concentrations. This is likely due to curcumin's highly non-polar nature, allowing it to partition more towards the oil phase and oil-water interface where hydroperoxides are predominantly located; and is the main location for LO reactions to occur in O/W emulsions (McClements and Decker, 2000). Therefore, although harbouring lower antioxidant activities than quercetin, it could be that the more effective positioning of curcumin molecules within these emulsions (due to its reduced polarity) was able to make up for this deficit. This is in agreement with the widely reported 'polar paradox' theory which states that non-polar molecules are more effective in aqueous (polar) systems due to their positioning at the oil-water interface and *vice-versa* (Shahidi and Zhong, 2011). Therefore, increased hydrophobicity is perhaps also why quercetin combatted LO more effectively than rutin hydrate, in addition to its superior antioxidant potency displayed in Figure 3-4. Furthermore, the smaller molecular size of quercetin (molecular weight 302g/mol) compared to rutin hydrate (molecular weight 611g/mol) would allow it to locate more efficiently at the oil-water interface leading to greater antioxidant concentrations at the primary site of oxidative reactions (Yi et al., 2017).

3.4.3 Iron concentration

Metal contaminants are common in water (Yang et al., 2015), and all food-grade oils are known to contain a degree of iron and other prooxidant metals (Villière et al., 2005). Even trace quantities (< ~10 parts per billion) of these prooxidant metals within emulsions is thought to be sufficient to have a significant impact on oxidative stability (Mozuraityte et al., 2016), particularly in the presence of antioxidants. Ferrous iron (in the form of ferrous sulphate heptahydrate (FSH)) was chosen as the metal contaminant in these experiments as it is one of the most common, prooxidant and important transition metals in determining LO within O/W emulsions (Waraho et al., 2011). Results are displayed in Figure 3-6.

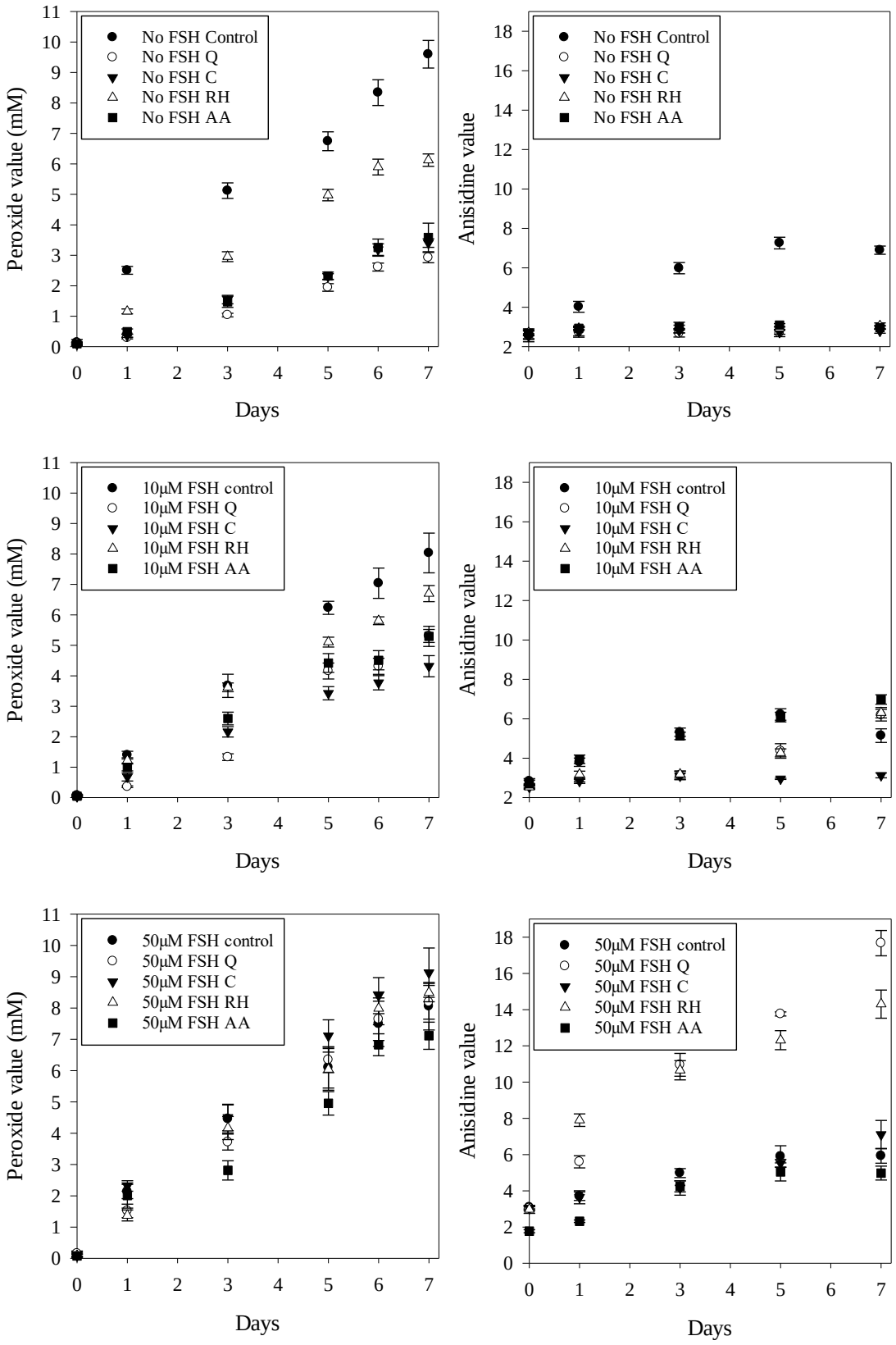

Figure 3-6: Oxidative stabilities of emulsions containing 1mg antioxidant under varying FSH concentrations. Where Q = quercetin, C = curcumin, RH = rutin hydrate, and AA = ascorbic acid.

Interestingly, control emulsions which varied only in FSH concentrations showed the lowest oxidative stability when no iron was added and no significant difference between samples containing either 10 or 50µM FSH. For example, with P20 control emulsions on day 7, as FSH concentration was increased from 0 to 10µM the PV decreased from 9.6 to 8.0mM and the AV decreased from 6.9 to 5.1. This is in contrast to a number of studies which found that the addition of iron to P20 emulsions resulted in a prooxidant effect with increasing concentration (Cengiz et al., 2019, Yi et al., 2016). This is possibly because P20 is known to harbour significant quantities of peroxides (Mancuso et al., 1999), which can build up over prolonged periods of storage or, in the case of this study, through emulsion storage at 40°C for 7 days. A study investigating the oxidation of alpha-tocopherol in surfactant micelles (Mancuso et al., 1999) found that addition of higher iron concentrations (50-250µM) caused decomposition of peroxides in P20 samples. This would explain the reduced PV's and AV's in P20 control emulsions with increased FSH concentration from 0 to 10 or 50µM. The reduced AV's with increased iron concentrations from 0 to 10 or 50µM were also observed in a study which assessed the oxidative stability of methyl linoleate dispersions in different emulsion environments (Nuchi et al., 2001). When higher FSH concentrations of 100µM were used in this current study, P20 emulsions were observed to physically destabilise via phase separation after one day; hence addition of FSH could have caused P20 to be removed from the oil-water interface, physically destabilising the emulsions and also resulting in the removal of prooxidant species (particularly peroxides) with it, making FSH appear to possess a form of antioxidant activity within P20 emulsions.

When no FSH was added to 1% P20 emulsions, all added compounds caused significant reductions in PV's and AV's, enhancing oxidative stability. With the addition of 10µM

FSH, all compounds show reduced difference in oxidative stability in terms of PV's and AV's compared to the control; ascorbic acid and quercetin even showed increased AV's. At maximum FSH addition of 50µM there was little to no significant difference in PV's, however at this concentration quercetin and rutin hydrate caused large increases in AV's, illustrating their prooxidant nature under higher ferrous iron concentrations. The prooxidant nature of flavonoids such as quercetin and rutin hydrate in the presence of iron stems primarily from their possession of a catechol moiety, which becomes oxidised by ferric iron to a quinone (Rietjens et al., 2002). This results in the formation of electrophiles which act as potent prooxidants. This finding was echoed in another previous study which investigated the behaviour of quercetin in combination with iron (Osborn and Akoh, 2003). This also explains why curcumin (which was shown to be a less effective chelator of ferrous ions than quercetin or rutin hydrate through the Ferrozine assay) is able to provide greater oxidative stability in the presence of higher FSH concentrations as it does not possess a catechol group that can become oxidised. A study assessing the impact of quercetin on O/W emulsions with added ferrous ions found that the quercetin concentration needed to be high enough, relative to ferrous iron, in order to exhibit an antioxidant effect (Yi et al., 2017). Another study found that rutin acted as a potent antioxidant with the addition of no iron, but its efficacy was greatly reduced and it exhibited prooxidant behaviour with the addition of 50µM ferric chloride (Yang et al., 2015). All four antioxidants investigated would have also undergone a degree of metal-catalysed oxidation in the presence of ferrous iron causing the generation of hydrogen peroxide which may then reduce to the highly prooxidant hydroxyl radical (Zhou and Elias, 2012) which further explains their increased prooxidant nature under the addition

of FSH. From these results it is clear that the efficacy of all four antioxidants to combat LO is only hindered by the addition of ferrous iron.

It was initially hypothesised that compounds which were found more capable of chelating ferrous iron via the Ferrozine assay would therefore provide greater oxidative stability in the presence of added FSH. However, these results indicate that the prooxidant behaviour of these compounds in the presence of iron has far greater influence on LO than their antioxidant ability to chelate ferrous iron.

3.4.4 Effect of emulsifier type

The choice of emulsifier is widely regarded as one of the most important factors in determining the oxidative stability of O/W emulsions as it affects surface charge, interfacial thickness, and droplet size. These experiments specifically investigated the efficacy of four different antioxidants within emulsions formulated using different emulsifiers and assessed the reasons for this. Three emulsifiers were used in this study which were SDS (anionic), P20 (non-ionic) and CAT (cationic) surfactants and these were chosen to provide different surface charges to emulsion droplets. Droplet sizes of these formulated emulsions together with their native pH and zeta potential (ZP) values along with ZP values of the four antioxidants at the corresponding emulsion pH values are given in Table 3-1.

Emulsion	Emulsion droplet size D [3,2] µm	Emulsion pH	Emulsion zeta potential (mV)	Antioxidant zeta potential at emulsion pH (mV)			
				Quercetin	Curcumin	Rutin hydrate	Ascorbic acid
Anionic (SDS)	5.74 ± 0.20	6.94 ± 0.12	-110.0 ± 2.1	-44.1 ± 1.1	-59.7 ± 1.1	-32.8 ± 1.2	-29.4 ± 2.0
Non-ionic (P20)	5.86 ± 0.07	5.99 ± 0.07	-31.4 ± 0.2	-44.1 ± 1.3	-43.8 ± 2.8	-32.5 ± 0.4	-11.5 ± 1.5
Cationic (CAT)	6.82 ± 0.14	3.29 ± 0.10	86.0 ± 2.4	-8.6 ± 0.4	-9.1 ± 1.5	-10.4 ± 0.8	-19.9 ± 0.5

Table 3-1: Native emulsion pH values along with zeta potentials of these emulsions and antioxidants at the corresponding emulsion pH.

From Table 3-1 it can be seen that CAT caused the formation of acidic emulsions whereas SDS and P20 formed fairly neutral ones. As expected SDS and CAT exhibited strongly negative and positive zeta potential values respectively indicating their droplet charge status. P20 however also exhibited a significantly negative zeta potential in spite of its non-ionic character; this phenomenon can primarily be attributed to the presence of surface-active free fatty acids within the dispersed phase of sunflower oil which migrate to the oil-water interface and impart a negative charge (Waraho et al., 2011). In addition, OH^- ions present within these emulsions are known to preferentially adsorb onto the polar head groups of P20 (McClements, 2004) which locate themselves at the oil-water interface and impart further negative charge. All antioxidants possessed negative zeta potentials as particles which decreased under lower pH values encountered within CAT emulsions however, they constantly remained negative, which gives indication of the predominantly negative charge associated with these antioxidants within each emulsion formulation.

Oxidative stabilities of emulsions formulated with the three different emulsifiers in the presence and absence of each antioxidant are shown in Figure 3-7. In SDS emulsions,

ascorbic acid acted as a prooxidant which was illustrated through its high AV's compared to the control. This is due to the ability of ascorbic acid to reduce ferric iron (a prooxidant naturally present in sunflower oil) to the far more potent prooxidant ferrous iron (Lynch and Stoltzfus, 2003) which is then strongly attracted towards the oil-water interface due to the negative surface charge which SDS imparted. Quercetin, curcumin and rutin hydrate in SDS emulsions were all however able to exert substantial antioxidant effect in spite of possessing a negative emulsion surface charge; this is perhaps because these compounds are able to be solubilised and incorporated into SDS micelles via hydrophobic interaction which was detailed with quercetin in one study (Liu and Guo, 2006). Furthermore, even when these antioxidants are kept away from the interface, they are still able to exert antioxidant activity through other antioxidant mechanisms such as through chelation of prooxidant metals in the aqueous phase.

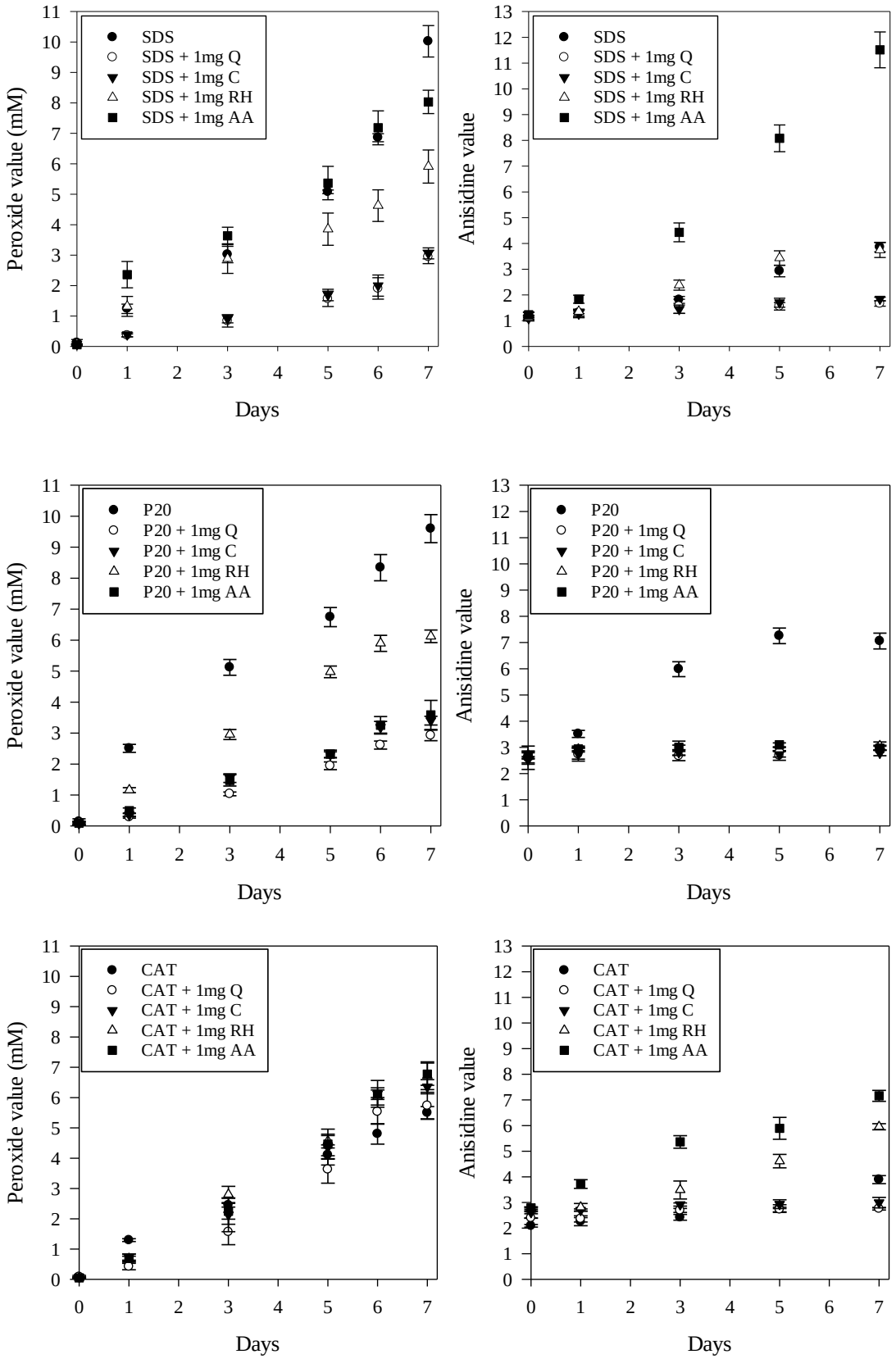

Figure 3-7: Oxidative stability of emulsions formed with different emulsifiers. Where Q = quercetin, C = curcumin, RH = rutin hydrate, and AA = ascorbic acid.

Antioxidants had either no significant effect or a prooxidant effect on CAT emulsions. This initially seemed counter-intuitive as these antioxidants possessed a negative charge so were expected to be attracted to positively charged CAT emulsion droplets and locate at the oil-water interface; however this was not the case. The lower pH of CAT emulsions meant that the solubility of ferric ions was higher (Nielsen et al., 2013), and all antioxidants used were capable of reducing ferric ions to more potent, prooxidant ferrous ions. However, again it seemed that ascorbic acid yielded the greatest potential to convert ferric iron to ferrous iron as this 'antioxidant' was found to be the strongest prooxidant within CAT emulsions.

As was seen earlier in the section on antioxidant concentration in P20 emulsions, all antioxidants were able to exhibit a significant antioxidant effect in contrast to the emulsions which used ionic emulsifiers. This is likely due to P20 emulsions possessing a more neutral pH than CAT, a lower negative surface charge than SDS and a larger polar head group which was able to situate at the oil-water interface and be able to accommodate more antioxidants within its micellar structure (Huang et al., 1997) which resulted in more antioxidants being brought to the interface where they could exert a greater antioxidant effect.

3.4.5 Effect of oil phase volume

The four antioxidants used in this study were known to differ in their polarity, which is understood to affect partitioning behaviour within emulsions. As it was widely reported that the partitioning of antioxidant molecules within emulsions has a substantial impact on their efficacy (Berton-Carabin et al., 2014, López-Martínez and Rocha-Uribe, 2018) it was of interest to understand how each antioxidant performed at combatting LO within

emulsions of different oil phase volumes. Experiments were first performed to assess the partitioning behaviour of the four antioxidants in a water-octanol mixture to obtain an indication of their preference for the polar or non-polar phase, results are displayed in Table 3-2.

Sample	**Log P**
Quercetin	1.95 ± 0.07
Curcumin	3.55 ± 0.07
Rutin Hydrate	0.40 ± 0.01
Ascorbic Acid	-1.86 ± 0.09

Table 3-2: Partition coefficients of the four antioxidant compounds studied

As can be seen from Table 3-2, quercetin and curcumin exhibited highly hydrophobic nature with Log P values >> 0, whereas ascorbic acid exhibited a hydrophilic nature. Curcumin was found to be by far the most hydrophobic molecule, and rutin hydrate showed only slight hydrophobicity with a Log P value close to 0.

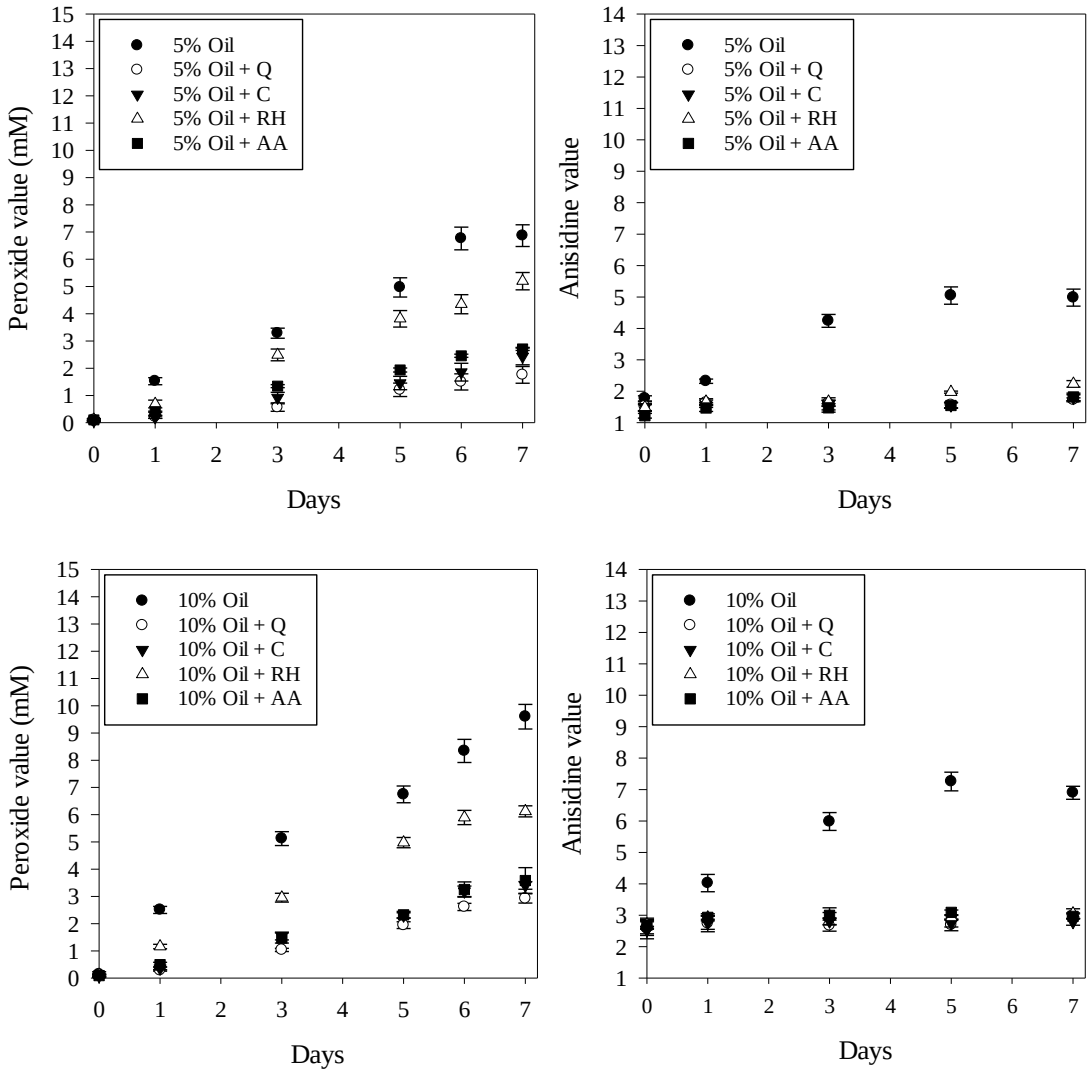

Figure 3-8: Oxidative stability of 1% (w/w) P20 emulsions with oil phase volumes of 5% and 10%. When antioxidants were used, 1mg of each were added to emulsions. Where Q = quercetin, C = curcumin, RH = rutin hydrate, and AA = ascorbic acid.

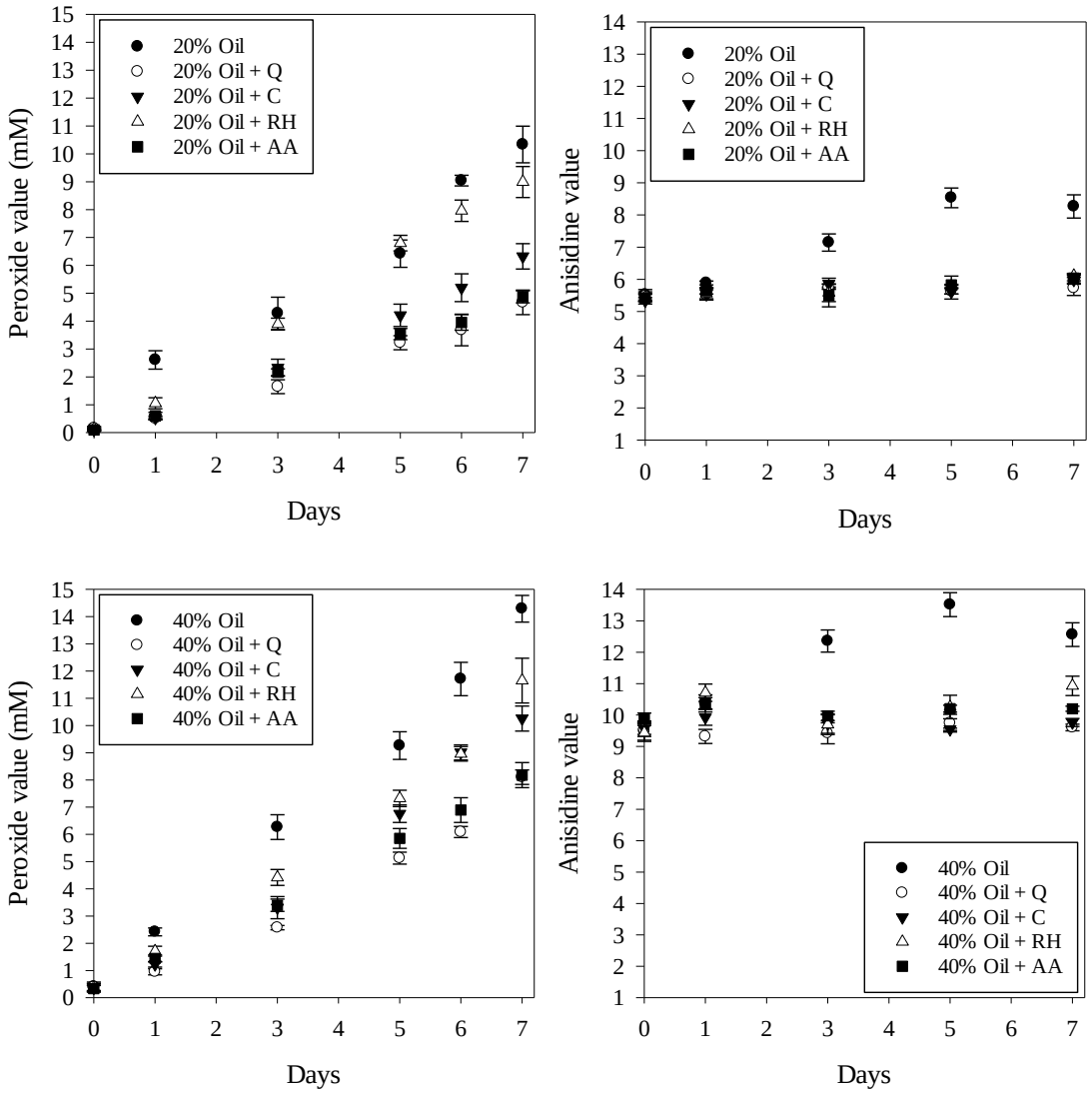

Figure 3-9: Oxidative stability of 1% (w/w) P20 emulsions with oil phase volumes of 20% and 40%. When antioxidants were used, 1mg of each were added to emulsions. Where Q = quercetin, C = curcumin, RH = rutin hydrate, and AA = ascorbic acid.

Considering emulsions created with no added antioxidants in Figure 3-8 and Figure 3-9 it can be seen that increasing oil phase volume leads to an increase in both PV's and AV's. Evidently however, looking at AV's, there is a certain quantity of secondary oxidation products contained within the sunflower oil prior to experiments being performed as on day 0 the AV roughly doubles when the oil phase volume is doubled. Therefore, it is pertinent to instead consider the increase in AV from day 0 to day 7 with each oil phase volume used which were 3.2 ± 0.4, 4.3 ± 0.2, 2.7 ± 0.3, and 3.1 ± 0.8 for 5%, 10%, 20%

and 40% oil phase volumes respectively which shows no correlation for AV's with increasing oil phase volumes in real terms. However, this is not the same for PV's which always began at around 0mM and only ended up at higher values with increased oil phase volumes which means that the overall impact of oil phase volume on LO was that it increased with increasing oil phase volume. This is because, increasing oil concentration will increase the amount of lipids available for oxidation, in addition to decreasing the separation distance between oil droplets which increases the potential for labile species (such as free radicals and hydroperoxides) on nearby oil droplets to react and propagate LO (Berton-Carabin et al., 2014). Interestingly however, other studies have reported the opposite effect, saying that increasing oil phase volume will (1) lead to the generation of larger oil droplets (as shown in this study in Table 3-3) which has been detailed to retard LO through generation of smaller oil droplet surface areas (Gohtani et al., 1999), (2) supress creaming which has been held responsible in a previous study for enhanced oxidative stability as it lowered the amount of oil droplets in contact with the air (Sun and Gunasekaran, 2009) and (3) will decrease aqueous phase volume, thereby decreasing the amount of dissolved water-soluble prooxidants such as transition metals and enhancing oxidative stability, as was noted in another study (Kargar et al., 2011b). The finding in this study that AV's roughly doubled with doubling oil phase volume confirmed that the sunflower oil used in these experiments contained significant amounts of secondary oxidation products; meaning that a significant amount of LO had taken place within this sunflower oil prior to its measurement in this study. Due to the known freshness of sunflower oil used in these experiments, it is likely that the particular type of sunflower oil used contained large amounts of prooxidants such as hydroperoxides which swiftly degraded and resulted in the generation of a significant amount of secondary oxidation

products over a limited storage time. It is therefore believed that the high amount of prooxidants contained within the sunflower oil was the main reason for the trend exhibited in this study with respect to control emulsions.

Oil phase volume (%)	Droplet diameter (μm)
5	3.9 ± 0.2
10	5.9 ± 0.1
20	8.5 ± 0.5
40	9.2 ± 0.6

Table 3-3: Droplet diameter of 1% (w/w) P20 emulsions formulated with different oil phase volumes.

The well referenced 'polar paradox' theory states that more polar antioxidants (such as ascorbic acid) are more effective in non-polar media (such as bulk oils or high oil phase volume emulsions), whereas non-polar ones are more effective in polar media (such as aqueous or high aqueous phase volume emulsions) (Shahidi and Zhong, 2011) as this helps their orientation at the oil-air/oil-water interface where LO is known to predominantly occur. In terms of AV's, the addition of antioxidants was able to prevent any significant increases compared to control emulsions over a 7-day period, and hence no differences in efficacy with oil phase volume could be established from this data. However, in terms of PV's, substantial differences could be found when antioxidants were added to emulsions with different amounts of oil. As PV's only ever increased, the

percentage reduction of PV's compared to control emulsions are given in Table 3-4 on day 7 only, as this day gave clearest indication of each antioxidants efficacy.

Antioxidant	PV reduction (%) on day 7 in:			
	5% Oil	10% Oil	20% Oil	40% Oil
Quercetin	74.4 ± 5.5	69.7 ± 2.2	54.8 ± 5.2	43.3 ± 2.3
Curcumin	64.6 ± 5.5	64.7 ± 1.8	38.8 ± 5.4	28.2 ± 3.9
Rutin hydrate	24.3 ± 5.7	36.5 ± 2.6	13.0 ± 6.6	18.5 ± 7.1
Ascorbic acid	60.6 ± 1.0	62.8 ± 6.0	52.9 ± 2.6	42.8 ± 3.9

Table 3-4: Reduction in PV's of emulsions containing different oil phase volumes and antioxidants on day 7 of LO measurement.

From Table 3-4, it can be seen that the two antioxidants with the highest Log P values (most hydrophobic), curcumin and quercetin, were able to prevent significantly more PV formation in 5% and 10% oil phase volumes than at 20% and 40% and thus behave in accordance with the 'polar paradox'. It is likely that when these highly hydrophobic molecules partition, they 'bury' themselves inside the core of oil droplets and away from the interface where LO is most prevalent; this phenomenon is further exacerbated by the larger droplet sizes with increasing oil phase volume meaning hydrophobic antioxidants are able to position even further away from the interface (deeper in the oil droplet core). This explains why the decrease in PV reduction with oil phase volume exhibits the most extreme change in the case of curcumin, as this was the most hydrophobic molecule assessed. This also explains why rutin hydrate, a molecule with both hydrophilic and

hydrophobic nature, exhibited an initial enhancement in PV reduction from 5-10% oil phase volume, followed by a decrease thereafter; as there is an optimal oil phase volume of 10% to allow for its most effective partitioning for combatting LO. As a hydrophilic molecule, ascorbic acid did not follow the opposite trend, and following the same logic it is probable that this is because water serves as the continuous phase, so even when there is less water at high oil phase volumes, there was less possibility of ascorbic acid being able to distance itself from the oil-water interface.

3.4.6 Antioxidant combinations

As shown in Figure 3-10, Quercetin-rutin hydrate emulsions were found to generally exhibit antagonistic behaviour however the effect only became statistically significant with the addition of 10µM FSH, as this caused a significant increase in AV's and no change to PV's. One study reported that the use of quercetin and rutin in combination caused a synergy in their ability to reduce ferric (Fe^{3+}) to the more prooxidant ferrous (Fe^{2+}) iron ions (Hajimehdipoor et al., 2014) which could be the reason for this antagonistic effect. This antagonism is likely to be due to quercetin harbouring higher reduction potential than rutin hydrate (Bors et al., 1995), meaning that quercetin acted as a primary antioxidant, and rutin hydrate acted as a secondary antioxidant by regenerating quercetin from its radical form; hence, as quercetin is known to reduce ferric ions to the more potent prooxidant ferrous ions more effectively than rutin hydrate, this causes an antagonistic effect on oxidative stability. Curcumin-rutin hydrate emulsions showed only additive behaviour in combination which likely means these compounds did not interact with each other which is perhaps because they share similar dominant antioxidant mechanisms.

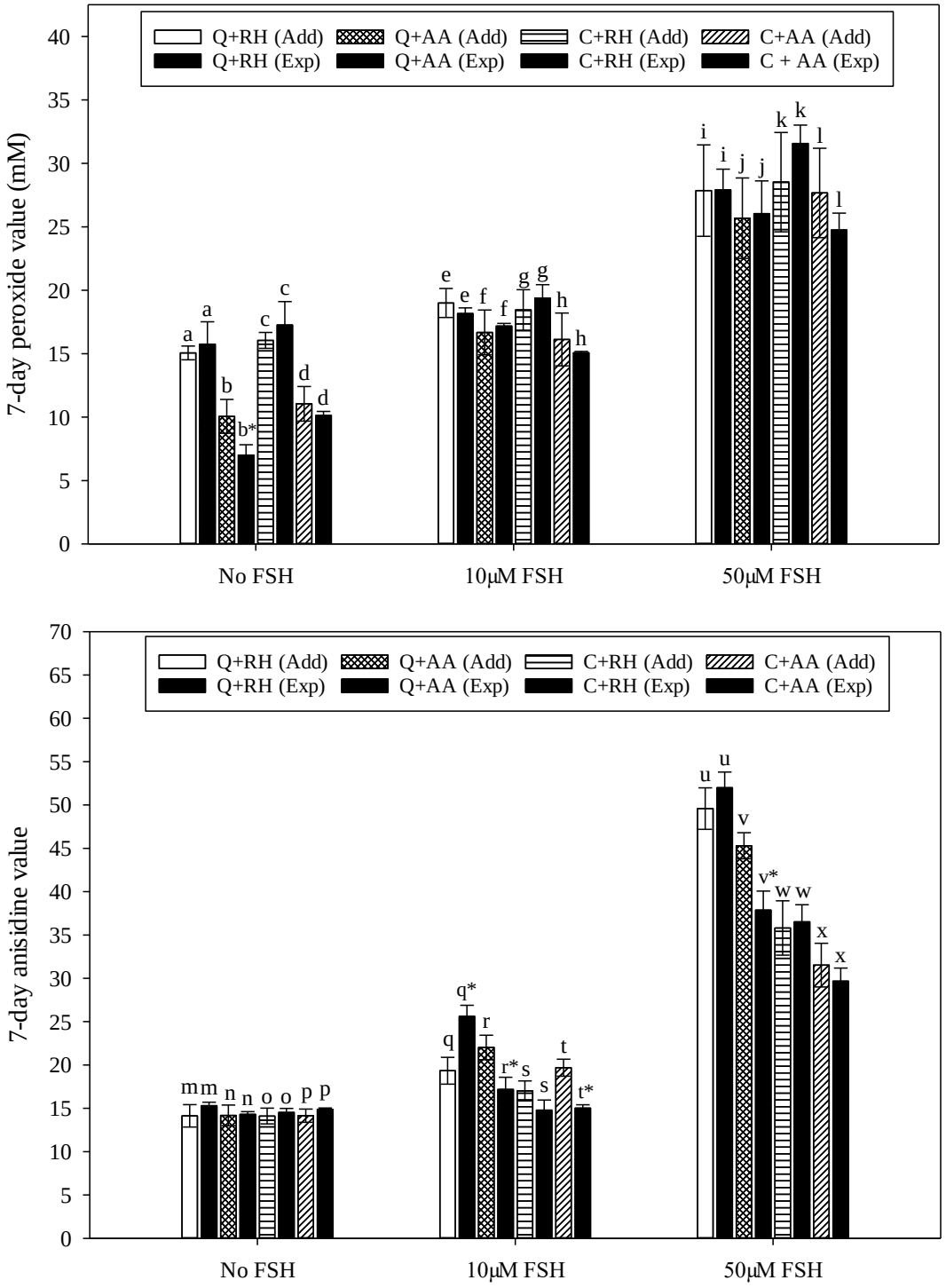

Figure 3-10: Effect of antioxidant combinations (500µg of each antioxidant added) on oxidative stability. Experimental values given to the right of additive (predicted) values as solid black bars. Where Q = quercetin, C = curcumin, RH = rutin hydrate, and AA = ascorbic acid. Letters with an asterisk (*) denote a significant difference ($P < 0.05$) between the experimental and additive values (but differences between different antioxidant combinations are not labelled).

Quercetin-ascorbic acid mixtures acted synergistically in combatting LO at all FSH concentrations, significantly increasing either PV's or AV's; and curcumin-ascorbic acid emulsions showed synergism in the presence of 10μM FSH with a significant decrease in experimentally obtained AV's compared to predicted additive values. Ascorbic acid has been reported to regenerate quercetin from its oxidised quinone structure through reducing it, and is widely reported to possess a protective/enhancing effect on polyphenolic compounds (Inoue et al., 2006, Skaper et al., 1997) such as quercetin and curcumin. However, as earlier results showed that ascorbic acid was able to combat LO either at least as effectively, if not more effectively than quercetin and curcumin this cannot be the reason for the synergy. Furthermore, as quercetin and ascorbic acid were shown to perform similarly in terms of their abilities to chelate ferrous via Ferrozine inhibition, it is likely that their synergism is owed to the fact that their different antioxidant strengths lie with mechanisms other than free radical scavenging or metal chelation. One study showed that ascorbic acid was capable of quenching singlet oxygen more effectively than quercetin (Fatima et al., 2016), whereas another concluded that quercetin was more effective at inhibiting lipoxygenase than ascorbic acid (Silva et al., 2000). Therefore, through combining antioxidants with different antioxidant mechanistic strengths, it is possible that a synergistic effect will occur as one antioxidant can account for the mechanistic shortfall of the other and enhance their overall effectiveness. In addition, it is also likely that the different physical properties of compounds, in particular polarity, will help multiple antioxidants locate in different locations and hence be able to more effectively combat LO throughout the entire emulsion matrix.

3.5 Conclusions

This study has shown the efficacy of four natural antioxidants to enhance oxidative stability of O/W emulsions under a range of different emulsion environments. In P20 emulsions with no added ferrous ions, ascorbic acid and quercetin were found to serve as the most potent antioxidants which was in line with what initial DPPH and Ferrozine assays predicted. Curcumin however was found to reduce the formation of primary and secondary oxidation products much more effectively than rutin hydrate, despite rutin hydrate being more effective at inhibiting DPPH and this was attributed to the highly hydrophobic nature of curcumin enabling more effective partitioning behaviour. The prooxidant effect of ferrous iron on these four antioxidants was concluded to be of far greater importance to these compounds than their ability to chelate ferrous iron as they all lost their antioxidant activities at higher ferrous iron concentrations. Antioxidants performed less effectively in emulsions stabilised by ionic compared to non-ionic surfactants which was believed to be due to a variety of reasons including changes in emulsion pH and a reduced antioxidant presence at the oil-water interface. Higher emulsion oil phase volumes were found to promote LO and reduced the efficacy of antioxidants, particularly highly hydrophobic ones, which was believed to be due to these compounds partitioning deep within oil droplets where they could not function as effectively at combatting LO. Synergy between compounds in combatting LO was exhibited when ascorbic acid was combined with either quercetin or curcumin; a finding attributed to different compounds performing particular antioxidant mechanisms more effectively than the other and hence making up for the antioxidant deficiencies of the partnering compound. Ultimately, the work in this chapter has shown how key formulation parameters impact upon the efficacy of common, naturally occurring

antioxidant compounds and thus will be highly useful in assessing their suitability for specific food applications.

CHAPTER 4: THE USE OF RUTIN HYDRATE PICKERING PARTICLES TO PROVIDE DUAL-PURPOSE FUNCTIONALITY WITHIN O/W EMULSIONS

Data and discussions from within this chapter have been published in:

Noon, J., Mills, T. B. & Norton, I. T. 2020. The use of antioxidant rutin hydrate Pickering particles to combat lipid oxidation in O/W emulsions. Journal of Food Engineering, 274, 109830.

4.1 Abstract

This chapter of work assessed the dual-purpose use of rutin hydrate (RH) Pickering particles to provide O/W emulsions both with physical and oxidative stability. The main hypothesis of this work was that antioxidant RH Pickering particles would be able to locate at the oil-water interface (which is known to be the primary site of action of lipid oxidation (LO) reactions within O/W emulsions) where they could use their antioxidant properties to effectively combat LO whilst simultaneously providing physical emulsion stability.

Results showed that formulated RH emulsions were physically stable for at least 14 days. The oxidative stability of RH emulsions was assessed in comparison to conventional emulsifiers polysorbate 20 (P20), whey protein isolate (WPI) and sodium dodecyl sulphate (SDS) in terms of each emulsifiers ability to combat lipid oxidation (LO) in emulsion samples. RH emulsions were found to combat LO more effectively than P20 and SDS in the absence of added ferrous iron; however the oxidative stability of RH emulsions greatly decreased with the addition of iron and this was attributed to the prooxidant nature of RH particles in the presence of higher iron concentrations. With high consumer demand for the removal of synthetic ingredients from food products, it is important that this study has shown the capability of RH, a natural antioxidant, to provide emulsions with both physical and oxidative stability.

4.2 Introduction

There is tremendous current interest in the use of food-grade Pickering particles for emulsion formulation, with research predominately focused on utilising particles derived from proteins, fats and starches to fulfil this purpose (Linke and Drusch, 2018). Through use of Pickering particles it has been possible to produce emulsions with unique advantages, such as excellent resistance to droplet coalescence and Ostwald ripening; making them highly desirable for a wide range of food applications. However, there has yet been limited research conducted to investigate the use of natural antioxidant particles such as flavonoids for emulsion formulation. Natural antioxidant Pickering particles used in O/W emulsions possess the potential to provide dual-purpose functionality to emulsions by providing them with both physical stability through acting as conventional Pickering particles, as well as oxidative stability through utilisation of their various antioxidant mechanisms, including their non-conventional antioxidant ability to form a thick interfacial barrier on the surface of oil droplets to safeguard the lipid phase from oxidative attack. In this study, rutin hydrate, a potent antioxidant flavonoid found widespread in nature (Luo et al., 2012) was investigated for this purpose.

4.3 Materials and methods

4.3.1 Materials

Distilled water was used as the continuous phase in all emulsions. This was obtained by pumping water through a reverse osmosis unit followed by milli-Q water system prior to usage. A large batch of consumer grade sunflower oil was purchased from a local Aldi supermarket and was used as the dispersed phase in emulsions throughout this study. Whey protein isolate (W994, S-493391) was obtained from Kerry Ingredients. The WPI had the following composition: 91.0% protein, 4.0% moisture, 3.5% ash, 1.0% fat, and

0.5% lactose. Polysorbate 20 was obtained from Acros Organics. Sodium dodecyl sulphate (> 99%), ethanol (≥ 99.8%), methanol (≥ 99.9%), butan-1-ol (≥ 99.9%), propan-2-ol (≥ 99.5%), iron (II) sulphate heptahydrate (≥ 98%), ammonium thiocyanate (≥ 97.5%), 2,4-decadienal aldehyde (85%), anhydrous barium chloride (≥ 97%), hydrochloric acid (37%) and glacial acetic acid (≥ 99.7%) were obtained from Fisher Scientific. Rutin hydrate (≥ 94%) and para-anisidine (99%) were obtained from Sigma Aldrich. Xanthan gum (MSK-0501) was obtained from MSK specialist food ingredients. Isooctane (> 98%) was provided by VWR international. Cumene hydroperoxide (80%) was provided by Scientific Laboratory Supplies Ltd.

4.3.2 Size reduction of rutin hydrate particles

Size reduction of RH particles was necessary in order to formulate stable emulsions and this was achieved via a dispersion-sonication route. Raw RH particles (initial particle size of 13.1 ± 0.4μm (D [3,2])) were added to 90 g of distilled water, heated to 50 °C and agitated via magnetic stirring for 30 minutes to encourage particle dispersion. Then the RH dispersion was placed in an ice bath (to avoid overheating) and sonicated using a high intensity ultrasonic vibracell processor (operating at 95% amplitude, 20 kHz and 700W) for 3 minutes.

4.3.3 Emulsion formulation

4.3.3.1 Surfactant emulsions

The desired concentration (either 0.01, 0.1 or 1% (w/w)) of P20, WPI or SDS were added to distilled water to make 90g and mixed under magnetic stirring at room temperature for 15 minutes to ensure total surfactant dissolution. 10g of sunflower oil was added to the aqueous surfactant phase (to make a 10% (w/w) oil phase volume O/W emulsion) and

the mixture was emulsified using a Silverson L5M high shear mixer using a fine emulsion screen, 57mm diameter head, and a homogenisation speed of 7000rpm for 5 minutes.

4.3.3.2 Rutin hydrate emulsions

The desired concentration (either 0.5, 1, or 1.5% (w/w)) of size-reduced RH (particle size of 1.2 ± 0.1μm (D [3,2])) obtained as outlined in Section 4.3.2) was added to distilled water to make 90g total weight. If necessary, the pH was adjusted using hydrochloric acid from native pH 5.74 to pH 5.00, 4.00, 3.00 or 2.00. 10g of sunflower oil was added to the dispersion and the mixture was emulsified using a Silverson L5M high shear mixer using a fine emulsion screen, a 57mm diameter head, and a homogenisation speed of 7000rpm for 5 minutes. If desired, iron sulphate heptahydrate (0.1mM) was also added post-emulsification.

To assess the impact of creaming, 0.2% (w/w) xanthan gum was added to emulsions post-emulsification and the mixture was stirred for 30 minutes at a temperature of 50°C (to ensure total dissolution of the xanthan gum).

To assess the impact of RH location, for emulsions in which RH was located primarily at the interface, a 1.5% (w/w) RH emulsion was formulated as stated previously and added to another 90g of distilled water. For emulsions in which RH was located primarily in the aqueous phase a 0.5% (w/w) RH emulsion was formulated as stated previously and this was added to a 90g 1% (w/w) RH dispersion in water. Different concentrations of iron sulphate heptahydrate (either 0.00, 0.02 or 0.10mM) were then added post-emulsification.

4.3.4 Effect of droplet size on lipid oxidation

The droplet size of 0.1% (w/w) SDS (aqueous phase) O/W emulsions (10% (w/w) oil phase volume) was modified through varying the speed of the rotor during high-shear

mixing. A mixing time of 5 minutes was coupled with high shear mixing speeds of 7000, 4500, 3000 and 2000rpm to produce emulsions of Sauter mean diameter droplet sizes 7.5, 11.4, 22.6 and 33.6µm respectively. Lipid oxidation measurements were then carried out as detailed in Section 4.3.8. From this data, linear regression was used to relate average Sauter mean diameter emulsion droplet sizes to quantities of primary/secondary oxidation products generated. Using these relationships, it was possible to create 'correction factors' for each emulsion formulated with different emulsifiers, emulsifier concentrations, pH levels (from native pH 5.74 to pH 2.00), and droplet sizes to account for differences in oxidative stability caused by emulsion droplet sizes. This worked by applying a correction factor of 1 to the emulsion encountered in this study with the lowest droplet size (1% (w/w) P20 emulsions at 5.7 µm Sauter mean droplet diameter) and any other emulsion created had its peroxide and anisidine value multiplied by a correction factor (obtained using the linear regression data) to eliminate the effects of droplet size from the system. Single factor ANOVA was used to assess statistical difference between measurements, a probability value of < 0.05 was deemed as significant and when this was the case, a post hoc t-Test was performed to assess between which specific measurements this significant difference occurred.

4.3.5 Size measurement

The Sauter mean diameter (D [3,2]) and size distributions of RH particles and emulsified oil droplets were calculated using a Mastersizer 2000. It was ensured that the Mastersizer was measuring >77% laser light transmittance prior to its operation. The stirring speed for all size measurements was selected at 1300rpm and sample was added via pipetting until laser obscuration reached a value of 5%. Refractive index values of sunflower oil (1.47) were selected for all emulsions. Single factor ANOVA was used to assess statistical

difference between measurements, a probability value of < 0.05 was deemed as significant and when this was the case, a post hoc t-Test was performed to assess between which specific measurements this significant difference occurred.

4.3.6 Dynamic interfacial tension measurements

Dynamic interfacial tension (IFT) measurements were conducted using a K100 Kruss tensiometer and Wilhelmy plate method. Experiments were conducted on distilled water-sunflower oil systems with different emulsifiers/concentrations and on control samples with no emulsifier. All experiments were conducted at room temperature. Measurements were performed for 5000 seconds to ensure equilibrium values of IFT had been reached.

4.3.7 Polarised light microscopy

Polarised light microscopy was used to visualise RH particles within formulated emulsions via a Leica DM2500 LED microscope. Images were taken at 10x and 40x magnifications.

4.3.8 Lipid oxidation study

The lipid oxidation study was conducted using the same methodology as that described in Section 3.3.7.

4.3.9 Statistical analysis

All experiments were carried out in triplicate, with error reported as plus/minus a standard deviation unless otherwise stated. Any additional statistical analysis is detailed within individual methodology descriptions.

4.4 Results and discussion

4.4.1 Size reduction of rutin hydrate particles

Preliminary experiments had shown that the use of RH as an emulsifier in its raw form produced emulsions which were unstable and phase separated after a very short time (< 1hour). Therefore, raw RH particles were size reduced from 13.1 ± 0.4μm to 1.2 ± 0.1μm prior to emulsification via the dispersion-sonication method. Further experiments showed that size-reduced RH was able to produce O/W emulsions which were physically stable for a period of at least 14 days. Therefore, size-reduced RH particles were used for all experiments involving RH in this chapter of work.

4.4.2 Interfacial tension

Interfacial tension (IFT) between oil and water phases was evaluated for the range of different emulsifiers studied. Figure 4-1 shows that sonicated RH was able to reduce the IFT between sunflower oil and water from 24.9 ± 0.1mN/m to 19.6 ± 0.2mN/m, although the reduction of IFT was not concentration dependent within the range used. This reduction in interfacial tension was most likely due to the partial solubilisation of RH by the aqueous phase which created free RH molecules that diffused to the oil-water interface and lowered IFT. Therefore, it appears that RH can stabilise emulsions via both a steric stabilisation mechanism as well as through a reduction of IFT. Using conventional emulsifiers P20, WPI, or SDS, at concentrations of either 0.1% or 1% (w/w) caused a significant reduction in interfacial tension.

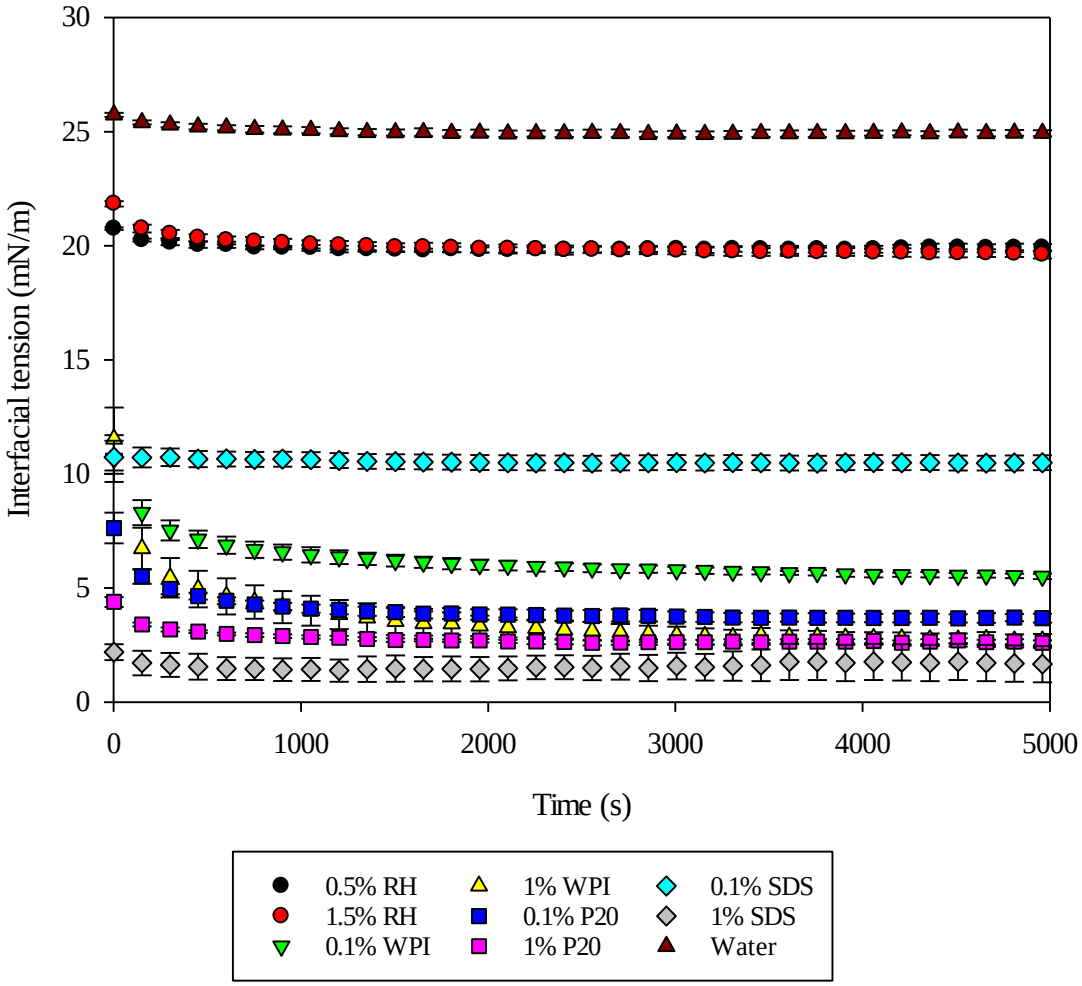

Figure 4-1: Dynamic IFT values of various emulsifiers at different concentrations.

4.4.3 Droplet size and physical stability of emulsions

The effect of emulsifier type and concentration on droplet size over a 14-day period is shown in Figure 4-2 (N.B. the scale on each graph is different). Using solely RH stabilised emulsions, with RH concentrations from 0.5%-1.5% (w/w) it was possible to produce emulsions which were physically stable for at least 14 days, as no significant droplet growth occurred during this period. This is because Pickering emulsions are known to possess excellent levels of physical stability, as particles situated at the interface reduce the possibility of droplet coalescence (Yang et al., 2017a). With increasing RH

concentration from 0.5%-1% (w/w) there was a significant reduction in average droplet size with initial sizes dropping from 21.3-11.0μm on day 0, which is attributed to a greater number of particles being available to stabilise a larger interfacial area. Interestingly however, at RH concentrations exceeding 1% (w/w) RH, particle concentration appears to no longer be a limiting factor in determining average droplet size and therefore other parameters, such as emulsification technique, would need to change to induce further size reduction.

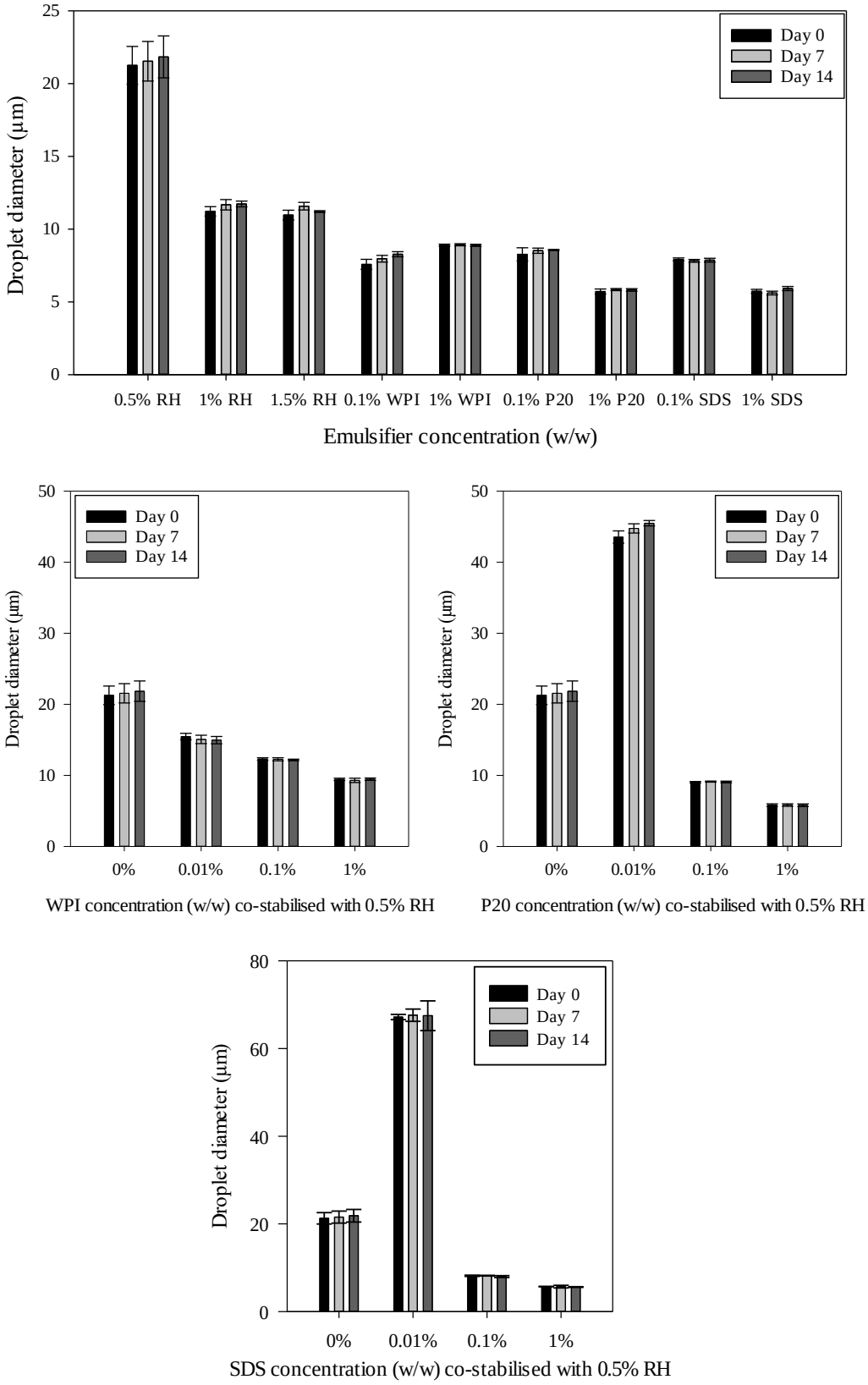

Figure 4-2: Droplet sizes over a 14-day period for a range of emulsifiers/co-stabilisers and concentrations. No significant differences ($P < 0.05$) between day 0, 7 and 14 measurements were found with any samples.

When used solely, conventional emulsifiers P20, WPI, and SDS were all able to form relatively stable emulsions at concentrations of 0.1% and 1% (w/w), however it was found that 0.01% (w/w) concentrations of any of these surfactants was insufficient to prevent almost immediate phase separation. Increasing P20 and SDS concentrations from 0.1-1% (w/w) caused a significant reduction in droplet size, due to a reduction in interfacial tension (as shown previously in Figure 4-1) which allowed for greater droplet break-up during emulsification. However, the same concentration increase for WPI did not share this effect and instead resulted in a slight increase in droplet size which could have been due to both the slower adsorption of bulkier WPI molecules (compared to P20/SDS) as well as the presence of lipids in the WPI powder which caused a destabilising effect on adsorbed proteins at the oil-water interface (Wilde et al., 2003) and consequently the formation of larger oil droplets.

The use of RH particles as a co-stabiliser with the other surfactants was investigated to see if this could impart a synergistic effect on emulsion formulation; with P20, WPI, and SDS lowering IFT to allow for the creation of smaller droplets upon which RH particles could locate and enhance coalescence and oxidative stability (which would be assessed later). Indeed, proteins such as WPI are known to bind to flavonoids such as RH (Arts et al., 2002), therefore it was hoped that these two emulsifiers would work in harmony. However, it was found in all cases that using surfactant concentrations of over 0.1% (w/w) resulted in the formation of emulsions of near identical sizes to those in which there was no RH at all, and only surfactant present. This finding was echoed in a previous study into O/W emulsions which were co-stabilised using silica Pickering particles and Tween 60 surfactant (Pichot et al., 2010); the finding was attributed to Tween 60 displacing silica particles at high Tween 60 concentrations and after a prolonged period these emulsions

were found to contain sedimented Pickering particles in the serum phase of the emulsion, which was also found to be the case when 0.5% RH co-stabilised with 1% (w/w) SDS was used in this current study.

Polarised light micrographs in Figure 4-3 clearly show the presence of partially crystalline RH particles (which appear as shiny blue particles) at the oil-water interface in emulsions stabilised solely by 0.5% (w/w) RH particles, and then conversely show none of these particles present at the interface when WPI surfactant concentrations of 0.1% (w/w) were used as a co-stabiliser; instead these particles now exist almost solely in the aqueous phase. Furthermore, as shown in Figure 4-2, when 0.01% (w/w) concentrations of WPI co-stabiliser were used, there was a significant reduction in droplet size from that of emulsions solely stabilised by RH particles, and at the same time it was found that RH particles were still present at the oil-water interface. This is likely because, 0.01% (w/w) WPI alone is unable to stabilise O/W emulsions and is unable to form a tight barrier around emulsion droplets or displace RH particles from the oil-water interface. However, even a concentration of 0.01% (w/w) WPI was able to significantly reduce IFT which is why there was still a significant reduction of droplet size using 0.01% WPI with 0.5% RH (w/w) emulsions as the RH was then able to sterically-stabilise formulated droplets in synergistic action with low concentrations of WPI. It should be noted however, that even at this low WPI concentration, visually it was observed that there were many more sedimented RH particles than emulsions in which there was no WPI; meaning even at 0.01% (w/w) WPI concentration RH was prevented from locating at the oil-water interface to some degree and there appears little synergy between these two emulsifiers in terms of providing physical stability. Using 0.01% (w/w) P20 or SDS with 0.5% (w/w) RH led to an increase in droplet size compared to using solely RH. This could be because,

a 0.01% (w/w) P20 or SDS concentration is enough to cause a significant reduction in interfacial tension (compared with 0%), meaning smaller droplets were formulated during emulsification, however these droplets could not effectively be covered by such low emulsifier concentrations and this made the system more prone to coalescence, a view which was echoed in another recent study (Zafeiri et al., 2017). Ultimately, there appears to be no synergy between RH and any tested surfactant in this study, with the surfactants seemingly behaving only to block or displace RH particles from locating at the oil-water interface.

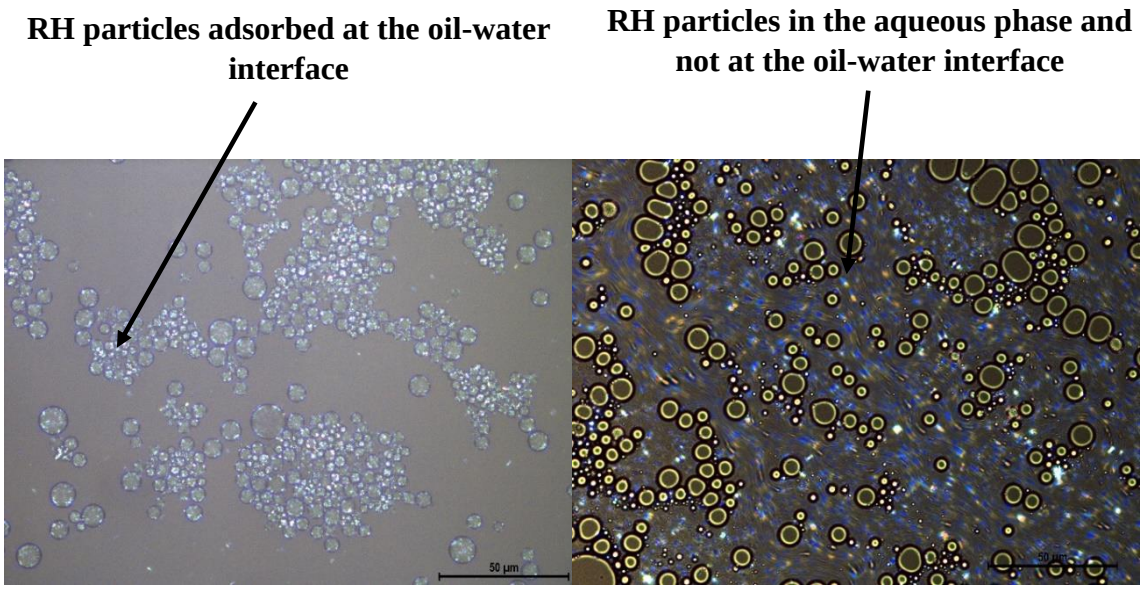

Figure 4-3: Polarised light micrographs showing 0.5% RH (left) and 0.5% RH with 0.1% WPI co-stabiliser (right).

4.4.4 Oxidative stability of emulsions

4.4.4.1 Effect of droplet size

LO is a process which is known to be accelerated through reactions which take place at the oil-water interface within emulsions (McClements and Decker, 2000). Therefore, the first step in this oxidative stability study was to quantify the impact of droplet size on LO

as this directly impacts droplet interfacial area and isolating this effect would then allow other factors, such as emulsifier type and concentration, to be assessed more independently. Figure 4-4 shows the effect of droplet size on the amounts of primary and secondary oxidation products formed on different days.

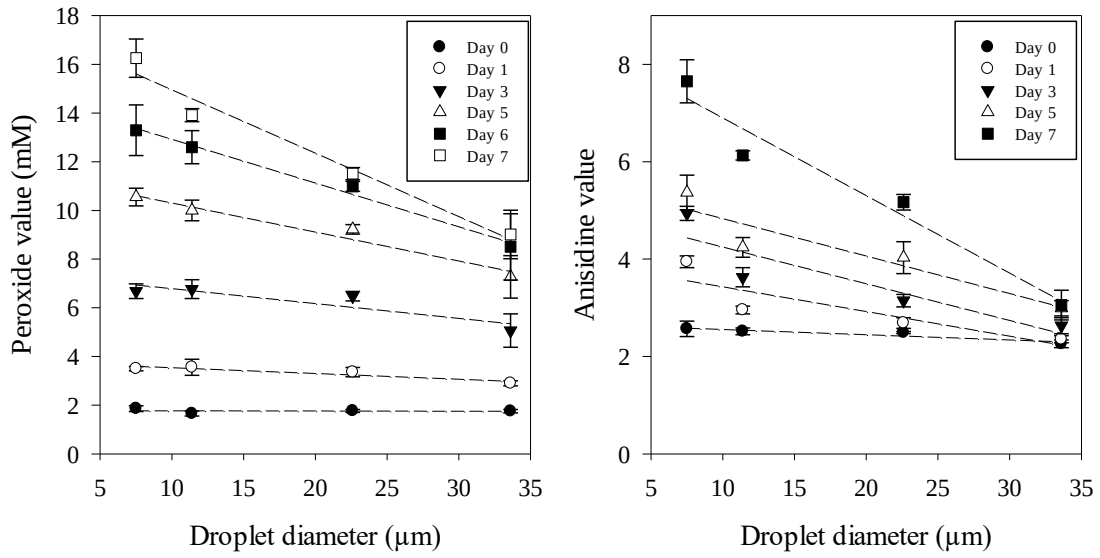

Figure 4-4: Effect of droplet size on the amount of primary and secondary oxidation products generated on different days with 0.1% (w/w) SDS stabilised emulsions.

Graphs for the peroxide and anisidine values in Figure 4-4 show that droplet size has a significant effect on the oxidative stability of emulsions, with larger droplet sizes offering superior oxidative stability. This is because as droplet size is decreased, there is an increase in the surface (interfacial) area of oil droplets. It is also clear from this data that the effect of droplet size is amplified with time following emulsion formulation. Therefore, for all following LO results in this study, a correction factor has been applied to formulated emulsions which adjusted peroxide and anisidine values so that droplet size effects were negated. To calculate correction factors, linear regression was performed to obtain a relationship between number of days and PV's/AV's. Table 4-1 shows the linear

regression constants used. Table 4-2 and Table 4-3 show a list of correction factors used for PV's and AV's respectively for each emulsion formulation examined.

Peroxide values						
Day	**0**	**1**	**3**	**5**	**6**	**7**
m	-0.001	-0.024	-0.061	-0.120	-0.180	-0.260
c	1.778	3.774	7.390	11.505	14.717	17.557
Anisidine values						
Day	**0**	**1**	**3**	**5**	**7**	
m	-0.011	-0.051	-0.076	-0.077	-0.160	
c	2.661	3.937	5.003	5.606	8.500	

Table 4-1: Linear regression curve constants for data showing the effect of droplet size on oxidation products in Figure 4-4 where m is the gradient and c is the y-intercept in the linear curve with equation $y = mx + c$.

Sample	Droplet diameter (μm)	Peroxide value correction factor (Day)					
		0	1	3	5	6	7
1% P20	5.71	1.00	1.00	1.00	1.00	1.00	1.00
0.1% P20	8.27	1.00	1.02	1.02	1.03	1.03	1.04
0.1% WPI	7.58	1.00	1.01	1.02	1.02	1.03	1.03
1% WPI	8.90	1.00	1.02	1.03	1.04	1.04	1.05
0.1% SDS	7.74	1.00	1.01	1.02	1.02	1.03	1.03
1% SDS	5.91	1.00	1.00	1.00	1.00	1.00	1.00
0.5% RH	21.25	1.01	1.11	1.16	1.21	1.26	1.34
1% RH	11.23	1.00	1.04	1.05	1.06	1.08	1.10
1.5% RH	10.97	1.00	1.04	1.05	1.06	1.07	1.09
0.5% RH pH 5.74	21.25	1.01	1.11	1.16	1.21	1.26	1.34
0.5% RH pH 4.00	16.70	1.01	1.08	1.10	1.14	1.17	1.22
0.5% RH pH 2.00	16.86	1.01	1.08	1.11	1.14	1.17	1.22

Table 4-2: Peroxide value correction factors for formulated emulsions on each day.

Sample	Droplet diameter (µm)	Anisidine Value Correction factor (Day)				
		0	1	3	5	7
1% P20	5.71	1.00	1.00	1.00	1.00	1.00
0.1% P20	8.27	1.01	1.04	1.04	1.04	1.06
0.1% WPI	7.58	1.01	1.03	1.03	1.03	1.04
1% WPI	8.90	1.01	1.05	1.06	1.05	1.07
0.1% SDS	7.74	1.01	1.03	1.03	1.03	1.04
1% SDS	5.91	1.00	1.00	1.00	1.00	1.00
0.5% RH	21.25	1.07	1.28	1.35	1.30	1.49
1% RH	11.23	1.02	1.08	1.10	1.09	1.13
1.5% RH	10.97	1.02	1.08	1.10	1.09	1.12
0.5% RH pH 5.74	21.25	1.07	1.28	1.35	1.30	1.49
0.5% RH pH 4.00	16.70	1.05	1.18	1.22	1.20	1.30
0.5% RH pH 2.00	16.86	1.05	1.18	1.23	1.20	1.31

Table 4-3: Anisidine value correction factors for formulated emulsions on each day.

4.4.4.2 Effect of emulsifier type, concentration and added iron

The effects of different emulsifiers and emulsifier concentrations on LO were investigated, both in the presence and absence of added prooxidant ferrous iron. Following what was found in Section 4.4.4.1, both peroxide and anisidine values used to quantify LO from here on in use droplet size corrected values.

For emulsions with added iron, 0.1mM iron sulphate heptahydrate was added post-emulsification, this concentration was chosen as it provided an iron concentration similar to those found in commercial oils (Nnorom and Ewuzie, 2015, Szyczewski et al., 2016). Two figures are presented, Figure 4-5 details the oxidative stability of P20 and WPI emulsions, whereas Figure 4-6 shows this for RH and SDS; these graphs were separated for clarity due to the large differences in oxidative stability between P20 and WPI vs. RH and SDS, and hence, the scale on the graphs in each of these figures is different. Note that, in Figure 4-5 there is no data set for P20 emulsions with added iron, as these emulsions became unstable and partially phase separated after 1 day, with near total phase separation after 7 days.

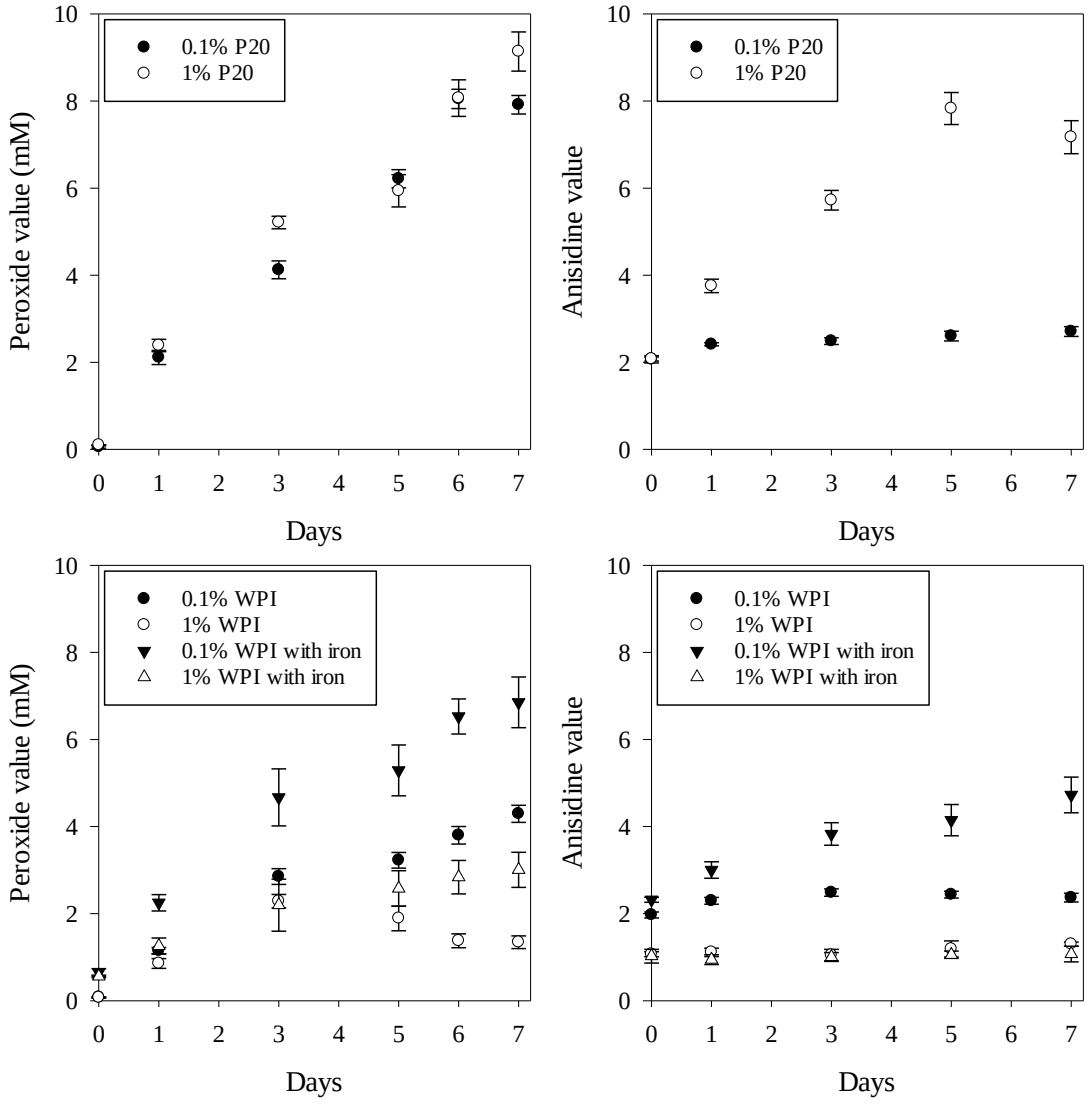

Figure 4-5: Oxidative stability (using size corrected PV's and AV's) of P20 and WPI emulsions at various concentrations with and without added iron.

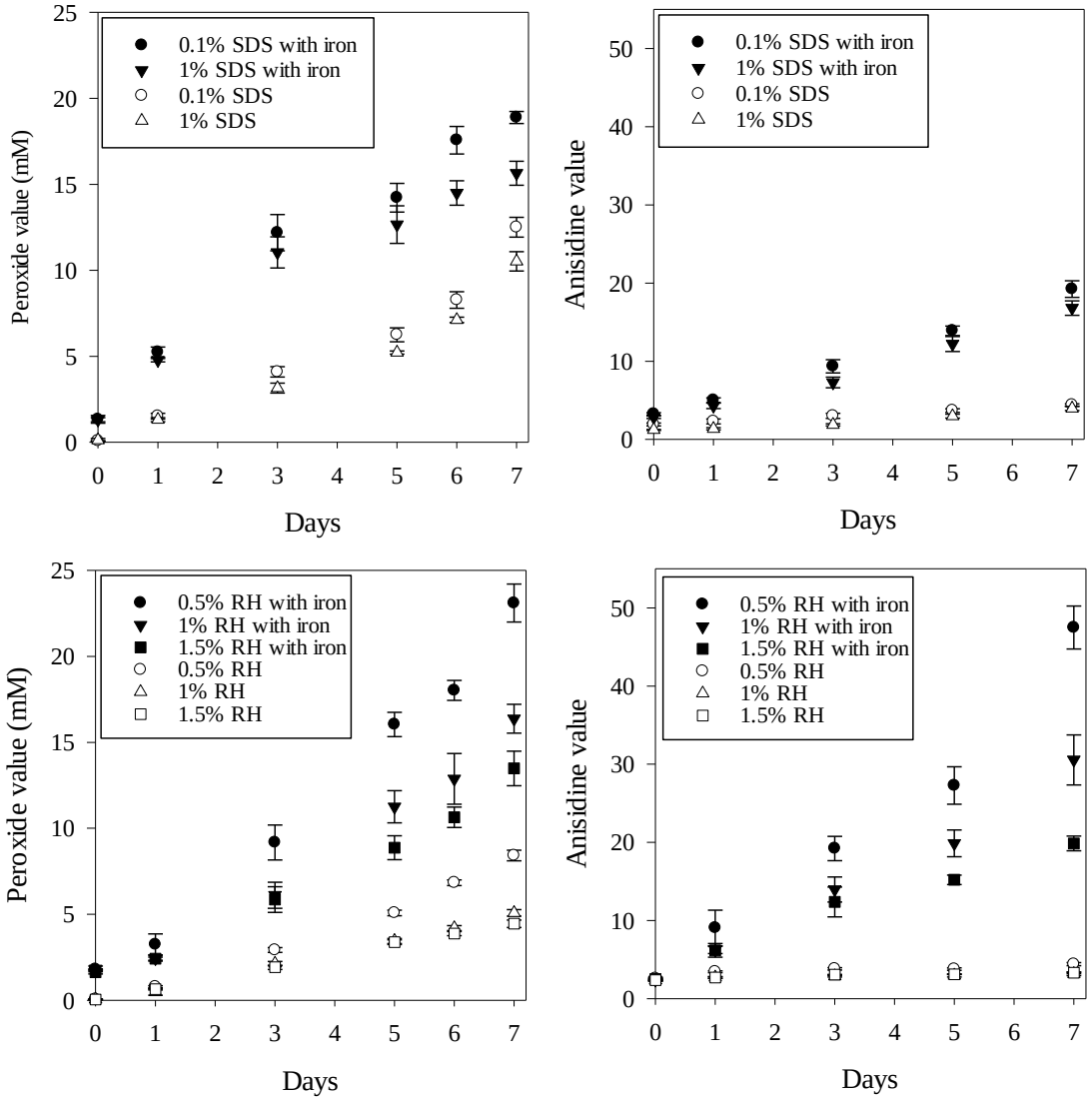

Figure 4-6: Oxidative stability (using size corrected PV's and AV's) of SDS and RH emulsions at various concentrations with and without added iron.

Making a comparison between the four different emulsifiers used in the absence of iron at 1% (w/w) concentrations in Figure 4-5 and Figure 4-6, these emulsifiers can be ranked in terms of their oxidative stability which was in the order of WPI > RH > SDS > P20 (ranking made in terms of PV and AV levels over the 7-day period). P20 emulsions exhibited the poorest overall oxidative stability under these conditions. P20 emulsions were also found to exhibit decreased oxidative stability with increased concentration from

0.1-1% (w/w), as although there were no major changes in PV's there were major changes in AV's. Results in Chapter 3 (Table 3-1) showed that although P20 is a non-ionic surfactant, it still harboured a significant negative zeta potential and therefore by increasing its concentration this could enable greater attraction of positively charged prooxidants to the oil-water interface and thus promote LO in this way. Furthermore, surfactants such as P20 are known themselves to contain prooxidant hydroperoxides (Nuchi et al., 2001); indeed one previous study found that P20 contained 35µmol of peroxide/g of surfactant which was substantially higher than other surfactants investigated including polysorbate 40, polysorbate 60, Brij 10 and Brij 35 (Mancuso et al., 1999). Therefore, increased P20 concentrations would have likely resulted in decreased oxidative stability due to both possession of a negative zeta potential and increased levels of peroxide prooxidants which would decompose relatively quickly into secondary oxidation products.

SDS emulsions also exhibited poorer oxidative stability than RH and this can primarily be attributed to the fact that it is an anionic surfactant, meaning that emulsion droplets harboured a highly negatively charged oil-water interface which served to attract positively charged prooxidant transition metals in the aqueous phase to the surface of oil droplets where they could react with hydroperoxides and accelerate the LO process. Interestingly, when the concentration of SDS were increased from 0.1-1% (w/w), there was little change in PV's or AV's in the absence of iron. This is likely because increasing SDS concentration will have opposing effects, firstly it will increase the negative surface charge of emulsion droplets, accelerating LO; on the other hand it is believed that high SDS concentrations can lead to the formation of negatively charged micelles in the aqueous phase which will attract prooxidants, thereby holding them away from oil

droplets (McClements and Decker, 2000). In addition, higher SDS concentrations provide tighter surfactant packing at the oil-water interface which enables enhanced shielding of oil droplets from prooxidants in the aqueous phase

In the absence of added iron, 1% (w/w) RH and WPI emulsions exhibited consistently lower PV's and AV's compared to P20 emulsions and showed consistently lower PV's than SDS emulsions over a 7-day period, illustrating their superior oxidative stability. This is because RH and WPI are more able to effectively retard LO through their various antioxidant mechanisms. One such mechanism of RH is due to its significant free radical scavenging ability (Ojha et al., 2016) which, like all flavonoids, it harbours primarily through possession of a hydroxyl group (OH) , which allows transfer of a hydrogen atom (Amić et al., 2013) to a free-radical to create a more stable radical as is shown in Equation 4-1 (where L = lipid):

$$RH - OH + OH^{\cdot} \rightarrow RHO^{\cdot} + H_2O \qquad \textbf{(Equation 4-1)}$$

Another important antioxidant mechanism of RH is through its effective metal chelating ability. Metal ions present in emulsions, such as Fe^{2+}, are able to catalyse LO reactions via the Fenton reaction (de Souza and De Giovani, 2004) and therefore through their chelation, RH is able to combat LO. Furthermore, as was illustrated in interfacial tension (IFT) experiments in Figure 4-1, RH as a Pickering emulsifier caused significantly less reduction of IFT than P20 or SDS; this higher IFT within emulsions would likely hinder the diffusion of oxygen between phases thus combatting oxidation (Frankel, 2001).

WPI is also known to possess antioxidant activity which stems from the fact it is able to: (1) form a tightly-packed interfacial barrier at the surface of oil droplets, typically up to

15nm thick, as opposed to up to just 1nm for surfactants such as P20 and SDS (Berton-Carabin et al., 2014). The relatively thick interfacial layer formed by WPI serves as an effective barrier to prooxidants such as transition metals present in the aqueous phase. This same barrier could also prevent contact from reactants present on the surfaces of adjacent oil droplets, which would also aid the fight against LO. Furthermore (2), WPI is an effective metal chelator and (3) is able to terminate free radicals through use of its amino acids and sulfhydryl groups (Hu et al., 2003a). Although WPI may not be able to terminate free radicals as effectively as RH, its other antioxidant mechanisms evidently make up for this deficit which made it the most effective emulsifier used in this study for combatting LO.

With increasing RH concentration, the oxidative stability of emulsions increased. RH was observed microscopically to be present in and around flocs of oil droplets which is shown in Figure 4-7. The amount of RH in and around oil droplets was of course dependent on concentration of RH in emulsions, and greater concentrations allowed for enhanced shielding from prooxidants in the aqueous phase, and hence, a reduction in LO.

However, it was also observed that RH particles were unable to form a continuous ‘shell’ to act as a barrier around oil droplets, which is most likely why they were not as effective at combatting LO as WPI. RH particles used in this study had an average Sauter mean diameter of 1.2 ± 0.1μm, which is large in comparison to conventional Pickering particles such as silica which tend to be less than 0.02μm. Furthermore due to sonication being employed for the initial size reduction of RH the particles of RH will be irregularly shaped, and the RH particles were polydispersed post sonication; consequently formulated RH emulsions exhibited numerous gaps at the oil-water interface with no RH

coverage, leaving oil droplets exposed to oxidative attack. Polarised light micrographs taken in Figure 4-7 and Figure 4-8 support this claim by showing the appearance of semi-crystalline RH particles at the oil-water interface, but also large areas of oil droplets with no RH coverage or shielding.

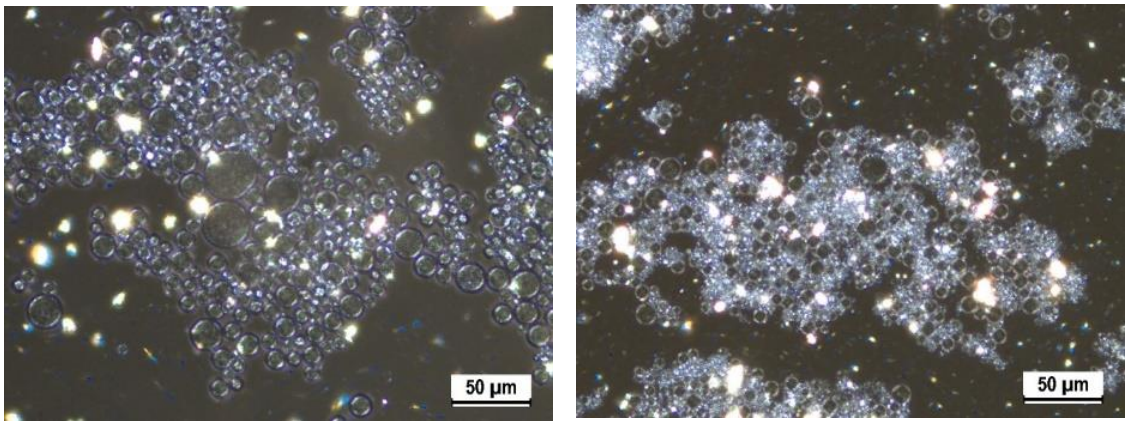

Figure 4-7: Polarised light micrographs showing 0.5% and 1.5% RH emulsions at 40x magnifications after 14 days.

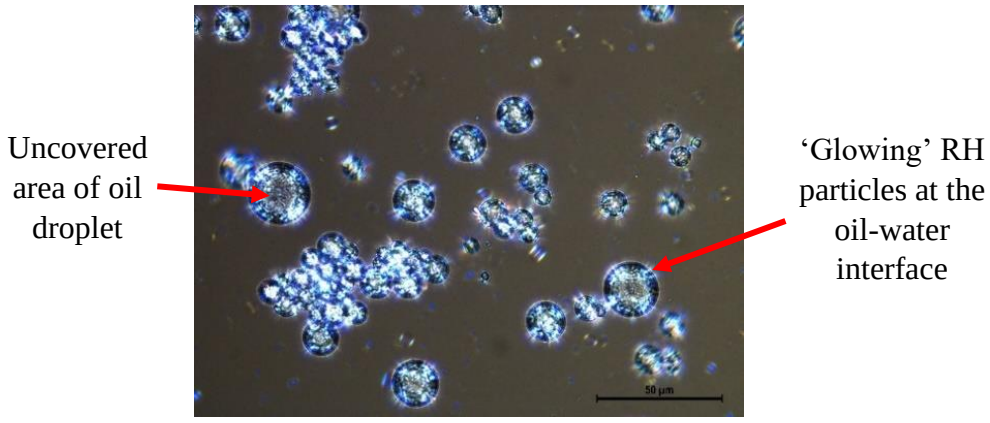

Figure 4-8: Polarised light micrographs of 0.5% RH emulsions after 14 days showing interfacial regions which contain large gaps with no RH coverage.

With the addition of ferrous iron there is an increase in the formation of both primary and secondary oxidation products, and therefore reduced oxidative stability at all emulsifier concentrations investigated except 1% (w/w) WPI. This is because ferrous iron acts as a prooxidant through catalysing initiation reactions in lipid oxidation processes, with 1%

(w/w) WPI showing no change due to its strong antioxidant properties at this concentration. RH was found to act as a prooxidant in the presence of added ferrous ions. The prooxidant nature of flavonoids such as RH in the presence of iron stems from their possession of phenolic groups, which was previously discussed in Section 3.4.3.

4.4.4.3 Effect of pH on RH emulsions

The zeta potential of RH emulsions was measured at pH values ranging from 2.00 to 5.74 (pH 5.74 was found to be the native pH value of RH). From Figure 4-9 it can be seen that as pH is increased from 2.00 to 5.74, there was a sharp decrease in zeta potential of RH Pickering particles. This is due to the ionisation of rutin which results from its deprotonation at higher pH values, something which has been reported to occur with other flavonoids such as the non-glycated rutin molecule, quercetin (Jurasekova et al., 2014). One study found that there was significant dissociation of quercetin hydroxyl groups between pH 4.00-8.00 which explains the increasing zeta potential values found in our study in the range pH 2.00-5.74 (Herrero-Martínez et al., 2005) .

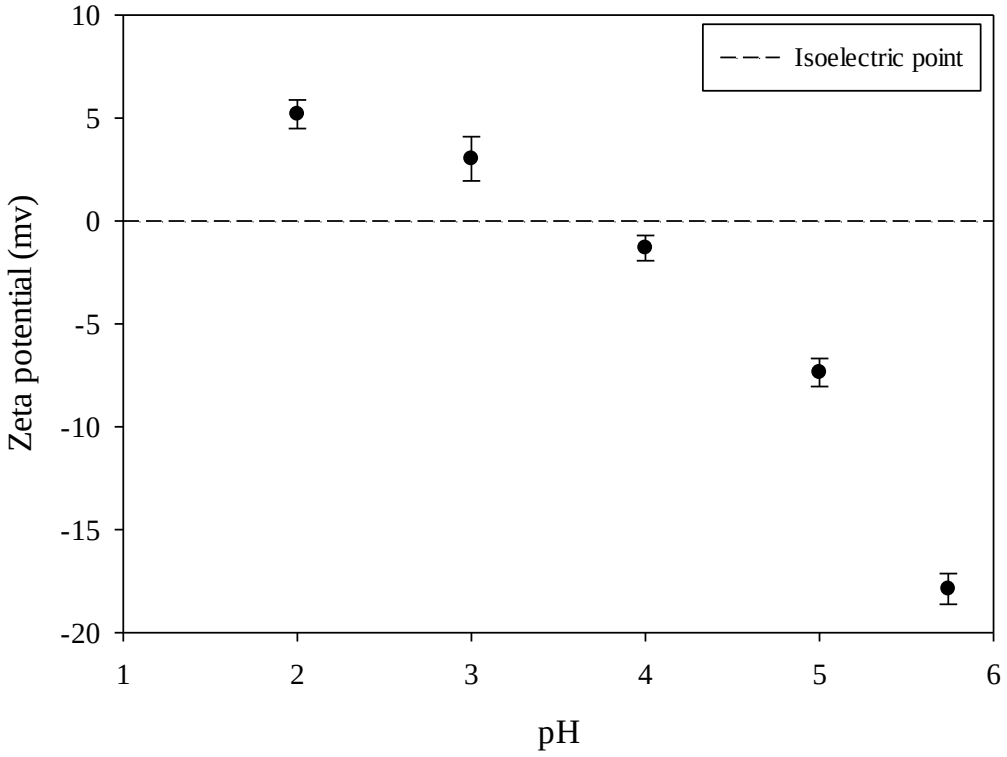

Figure 4-9: Zeta potential of RH emulsions was measured at pH values ranging from 2.00 to 5.74 (native pH)

Size measurements conducted on 0.5% (w/w) RH emulsions at pH values of 5.74, 4.00 and 2.00 are shown in Figure 4-10. RH emulsions at all pH values were physically stable throughout a 14-day period and showed no significant change in droplet size during this time. Interestingly, as the pH was reduced from 5.74 to 4.00, there was a dramatic reduction in droplet size. This can be attributed to a reduction of RH Pickering particle zeta potential from -17.9mv to -1.3mv (as was shown in Figure 4-9) meaning that Pickering particles were able to pack more tightly together due to reduced electrostatic repulsion and consequently form more stable, smaller droplets. This finding was exemplified in another study which found precisely this in the case of silica stabilised emulsions (Pichot et al., 2010); the silica particles exhibited decreased zeta potentials at low pH values which aided their stabilisation at the oil-water interface.

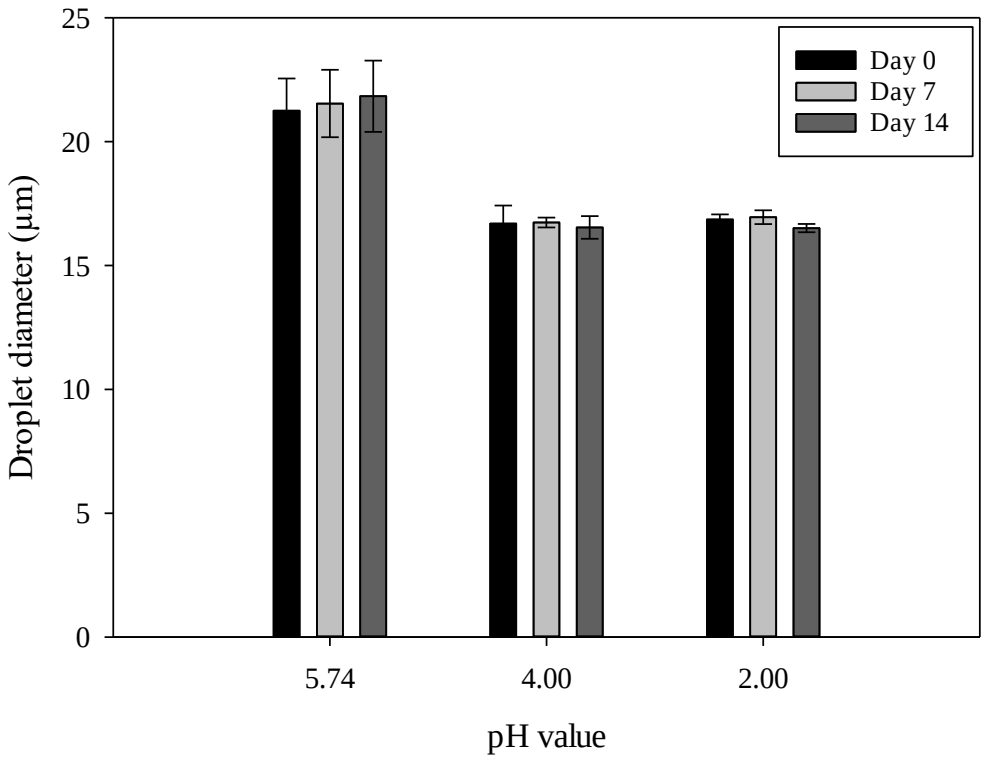

Figure 4-10: Droplet sizes of 0.5% RH emulsions over a 14-day period at different pH values.

The oxidative stability of 0.5% (w/w) RH Pickering emulsions over a 7-day period at different pH values is shown in Figure 4-11. Each of these emulsions contained 0.1mM ferrous sulphate heptahydrate (added to emulsions post-emulsification).

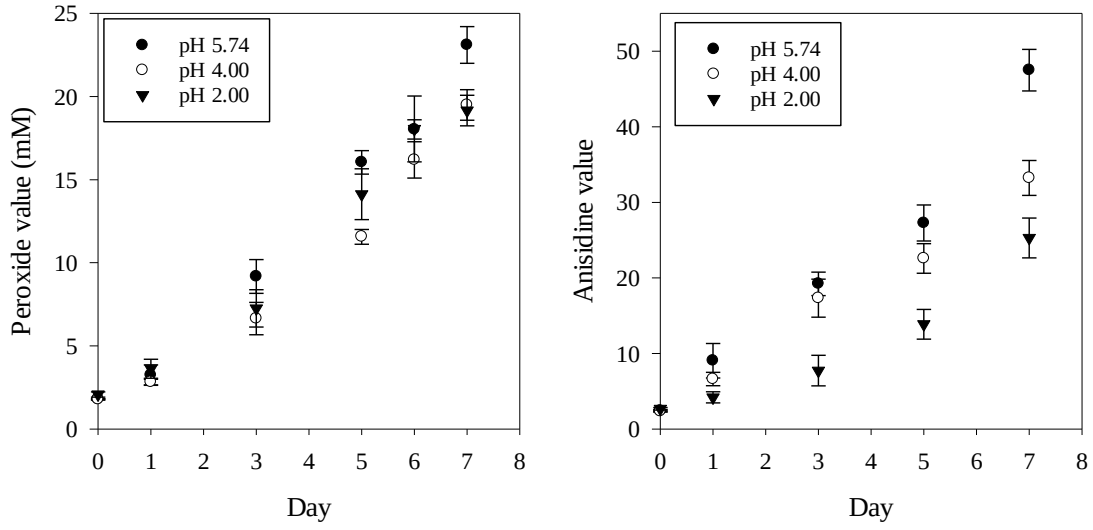

Figure 4-11: Effect of pH on oxidative stability (using size corrected PV's and AV's) of 0.5% RH emulsions.

Figure 4-11 shows that as pH is lowered from 5.74 to 2.00, there were no major changes in PV's over a 7-day period, but were significant reductions in AV's, which overall meant that reducing the pH of RH emulsions enhanced the oxidative stability of these emulsions. There are various different ways in which adjusting pH affects oxidative stability, for example prooxidant iron ions are known to be more soluble at low pH values (Nielsen et al., 2013) which would aid lipid oxidation reactions by making them more accessible. However, results in Figure 4-11 suggest that the most pertinent factor would be due to the decreased zeta potential of RH particles with increasing pH value. Decreasing zeta potential values from +5.19mv to -17.88mv as pH is increased from 2.00 to 5.74 (as shown in Figure 4-9) will enhance oxidative stability in one major way; at pH 2.00, the positive surface charge of RH particles which surround oil droplet interfaces will be able to repel away positively charged prooxidant transition metal ions present in the aqueous phase, whereas at pH 5.74 these RH particles will possess a negative charge which will attract these prooxidants to the oil-water interface where they were able to catalyse free-

radical lipid oxidation reactions and accelerate this process (this is shown schematically in Figure 4-12). One study (Mei et al., 1999) echoed this view by noting that transition metals have greater impact in emulsions in which the emulsifier carries a negative charge due to attraction of these prooxidants to the primary site of oxidation reactions (the oil-water interface). In addition, and as noted previously, as the pH decreases to pH 2.00 the solubility of prooxidant iron increases which would further accelerate the process of LO.

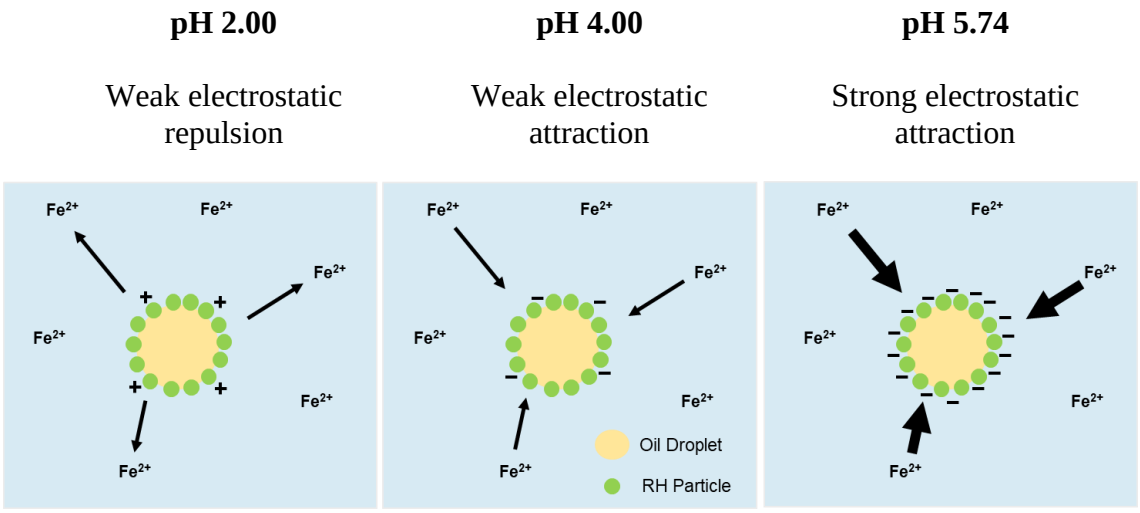

Figure 4-12: Schematic diagram illustrating the effect of pH on pro-oxidant ferrous ions.

4.4.4.4 Effect of Creaming

All formulated emulsions solely stabilised by RH particles were found to exhibit creaming, which is a key mechanism of emulsion instability. The reason creaming experiments were performed for RH emulsions was twofold; firstly, it was important to see to what degree creaming could be supressed using RH. Secondly, Figure 4-6 illustrated the effect of RH concentration on the rate of LO, however it is known that creaming can affect oxidative stability and it was important to know to what extent it did.

Figure 4-13 depicts the effect of RH concentration on emulsion creaming over a 14-day period, with pictures of the emulsions displayed below the creaming indices graph.

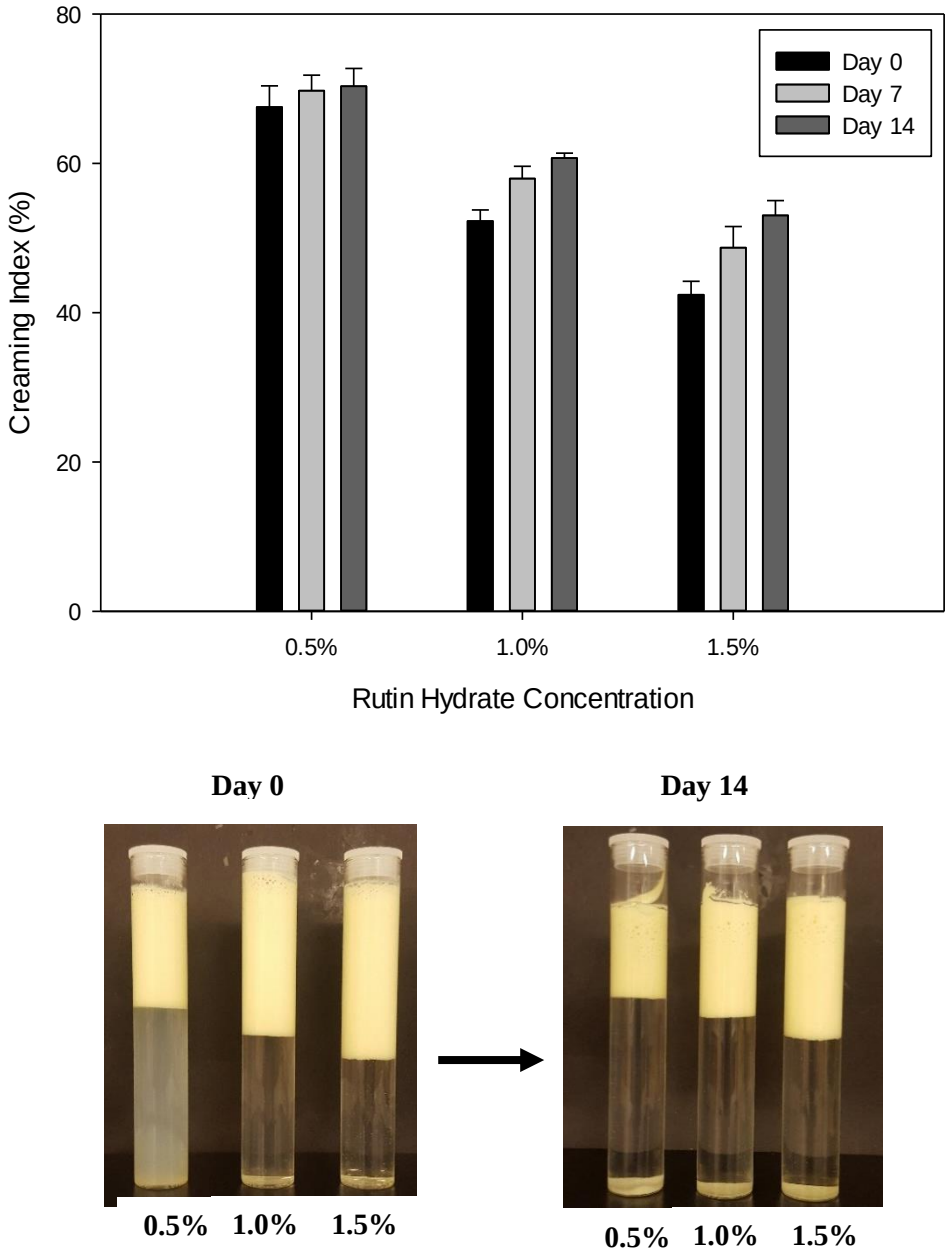

Figure 4-13: Creaming indices of RH emulsions prepared at different concentrations (above) with accompanying pictures (below).

Figure 4-13 shows that as RH concentration increased from 0.5-1.5% (w/w), there was a reduction in the rate of creaming. This is because when greater RH concentrations were used, more particles were able to attach to the surface of oil droplets which decreased the density difference between oil droplets and the aqueous phase and thus reduced the

driving force for creaming and hence, resulted in lower rates of creaming. This was exemplified by a study into the use of alginate Pickering particles for emulsion formulation found that lower Pickering particle concentrations increased creaming and attributed this to the low particle concentrations increasing droplet coalescence which led to the formation of larger droplets through emulsification and increased creaming rates (Zhang et al., 2018). Data in Figure 4-13 reinforces conclusions drawn earlier from experiments which showed increasing RH concentration reduced the extent of LO, because this data shows that more RH particles adsorb to the oil-water interface which suppresses creaming.

To assess the impact of creaming on RH emulsions made up of different RH concentrations, earlier experiments varying the concentration of RH (shown in Figure 4-6) were repeated in the presence of 0.2% (w/w) xanthan gum (XG). The role of XG was to supress creaming throughout the duration of the LO study, and by comparing these results to earlier ones in which no XG was used, the effects of creaming could be isolated. Figure 4-14 shows the impact of different RH concentrations, each made with 0.2% XG, on LO. The PV graph shows significantly lower PV's than for those in which creaming occurred, however, this was due to the presence of XG, which is known to be an effective metal chelator (Qiu et al., 2015, Shimada et al., 1994) due to the presence of negatively charged ketal-pyruvate and Beta-D-glucuronic acid moieties (Dow et al., 2010) which are able to bind to divalent transition metals (such as Fe^{2+}) in the aqueous phase rendering them ineffective. XG is also a thickening agent which gives emulsions greater viscosity and it has been suggested that this could slow down the diffusion of prooxidants (Sun et al., 2007) and hence retard LO. Of course, as XG is a high molecular weight polysaccharide, it would also be able to help shield oil droplets from oxidative attack.

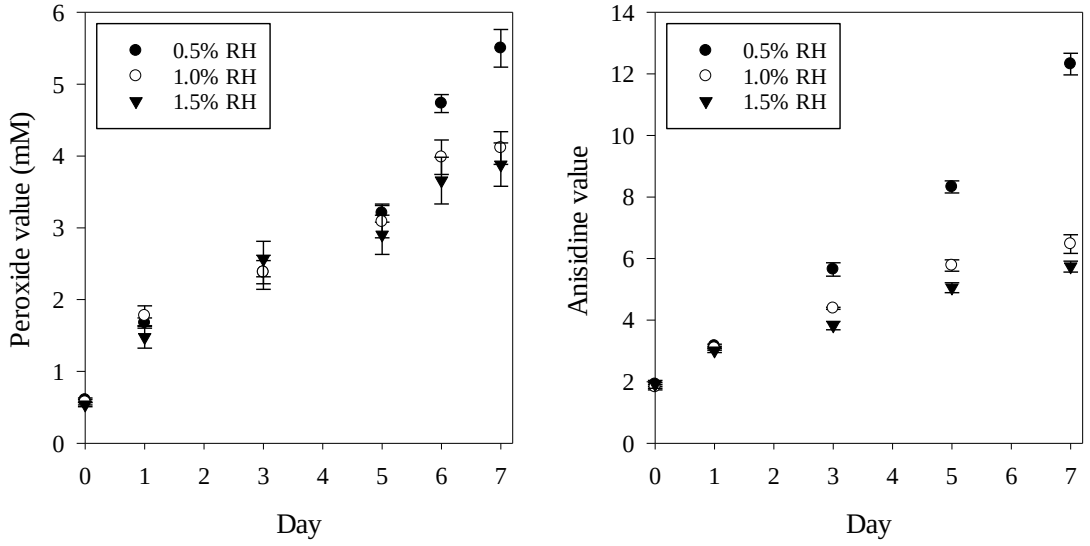

Figure 4-14: Effect of RH concentration on the oxidative stability (using size corrected PV's and AV's) of 0.2% xanthan gum stabilised emulsions.

By comparing the oxidative stabilities of RH in which there was creaming (Figure 4-6) and was no creaming (Figure 4-14), interesting conclusions can be drawn. Firstly, looking at PV's, it can be seen that before day 6, there was no significant difference between values for all tested concentrations, whereas when no XG was added, a difference could be seen much earlier (after just 3 days). This suggests that creaming is having a significant impact oxidative stability of emulsions. This is attributed to the fact that, when an emulsion creams, oil droplets are more tightly packed, and this can cause contrasting effects. On one hand, tighter packing of oil droplets could help shield vulnerable hydroperoxide molecules situated at the oil-water interface from prooxidants in the aqueous phase, decreasing lipid oxidation. On the other hand, tighter packing of oil droplets means it would be easier for free-radical chain reactions to occur (Gohtani et al., 1999), because after creaming the contact time between oil droplets is effectively infinite (Pichot, 2010), meaning that reactants situated at the oil-water interface on one droplet would be readily able to react with others on adjacent droplets. In addition, with greater

extents of creaming, a greater proportion of oil droplets accumulate at the top of emulsions and therefore more will be in contact with the air phase allowing for greater opportunity for them to react with oxygen and promote LO.

Importantly however, from Figure 4-14 it must be noted that the general overall trend for both PV's and AV's is similar to those exhibited in the absence of XG, with greater RH concentrations leading to significantly reduced PV's and AV's after a period of 7 days. Therefore, although creaming has been shown to affect oxidative stability in RH emulsions, it is clearly not the sole reason for the different extents of lipid oxidation encountered in RH emulsions.

4.4.4.5 Effect of rutin hydrate location

The effect of RH location was investigated. This was assessed by examining the effectiveness of RH particles at combatting LO when they were primarily located at either the oil-water interface or freely-dispersed within in the aqueous phase; these experiments were performed using different quantities of added ferrous sulphate heptahydrate (FSH), and results are displayed in Figure 4-15.

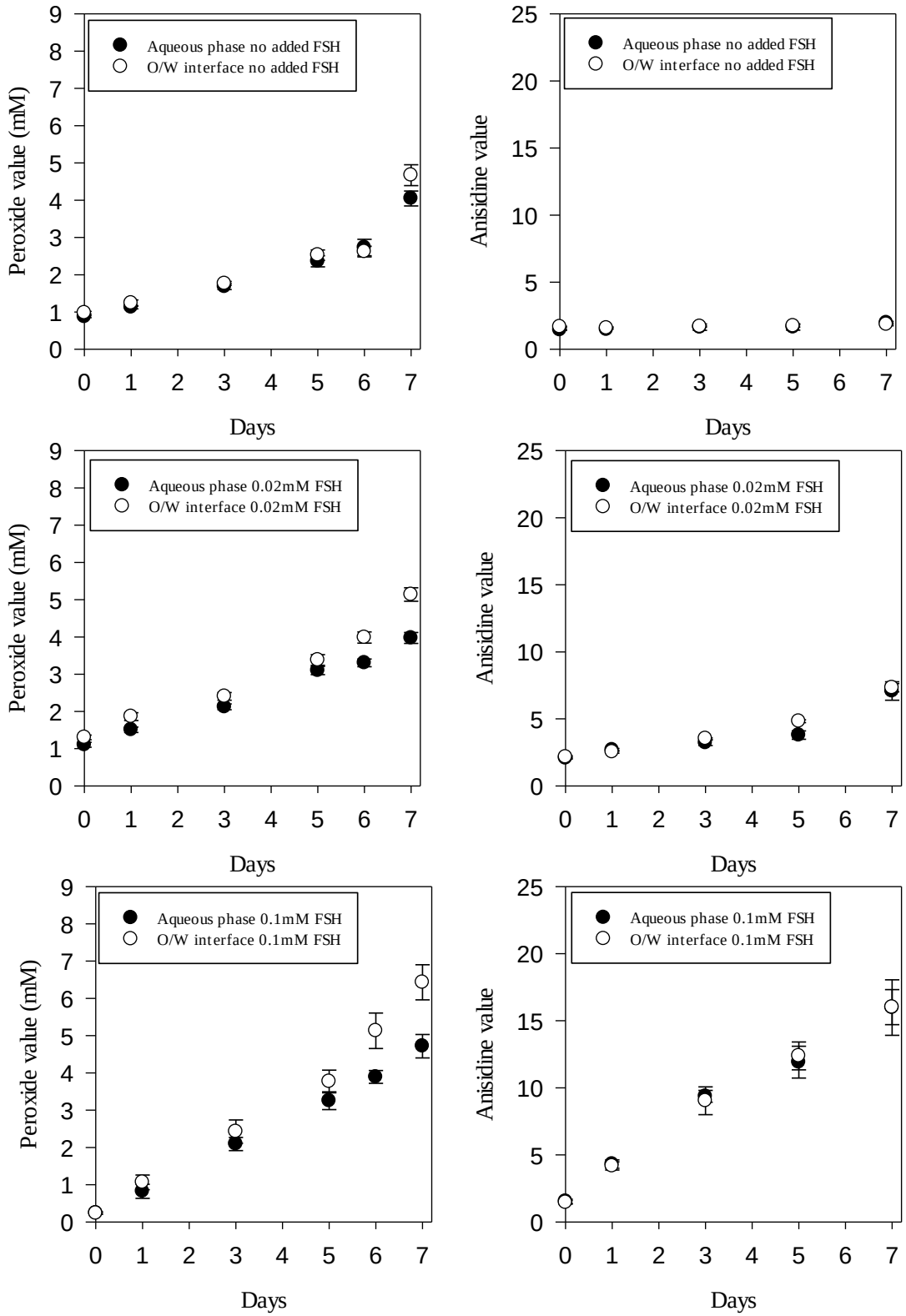

Figure 4-15: Effect of rutin hydrate location on oxidative stability (using size corrected PV's and AV's) of O/W emulsions.

Increasing the concentration of FSH led to reduced oxidative stability in all cases. Whether RH was primarily located at the oil-water interface, or the aqueous phase there were no significant differences in AV's and only minor changes in PV's over a 7-day period. With increasing FSH concentration, the difference in PV's on days 6 and 7 in which the RH is predominantly located at the oil-water interface or aqueous phase marginally increases. This is because at higher prooxidant FSH concentrations, the RH itself becomes more prooxidant (as was established in Sections 3.4.3 and 4.4.4.2) which means emulsion oxidative stability is now decreased through positioning of RH predominantly at the oil-water interface.

Ultimately however, from these results it is clear that beyond RH particles providing physical stability to oil droplets, the location of these particles has little bearing on oxidative stability. This is likely because, as was seen in earlier micrographs taken in Figure 4-8, RH particles were unable to form a continuous and effective barrier at the oil-water interface and therefore even when located here its efficacy is relatively unchanged from being located in the aqueous phase. Also, even when RH particles are freely dispersed in the aqueous phase, they are still able to interact with positively charged prooxidants such as ferrous ions due to their negative surface charge at native pH values. This ensures that RH is still able to enhance oxidative stability when positioned at either location within an O/W emulsion. RH particles may need to be nanonised and formed to a high degree of monodispersity to allow them to form a more effective, continuous barrier before significant benefits of them being located at the oil-water interface could be seen.

4.5 Conclusions

Through this study it has been found that RH is capable of providing dual-purpose functionality to O/W emulsions through functioning both as a conventional Pickering particle by providing physical stability; and through acting as an antioxidant to combat the process of LO and thereby provide oxidative stability. Formulated RH emulsions were physically stable throughout the duration of this study (14 days).

The impact of several factors on oxidative stability of O/W emulsions were assessed. It was found that the droplet size of emulsions significantly affected oxidative stability, and these effects were amplified with time following emulsification. RH emulsions showed enhanced oxidative stability over conventional surfactants P20 and SDS in the absence of added ferrous iron, but were found to be far less effective with the addition of higher concentrations and this was attributed to RH acting as a prooxidant in the presence of greater iron quantities. WPI-stabilised emulsions were able to combat LO more effectively than all other tested emulsifiers, and this was attributed to WPI being able to form a continuous and effective barrier at the oil-water interface in contrast to RH particles, which hindered their antioxidant prowess. This study suggests that a major challenge in the utilisation of natural flavonoid particles such as RH as Pickering particles is producing them in a form, and great enough quantity, to enable them to act as an effective interfacial barrier; this could possibly be achieved through attainment of concentrated flavonoid suspensions (> 0.5% (w/w)) which contain particles that are nanosized, relatively monodispersed, regularly shaped and resistant to aggregation.

RH emulsions gained oxidative stability at reduced pH values, which was attributed to the positive zeta potential gained by RH particles at low pH values which acted to repel

away positively charge prooxidants. Creaming was found to be supressed when emulsions formulated contained greater RH concentrations, and this was due to more RH particles adsorbing to the oil-water interface, lowering the density difference and reducing the rate of creaming.

For the first time in this study, a flavonoid particle, RH, has been assessed and determined to be successful in formulating physically stable O/W emulsions of enhanced oxidative stabilities. As a natural, and non-toxic particle, RH offers several key advantages over conventional emulsifiers. Something not considered in this study is the added health benefits which incorporating RH into food emulsions could offer in addition to providing physical and oxidative stability. Thus, the use of RH for emulsion formulation has tremendous opportunities in the food industry.

CHAPTER 5: THE PRODUCTION OF ANTIOXIDANT NANOPARTICLES VIA THE MICROWAVE-ASSISTED ANTISOLVENT PRECIPITATION (MAP) TECHNIQUE

Data and discussions from within this chapter have been published in:

Aditya, N. P., Hamilton, I. E., Noon, J. & Norton, I. T. 2019. Microwave-Assisted Nanonization of Poorly Water-Soluble Curcumin. ACS Sustainable Chemistry & Engineering, 7, 9771-9781.

5.1 Abstract

The microwave-assisted antisolvent precipitation (MAP) technique represents a novel method for the synthesis of antioxidant nanoparticles. This technique uses dielectric heating for the rapid removal of solvent from solvent-antisolvent mixtures (in which a solute is dissolved in the solvent) following the mixing of the two phases to generate a 'second wave' of supersaturation and the formation of aqueous nanosuspensions. Two naturally occurring model polyphenolic antioxidant compounds, curcumin and silymarin, were used for this study.

Using the MAP technique, curcumin and silymarin compounds were size reduced from initial sizes of ~20µm and ~10µm to 0.2µm and 0.1µm respectively. Both these materials were transformed from exhibiting crystalline structures to becoming amorphous post nanonisation via the MAP technique. These physical changes in size and crystallinity are known to enhance dissolution velocity as well as apparent solubility and are key factors in improving oral bioavailability upon the incorporation of these compounds into food or pharmaceutical products.

MAP was found to be more suitable for the synthesis of curcumin rather than silymarin nanoparticles, and this was primarily attributed to the far lower aqueous solubility of curcumin compared to silymarin. The main hypothesis of this work was that using microwave energy, solvent could be rapidly removed from solvent-antisolvent mixtures resulting in a higher degree of supersaturation and consequently the formation of a larger number of particles than would be attained solely through mixing solvent and antisolvent phases. This was found to be the case for curcumin, which exhibited the formation of a larger number of smaller particles at greater solvent removal rates but was not the case

for silymarin. It was hypothesised that the MAP technique is more suitable for polyphenols with a low aqueous solubility similar to that of curcumin; if the aqueous solubility of a compound is too high then a negligible amount of particle formation will occur during the solvent removal step of the MAP technique and particle formation will instead be dictated almost solely through the solvent-antisolvent mixing step.

For the first time in this study, the MAP technique has demonstrated its capability to control nanoparticle size and enhance the physical stability of nanosuspensions. MAP processing represents a highly efficient and rapid technique for the nanonisation of polyphenolic antioxidant compounds and has been developed using a green solvent (ethanol) which can be evaporated, condensed, and re-used in this process. Thus, the MAP technique shows great promise for further development and commercialisation.

5.2 Introduction

Numerous natural antioxidant and other bioactive compounds exist which are known for their health promoting and disease preventing activities. However, upon their consumption, many of these compounds suffer from poor bioavailability which is often due to their limited aqueous solubility. Through particle nanonisation, it is possible to help overcome the issue of low compound aqueous solubility and boost efficacy of many natural compounds. Although many nanonisation techniques currently exist, they each suffer their own drawbacks as was previously discussed in Section 2.10.2. Thus, the focus of this chapter was on the development of a novel and scalable nanonisation technique which could help overcome limited aqueous solubility issues associated with two model antioxidant compounds, curcumin and silymarin.

5.3 Materials and methods

5.3.1 Materials

Curcumin (≥ 80%) and silymarin (flavonolignan mixture containing ≥ 30% Silibinin) were obtained from Sigma Aldrich. Ethanol (≥ 99.8%) was obtained from Fisher Scientific. Distilled water was passed through a reverse osmosis unit followed by a milli-Q water system prior to usage.

5.3.2 Nanosuspension production through microwave-assisted antisolvent precipitation (MAP)

Firstly, the antioxidant of choice was dissolved in ethanol (at room temperature) at the desired concentration (either 1, 2 or 4mg/ml for curcumin or 20, 35 or 50mg/ml for silymarin) to obtain a stock solution. Next, the required amount of stock solution (solvent) was mixed with 30ml of distilled water (antisolvent) at a temperature of ~15°C. Immediately after the addition of antisolvent to solvent, the reaction vessel was placed in the reaction chamber of a single-mode microwave (Sairem 2kW, 2.45GHz microwave generator), in which a vacuum was (usually) applied at different gauge pressures (either 0, -90 or -93kPa), and after which equivalent amounts of microwave energy were directed at the reaction vessel at varying power levels and time durations (either 50, 100, 200, 400 or 800W for 240, 120, 60, 30, or 15s respectively) to facilitate solvent removal (evaporation) whilst keeping the total microwave energy used (power density) constant in all experiments.

Thus, in theory, MAP is able to produce two ‘waves’ of supersaturation and nanoparticle formation; the first during the mixing of solvent and antisolvent phases and the second during the solvent removal phase through microwave heating. A schematic diagram of

the single-mode microwave used is shown in Figure 5-1 and an outline of the MAP process is shown in Figure 5-2.

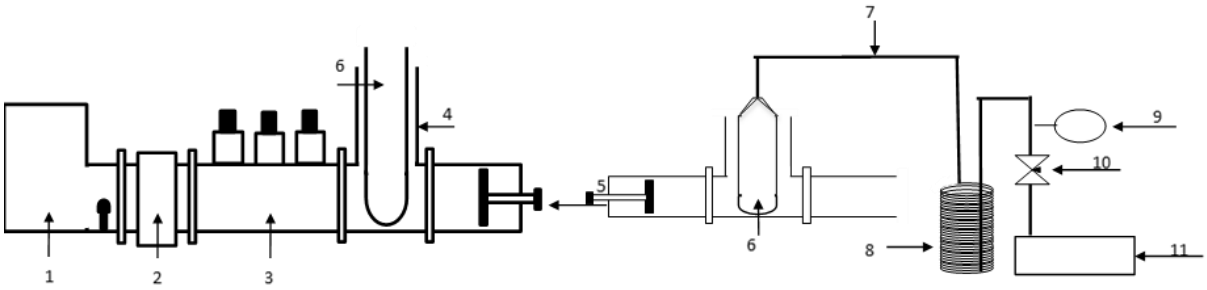

Figure 5-1: Schematic representation of microwave instrument used to fabricate curcumin nanosuspension using dielectric heating. This shows a microwave generator (1), isolator (2) and manual or automatic stub-tuning device (3). The tuning device is used to maximize power transference into the sample by reducing reflected power. Choke structure (4) allows the insertion of a sample into the wave-guide of the microwave whilst preventing microwaves being transmitted into the surrounding. This may be used, for example, to prevent leakage over 5mW/cm^2. A sliding short circuit (5) is typically used to allow the highest energy region (maxima) of the wave to be set over the sample to ensure efficient energy transfer. This also acts as a reflecting device that allows for a standing wave to form. Sample chamber (6) allows keeping vessel in a single mode wr340 cavity where the vessels diameter was kept below 2 1/4 guided wavelengths. This makes sure that microwave energy is evenly applied throughout the reaction vessel. Further it consists of transfer line (7) attached to the sample container (6). A condenser (8), vacuum/pressure gauge (9), isolation valve (10) and pump (11) which is used to reduce the pressure and condense evaporated solvent.

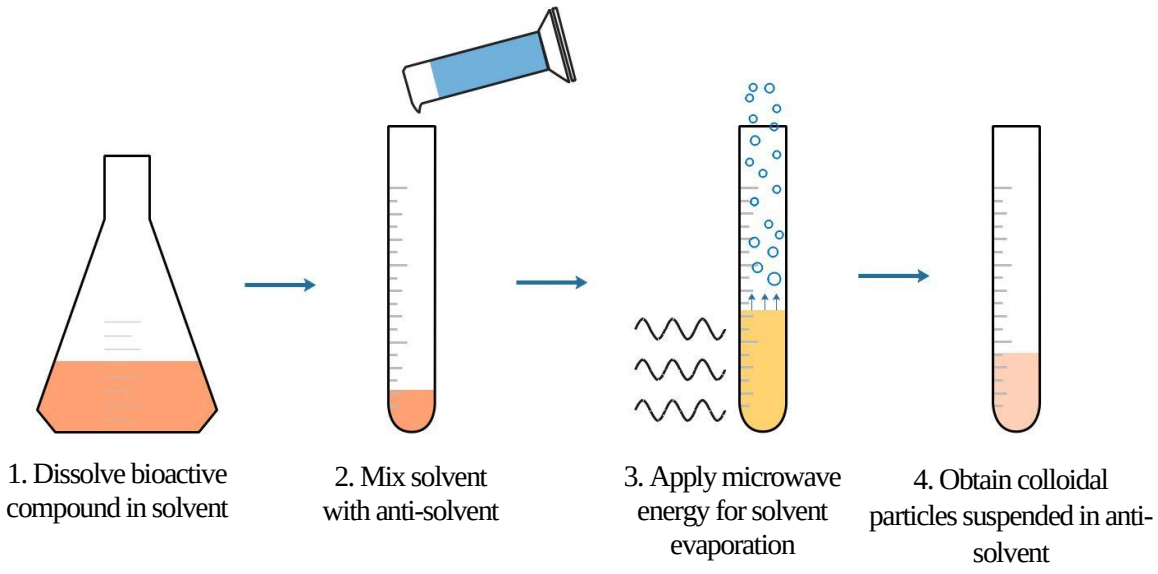

Figure 5-2: Schematic representation of the MAP technique.

5.3.3 The impact of solvent removal on nanosuspension stability

To assess the impact of solvent removal on the physical stability of formulated nanosuspensions, solvent and antisolvent phases were mixed at the desired solvent to antisolvent (SAS) ratio (either 1:30, 1:20 or 1:10). Then solvent was either removed (SR) via step three of the MAP technique or it was kept in the solvent-antisolvent mixture (NSR). Size measurements were performed in triplicate (as detailed in Section 5.3.6) and taken on days 0, 1, 7, and 30.

5.3.4 The effect of solvent-antisolvent mixing

To elucidate the impact of solvent-antisolvent mixing, 30ml of distilled water was placed upon a magnetically stirred plate and stirred (at room temperature) at the desired rates (100-1500 revolutions per minute (rpm); these rates were chosen as 1500rpm was the upper rpm limit of the magnetic stirrer). Solute-laden solvent was then added to the distilled water (antisolvent) at a controlled rate (2-30ml/min) through use of a syringe pump. Mixing was always carried out for a total time of 30 seconds.

5.3.5 Nanosuspension production through use of thermal heating

Experiments performed using thermal (conductive) heating as opposed to dielectric (microwave) heating used a rotary evaporator (Buchi Rotavapor) for the solvent removal stage of the MAP process, otherwise identical processing and formulation conditions to the ones described with the MAP method were implemented.

The rotary evaporator water bath was maintained at a temperature of 40°C as this resulted in solvent-antisolvent mixtures reaching the same final temperature (~39°C) as those achieved in mixtures which had undergone dielectric heating for the same duration.

5.3.6 Size measurement

The hydrodynamic diameter (herein referred to as particle 'size') and size distributions of particles were measured through dynamic light scattering using a Zetasizer (Malvern Zetasizer Nano ZS) at 25°C. Samples were diluted appropriately using distilled water prior to their size measurement.

5.3.7 Crystallinity of fabricated nanoparticles

In order to obtain solid particles required for solid-state characterisation, formulated curcumin and silymarin nanosuspensions (~30ml) were frozen in liquid nitrogen, prior to being freeze-dried using a freeze dryer (Scanvac 110-4 pro) for 96 hours in order to obtain dry powders.

5.3.7.1 X-ray powder diffraction (XRPD)

XRPD studies were performed using a Bruker Phaser D2 X-ray diffractometer which utilised a beam of Cobalt Kα radiation (λ=1.79Å). Freeze dried powder samples of curcumin and silymarin were scanned over an angular range of 2θ from 5-45° with a step

size of 0.02° and a scanning rate of 5°/min. The voltage was set up at 40kV and the current was 40mA.

5.3.7.2 Differential scanning calorimetry (DSC)

DSC studies were performed using a TA Instruments DSC 25 differential scanning calorimeter. 5mg of freeze-dried curcumin and silymarin samples were weighed and loaded into hermetically sealed aluminium pans prior to being heated at range of 40-200°C at a scan rate of 10°C/min under a nitrogen purge gas flowrate of 50ml/min. An empty but otherwise identical pan was used as a reference.

5.3.8 Surface tension measurements

Surface tension measurements were conducted using a tensiometer (Kruss K100) via the Wilhelmy-plate method. All experiments were performed at room temperature for a duration of 300 seconds to ensure equilibrium surface tension values were reached.

5.3.9 Zeta potential measurements

Zeta potential measurements were carried out using a Malvern Zetasizer Nano ZS at 25°C. Malvern folded capillary zeta cells (DTS1070) were used to house the samples.

5.3.10 Scanning electron microscopy

Nanosuspension morphology was studied using a Philips XL-30 FEG ESEM high vacuum environmental scanning electron microscope (SEM). Liquid samples at different time intervals were placed on the coverslip. Cold air was blown to strip the antisolvent which resulted in a thin layer of nanoparticles on the coverslip. Each coverslip was then placed on double-sided tape and gold-coated under a vacuum using a sputter coater. Observations were made under an accelerating voltage of 10.0 kV.

5.3.11 Statistical analysis

All measurements were made in at least triplicate with error reported as plus/minus a single standard deviation unless otherwise stated.

5.4 Results and discussion

5.4.1 The impact of solvent removal on nanosuspension stability

In antisolvent precipitation (AP) processes, a solute is first dissolved in a solvent, which is then added to an antisolvent and, upon addition, the drastic and sudden change in solubility generates a high level of supersaturation resulting in the nucleation and growth of nanoparticles. However, upon mixing of solvent and antisolvent phases the reaction is incomplete, due to the presence of diffusible solute in the mixture. Diffusible solute refers to the dissolved solute molecules within a solvent-antisolvent mixture and remains primarily due to the presence of solvent. Over time, diffusible solute will preferentially attach onto larger nucleated particles through Ostwald ripening, promoting increased particle size, polydispersity, and instability. The hypothesis of this work was that the rapid removal of solvent using the MAP technique (immediately following the mixing of solvent and antisolvent phases in which nuclei are initially formed) would generate a 'second wave' of high supersaturation resulting in the formation of a larger number of nuclei than would be obtained solely through mixing the solvent and antisolvent phases. Thus, the MAP technique would lead to the generation of highly monodispersed nanosuspensions of low average particle sizes and a relatively high degree of stability through reducing the effects of Ostwald ripening. To attest this hypothesis, the impact of solvent removal on nanosuspension stability had to be investigated, and this is illustrated for both curcumin and silymarin at different solvent to antisolvent (SAS) ratios in Figure 5-3 and Figure 5-4 respectively.

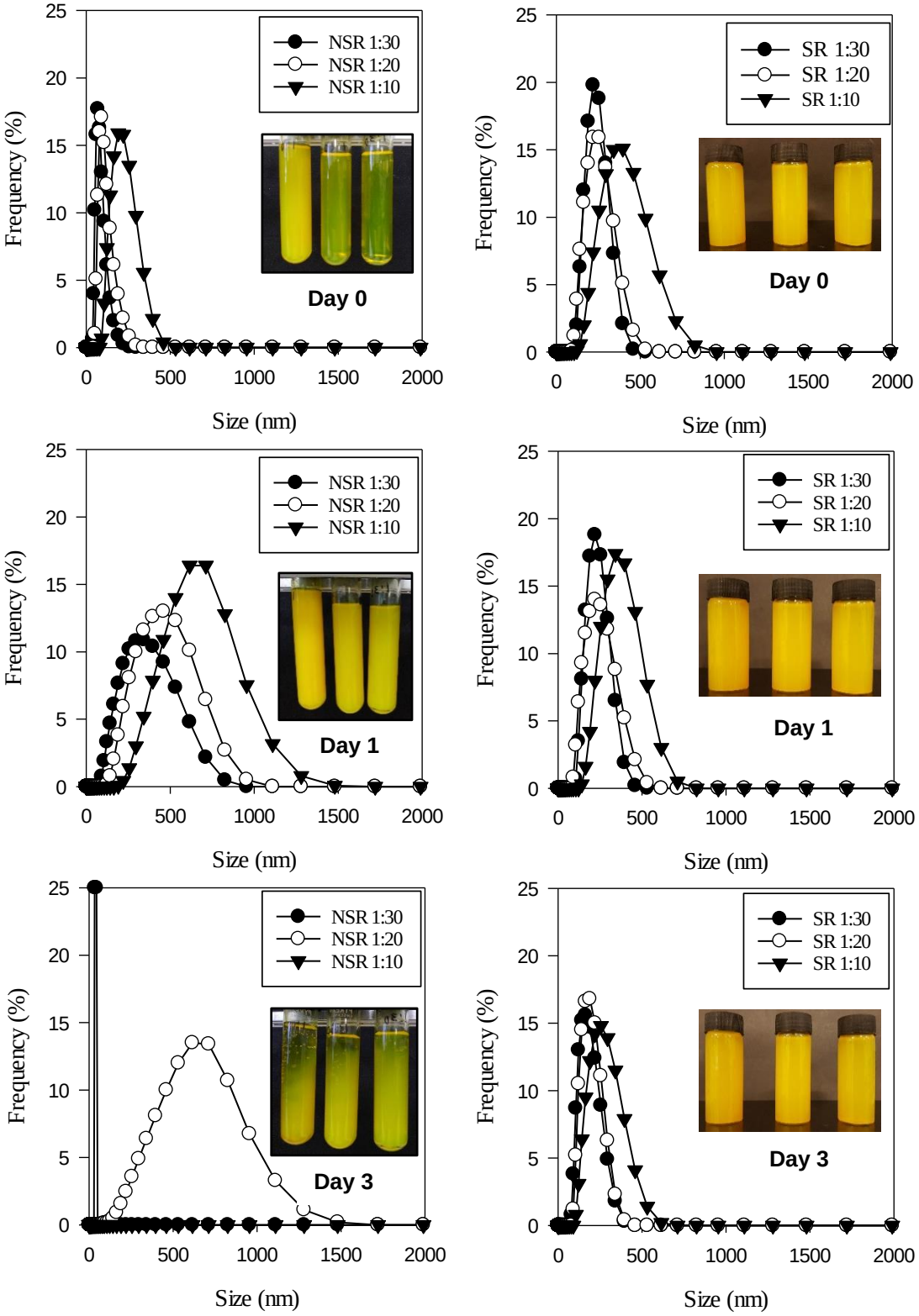

Figure 5-3: Size of curcumin nanosuspensions in which there was no solvent removal (NSR) (left) and solvent removal (SR) (right) over a 3-day period. Inset: pictures of samples at 1:10, 1:20 and 1:30 SAS ratios (from left to right).

In the case of NSR curcumin nanosuspensions, initial particle sizes were ~90nm for SAS ratios of 1:30 and 1:20, and ~200nm at an SAS ratio of 1:10. However, it can be seen that these nanosuspensions were unstable, and, over a period of three days the contained particles grew and their size distributions widened; a process which was accelerated at greater SAS ratios. The process of growth and instability in samples which had no solvent removed is illustrated in photographs taken of the samples in Figure 5-3 which show that the nanosuspensions became opaque after 1 day due to their increased size, and then underwent sedimentation after 3 days at which time all three samples became too polydispersed for size analysis. These observations can be explained using the LaMer theory of particle formation, which was previously described in Section 2.10.3. In curcumin samples with NSR, a lower degree of overall supersaturation and particle formation was attained compared to samples in which solvent was removed via microwave heating. This caused the formation of larger particles with greater polydispersity. The higher degree of polydispersity provided a key driving force for Ostwald ripening over time (Thorat and Dalvi, 2012). The process of Ostwald ripening was further promoted due to the presence of solvent over three days, which increased the solubility of curcumin within the nanosuspension thus providing a greater driving force for this process. Ultimately, increased Ostwald ripening resulted in the destabilisation of curcumin nanosuspensions in these experiments due to solvent not being removed following mixing of the solvent and antisolvent phases.

On the other hand, solvent removal from curcumin samples via MAP led to the formation of initial (day 0) particle sizes of ~240nm, ~200nm, and ~180nm at SAS ratios of 1:10, 1:20, and 1:30 respectively. Although these initial sizes were larger than samples in which there was no solvent removal, these nanosuspensions were far more stable in terms of

their physical size which instead remained relatively constant for the 3-day period. In addition, these samples were now observed to form homogenous suspensions which remained visually unchanged for three days (as shown in Figure 5-3). With the removal of solvent, a ‘second wave’ of high supersaturation in curcumin nanosuspensions was attained following the first wave upon mixing solvent and antisolvent phases. This caused the generation of a greater number of particles as particle nucleation was favoured over particle growth at higher levels of supersaturation (Celikbilek Ersundu et al., 2012); this enhanced nanosuspension stability as it ensured that the process of growth occurred over a larger number of particles, consequently lessening the effect of particle growth on nanosuspension stability. In addition, and *vice-versa* to formulated samples with no solvent removal, the greater level of supersaturation generated ensured a more monodispersed nanosuspension was formed which, along with the reduction in curcumin solubility following solvent removal, served to enhance the resistance of these nanoparticles to destabilisation by Ostwald ripening.

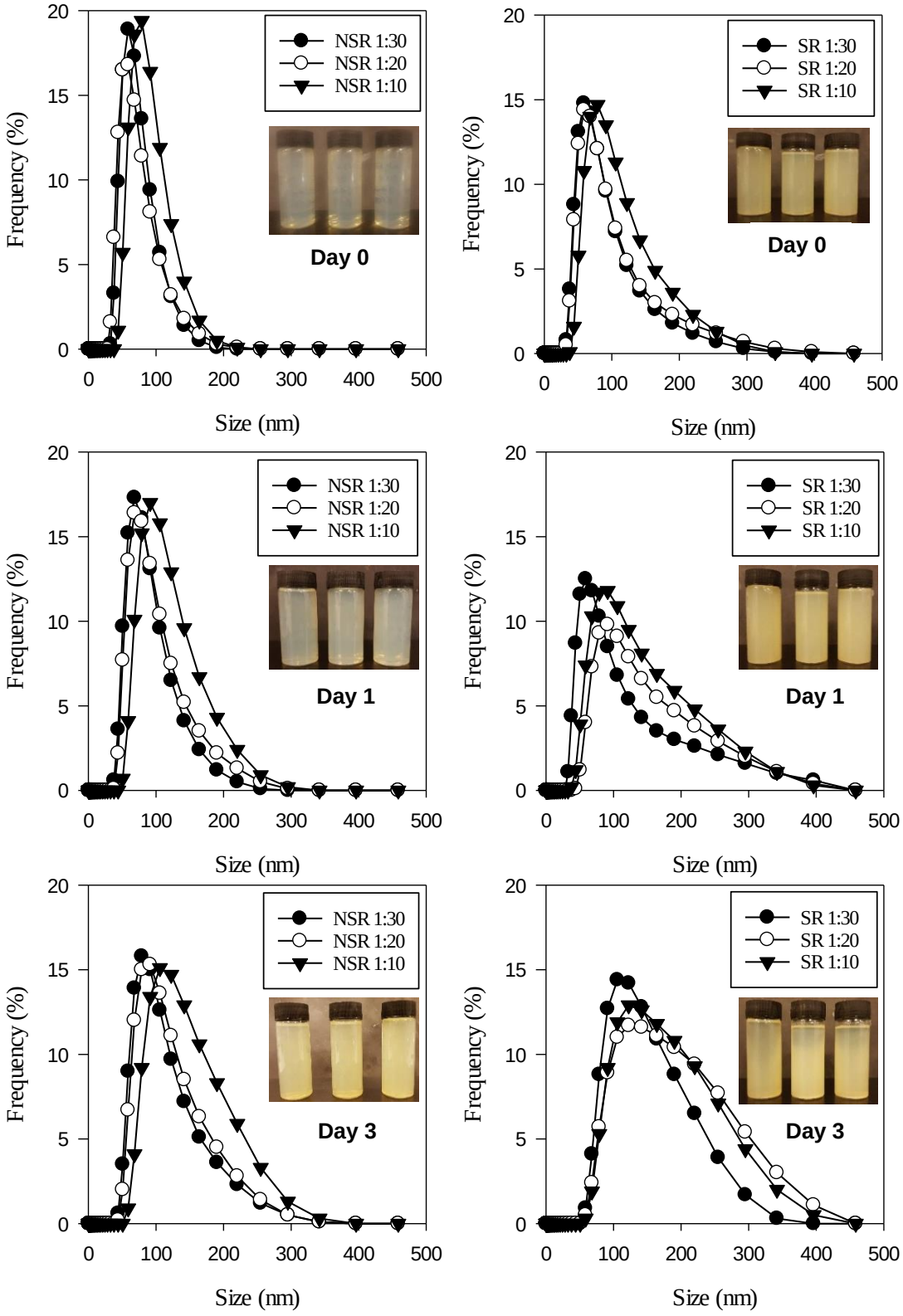

Figure 5-4: Size of silymarin nanosuspensions in which there was no solvent removal (NSR) (left) and solvent removal (SR) (right) over a 30-day period. Inset pictures of samples at 1:10, 1:20 and 1:30 SAS ratios (from left to right).

Conversely, there were no major differences in the stability of formulated silymarin nanosuspensions with and without solvent removal, as is depicted in Figure 5-4. These nanosuspensions were both visually observed to remain as dispersions throughout a 30-day period. The reason for the difference in behaviour of curcumin vs. silymarin nanosuspensions with and without solvent removal is most likely due to the vastly different aqueous solubility's of 0.6-2.7µg/ml (Modasiya and Patel, 2012, Shin et al., 2016) and 400µg/ml (Javed et al., 2011, Li et al., 2010) for curcumin and silymarin respectively. The far higher aqueous solubility of silymarin meant that the amount of diffusible solute present in silymarin nanosuspensions was high, whether the relatively low fraction (up to a maximum SAS ratio of 1:10) of solvent was removed. It appeared that the growth of suspended silymarin nanoparticles was determined primarily through the presence of water rather than the relatively low volumes of ethanol solvent, which is why particle growth was only marginally faster with no solvent removal at higher SAS ratios. Therefore, silymarin particles grew through Ostwald ripening at roughly equal rates at all SAS ratios, whether or not solvent is removed. For curcumin, although the volume fraction of ethanol in the mixture was the same as with silymarin, the low amount made a substantial difference on longer-term stability as curcumin has a significant solubility in ethanol (~5mg/ml) and near zero solubility in water, whereas with silymarin, even with ethanol removed, the suspended silymarin nanoparticles still possessed relatively high solubility in 30ml of water.

5.4.2 The effect of processing and formulation parameters on nanoparticle size

Experiments were performed to assess the impact of several processing and formulation parameters on curcumin and silymarin nanosuspensions. The parameters changed along with formulation identifiers for curcumin and silymarin are shown in Table 5-1 and Table 5-2 respectively.

Formulation	Pressure (kPa)	Power (W)	Time (s)	SAS Ratio	Solute concentration (mg/ml)
C1	0	50	240	1:30	2
C2	-90	50	240	1:30	2
C3	-93	50	240	1:30	2
C4	-93	50	240	1:30	2
C5	-93	100	120	1:30	2
C6	-93	200	60	1:30	2
C7	-93	400	30	1:30	2
C8	-93	800	15	1:30	2
C9	-93	50	240	1:10	2
C10	-93	50	240	1:20	2
C11	-93	50	240	1:30	2
C12	-93	50	240	1:30	1
C13	-93	50	240	1:30	2
C14	-93	50	240	1:30	4

Table 5-1: List of process and formulation parameters with sample identifiers for curcumin.

Formulation	Pressure (kPa)	Power (W)	Time (s)	SAS Ratio	Solute concentration (mg/ml)
S1	0	50	240	1:30	20
S2	-90	50	240	1:30	20
S3	-93	50	240	1:30	20
S4	-93	50	240	1:30	20
S5	-93	100	120	1:30	20
S6	-93	200	60	1:30	20
S7	-93	400	30	1:30	20
S8	-93	800	15	1:30	20
S9	-93	50	240	1:10	20
S10	-93	50	240	1:20	20
S11	-93	50	240	1:30	20
S12	-93	50	240	1:30	20
S13	-93	50	240	1:30	35
S14	-93	50	240	1:30	50

Table 5-2: List of process and formulation parameters with sample identifiers for silymarin.

The effect of each parameter investigated on the volume averaged mean particle size of both curcumin and silymarin is shown in Figure 5-5.

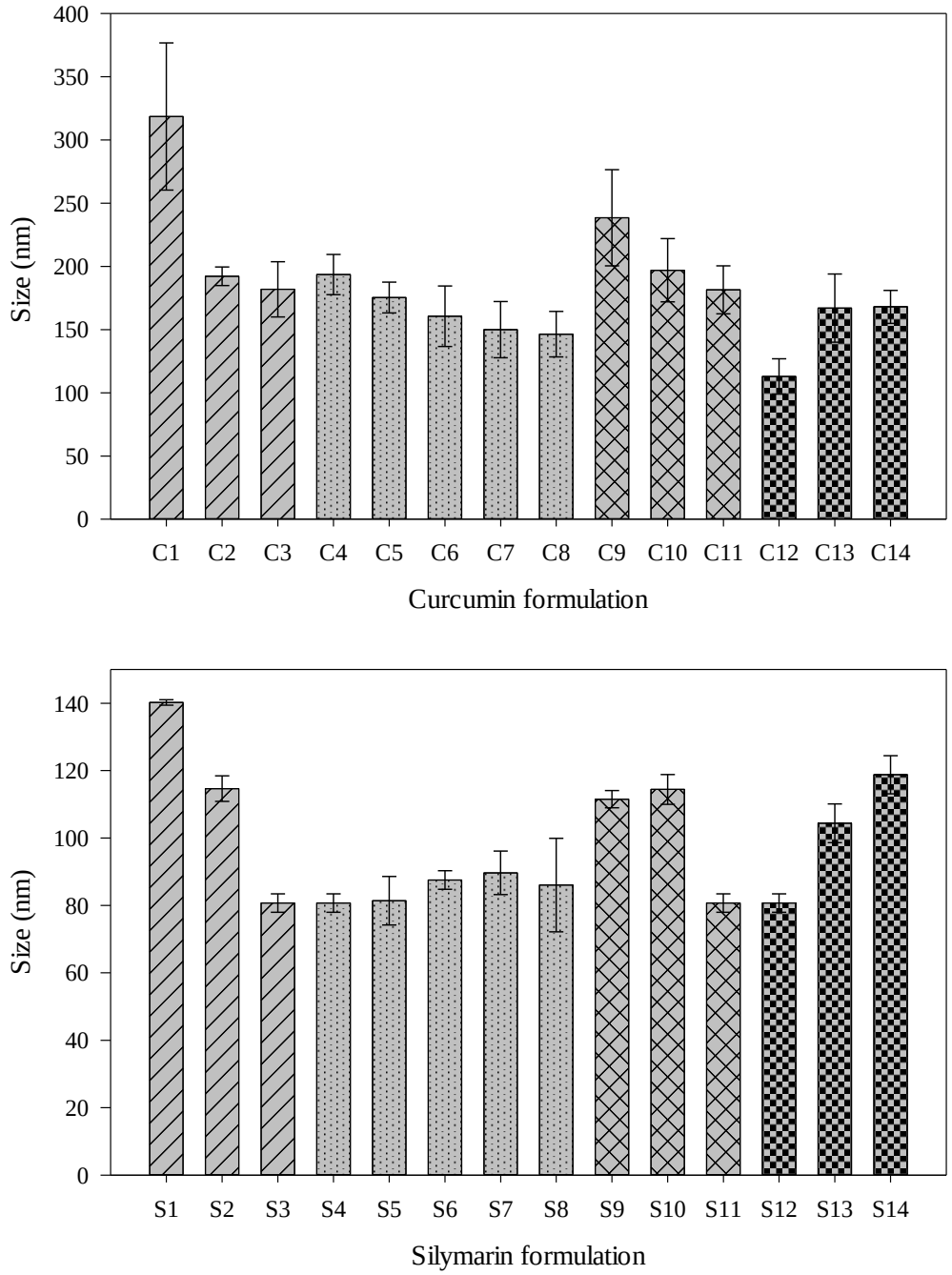

Figure 5-5: Impact of processing and formulation parameters on curcumin (top) and silymarin (bottom) nanosuspensions (N.B. the scale on the y-axis is different for these two graphs).

In analysis of results in Figure 5-5, firstly looking at the impact of the pressure (C1-C3 and S1-S3) used with the MAP technique during solvent evaporation, it can be seen that the use of lower pressures led to a reduction in average particle size in both the case of curcumin and silymarin. This is primarily due to the lower processing temperatures encountered when lower pressures were used; at pressures of 0, -90, and -93kpa, the maximum temperature reached by the nanosuspensions were 73°C, 45°C, and 39°C respectively. At higher temperatures, the diffusion rate and collision frequency between particles increases (Joye and McClements, 2013), which leads to the formation of larger particles through growth and agglomeration respectively. Higher temperatures will also increase the solubility of solutes and, after processing, these nanosuspensions will gradually cool, slowly reducing solute solubility and this will inevitably cause particle growth as diffusible solute migrates, which would preferentially be towards the surface of larger particles. Lower pressures are also responsible for increasing the rate of solvent evaporation which will generate an increased level of supersaturation, particle formation and consequently, a reduced particle size. The use of lower pressures in the MAP technique adds novelty as it is possible to process thermolabile compounds under vacuum conditions with no detrimental impact on particle size.

The amount of microwave energy applied to the solvent-antisolvent mixture in all experiments was kept the same, as this is directly proportional to both the microwave power and duration used. This meant that the ratio of power-time could be changed whilst keeping the microwave energy constant (i.e. 50W for 240 seconds vs. 100W for 120 seconds). This allowed for the impact of the rate of solvent evaporation to be investigated and this was found to have different effects for curcumin and silymarin nanosuspensions. Looking at curcumin samples (C4-C8), as the rate of solvent evaporation is increased

with increasing microwave power, there is a significant reduction in the size of generated nanoparticles from 194 ± 16nm to 146 ± 18nm. According to the LaMer theory of nucleation which was previously discussed, through increased rates of solvent evaporation using higher microwave powers a greater level of supersaturation and therefore particle formation occurs. In the case of curcumin, this meant that a greater number of particles were formed using 800W for 15 seconds compared to 50W for 240 seconds, which was illustrated through a reduction in average particle size as there is the same overall mass of curcumin present in each sample formulation. However, in the case of silymarin, there were no significant differences found when utilising different rates of solvent evaporation. This again is due to the far greater aqueous solubility of silymarin which meant that removing this solvent caused little change on the solubility of silymarin in the nanosuspension and ultimately caused no significant change in the level of supersaturation or particle formation attained.

Decreasing the SAS ratios in formulations C9-C11 and S9-S11 was found to generate significantly smaller particles in the cases of both curcumin and silymarin. As has been reported on numerous occasions, when the solvent-antisolvent ratio is decreased, this generally results in decreased particle size (Kakran et al., 2012, Kakran M, 2015, Yadav and Kumar, 2014). With decreasing SAS ratio, the amount of supersaturation generated upon mixing the solvent and antisolvent phases was increased, due to the swiftness of change from a system in which the solute had relatively high solubility, to one in which it has a significantly reduced solubility, resulting in the generation of a high level of supersaturation. With increasing supersaturation, there was an increased nucleation rate and thus smaller particles were generated in the cases of both curcumin and silymarin. Furthermore, an increase in SAS ratios from 1:30 to 1:10 would increase the importance

of the solvent removal step in the MAP technique with larger amounts of solvent to remove and supersaturation to generate. As it was previously found that the rate of solvent removal has far greater effect on curcumin rather than silymarin nanosuspensions, this is likely only an important factor in the case of curcumin nanosuspensions. Therefore, essentially, decreasing SAS ratios leads to a significant reduction in particle size due to greater levels of supersaturation generated in both the mixing and solvent removal steps for curcumin, but only in the mixing step for silymarin nanosuspensions.

Increasing solute concentration was shown to cause a significant increase in the average size of both curcumin and silymarin nanoparticles shown in formulations C12-14 and S12-14. In the cases of both compounds, different concentration ranges were investigated due to the vastly different aqueous and ethanol solubilities of the compounds. This trend of increasing solute concentration causing increasing particle size in antisolvent precipitation processes has been previously reported in the literature (Kakran et al., 2012, Yadav and Kumar, 2014b). With increasing solute concentrations there are two opposing mechanisms; firstly increasing solute concentrations will generally result in a greater amount of nucleation and hence smaller particles, secondly however, increasing the solute concentration will also increase the collision frequency between formed nuclei (Joye and McClements, 2013) which promotes aggregation and results in greater particle size. Generally, at relatively low concentrations, the nucleation mechanism will dominate and increasing solute concentration will result in smaller particle sizes, however once a critical concentration is reached, the aggregation mechanism will become more dominant and further increase in solute concentration will generate larger particles. In the cases of both curcumin and silymarin in our study, it is hypothesised that the mechanism of aggregation

was dominant and therefore larger particles were generated as solute concentration was increased in this study.

Through nanonisation using the MAP technique, the size of curcumin and silymarin particles were shown to be reduced from ~20µm and ~10µm, to ~150nm and ~80nm respectively. This size reduction can potentially improve bioavailability of curcumin, silymarin, and numerous other antioxidant compounds through alteration of their physicochemical properties. For instance, the Noyes-Whitney equation describes how smaller particles display enhanced dissolution velocity. Enhanced dissolution velocity is important for the oral consumption of bioactive compounds, which, once ingested will only remain in the gastro-intestinal (GI) tract for a finite period of time and, generally, must undergo dissolution (unless they are already small enough to pass through the epithelial lining of the gut) during this time to become bioavailable. Many unprocessed bioactive compounds found in food, such as quercetin and resveratrol, are poorly solubilised during transit through the GI tract and possess poorer bioavailability as a result. In addition, nanoparticles are known to increase the GI residence time by decreasing the impact of intestinal clearance mechanisms on bioactive compounds (they therefore move through the GI tract at a reduced speed) as well as causing greater interactions between nanoparticles and the GI walls due to their increased surface area to volume ratio (Wang et al., 2014); again, this can increase bioavailability of bioactive compounds. Improving dissolution velocity, and GI residence time is particularly important for compounds already identified as biopharmaceutical classification system class II or IV compounds, as these all suffer from poor solubility (Patel and Velikov, 2011). Therefore, the MAP technique could also be of use for numerous other bioactive compounds.

Using the MAP technique, it was possible to obtain a narrow particle polydispersity index (PDI) of < 0.1 and < 0.2 for curcumin and silymarin respectively. The PDI refers to the particle size distribution which is an important parameter affecting nanoparticle stability and behaviour upon consumption (i.e. release profile). Furthermore, particles with lower PDI's are inherently more stable as they are less susceptible to the effects of Ostwald ripening.

5.4.3 Crystallinity of nanoparticles

The degree of crystallinity of bioactive nanoparticles, as well as particle size, is known to affect dissolution velocity and can have a substantial impact on bioavailability (Babu and Nangia, 2011). Therefore, x-ray powder diffraction (XRPD) and differential scanning calorimetry (DSC) experiments were performed on both curcumin and silymarin nanoparticles as both raw (unprocessed) compounds and post-MAP processing to alleviate changes in their physical structures. Results are displayed in Figure 5-6.

XRPD results reveal the crystalline nature of both raw curcumin and silymarin as both of these materials showed intense, sharp peaks, indicative of a crystalline structure on the spectral line from 5-30° and 15-35° for curcumin and silymarin respectively. However, post-MAP processing XRPD results showed complete disappearance of these peaks for both curcumin (C4) and silymarin (S4) nanoparticles, which indicated that these materials were transformed from possessing a crystalline structure, to an amorphous one. This structural change will enhance the dissolution velocity and apparent solubility of these compounds.

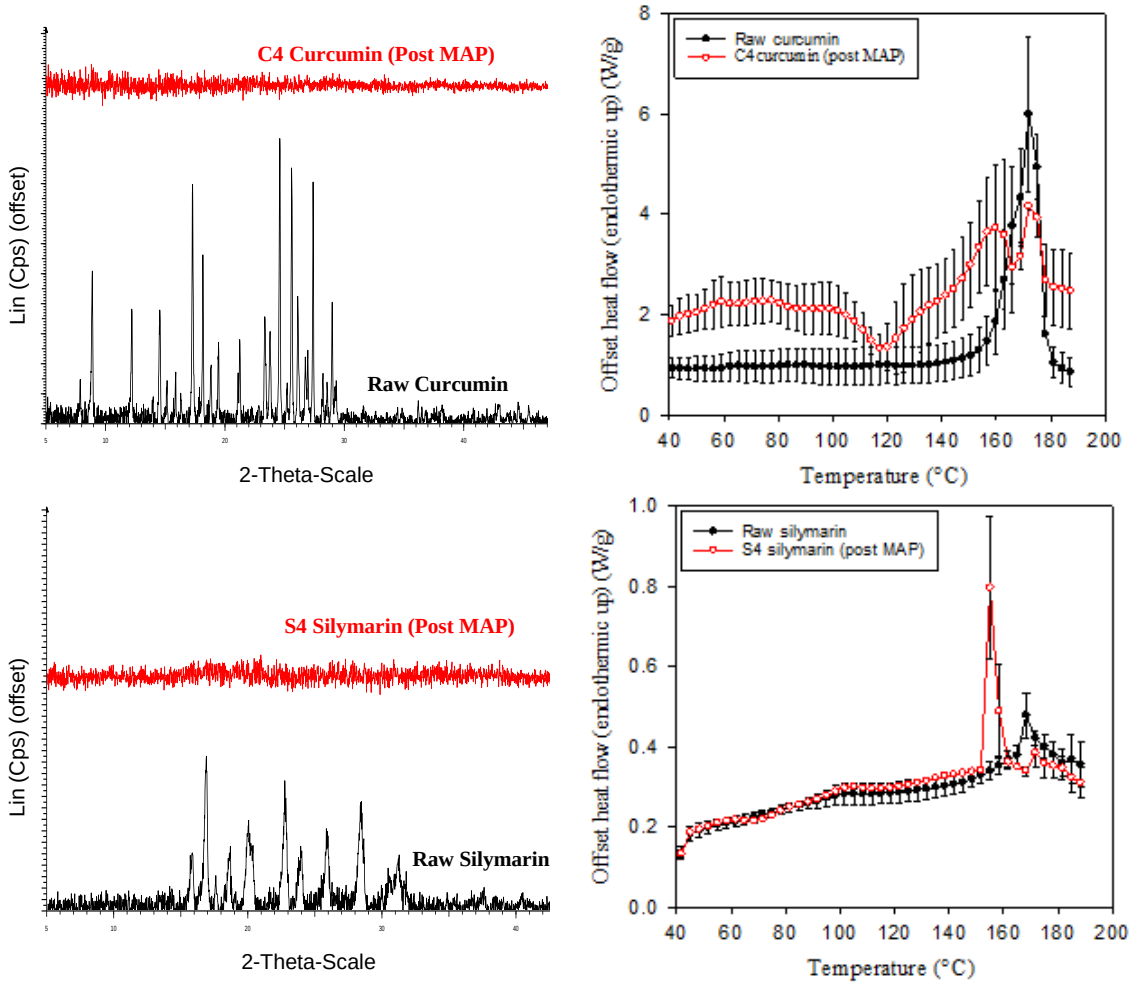

Figure 5-6: XRPD (left) and DSC (right) measurements for curcumin (above) and silymarin (below) compounds pre and post MAP processing.

A DSC study was conducted to provide further evidence to the changes in crystallinity of the two compounds. In its raw form, curcumin had a melting peak at 173°C, with a shoulder at 169°C. This shoulder at 169°C was likely due to the presence of curcumin polymorphs demethoxycurcumin and bisdemethoxycurcumin (Rege et al., 2012) which exist as impurities in the curcumin powder used in this study. However, post-MAP processing C4 curcumin now showed three peaks the first of which was an exothermic peak at around 119°C and this was likely the recrystallisation peak of amorphous curcumin. The next two peaks at 159°C and 172°C were endothermic, the first of which

was significantly less than the first melting peak (169°C) in the case of raw curcumin, which can be attributed to a reduction in crystallinity. However, the second endothermic peak at 172°C overlaps the endothermic peak found with raw curcumin, and this is likely due to the melting of the recrystallised curcumin encountered at 119°C. One further major difference between raw and MAP processed curcumin samples were in terms of their melting enthalpies (calculated by summating the enthalpies of each endothermic peak) which were found to be 132.0 and 51.3 J/g respectively. The significant reduction in melting enthalpy provides further evidence of a shift from a crystalline to a more amorphous structure (Centre, 2016) for curcumin post-MAP processing.

During the heating of silymarin samples from 40-200 °C, no melting peaks were found prior to the thermal decomposition of silymarin at temperatures over 155 °C. The effect of heating on unprocessed silymarin is depicted in Figure 5-7, showing images of the effect of thermal decomposition on both the hermetically sealed pan which becomes 'puffed up' as a result of vapour's given off during decomposition, and on silymarin powder of which only a black residue remained post-heating. There were two major endothermic peaks for silymarin as a result of thermal decomposition which were visible for both raw and MAP processed samples. With raw silymarin the first peak was very broad, with a peak temperature of 168°C, the second peak had a peak temperature of 185°C. However, post-MAP processing it was noted that these two thermal decomposition peaks had shifted to lower temperatures of 155°C and 172°C respectively, which meant there was a decrease in thermal decomposition temperature post-MAP processing. This could be for two reasons, firstly, the unprocessed silymarin is partially crystalline and therefore was able to withstand higher temperatures prior to decomposition than the amorphous post-processing silymarin. This view is reinforced by

a previous study on tobacco celluloses which found that the starting thermal decomposition temperature of these materials increased with increasing degree of crystallinity (Katō and Komorita, 1967). The decreased post-processing decomposition temperature could also be a result of decreased particle size following nanonisation, which increased contact area between the DSC pan and the sample; thus heat was transferred at an increased rate and lower temperatures were required to transmit the same amount of heat energy to initiate the thermal decomposition process.

Figure 5-7: Silymarin DSC pans pre (left) and post (right) heating (sealed (top) and uncovered (bottom) views).

5.4.4 Physical stability of formulated nanosuspensions

The majority of studies on antisolvent precipitation of polyphenolic nanoparticles tend to report on the use of surfactants to ensure stability of nanosuspensions (Hong et al., 2014, Nayak et al., 2017, Singh et al., 2018). However, in this study both curcumin and silymarin nanosuspensions were produced in the absence of any additional surfactants, thereby meaning these suspensions contained compound nanoparticles. The stability of several different formulations in terms of particle size were studied over a 30-day period and the results are displayed in Figure 5-8.

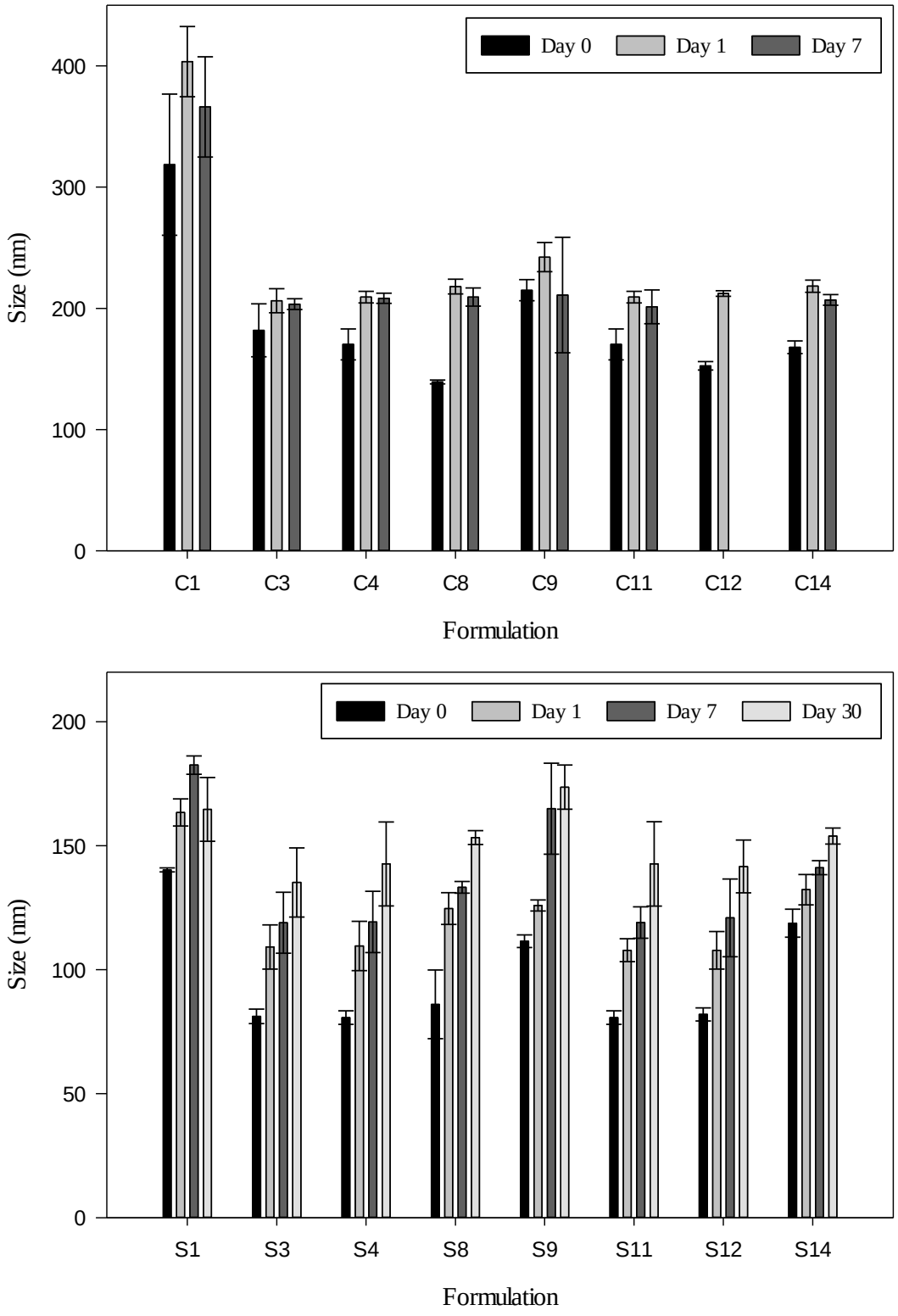

Figure 5-8: Physical stability of selected curcumin and silymarin formulations over a period of 7 and 30 days respectively.

In the case of all curcumin nanosuspensions there was an increase in size, even if sometimes minor, between day 0 and day 1 (e.g. C1 goes from 319 ± 58 nm on day 0 to 404 ± 29 nm on day 1). This can be attributed to the growth of nanoparticles following completion of nucleation via the MAP technique. This occurred due to refrigeration of nanosuspensions following initial size analysis on day 0 until they were sized again after one day. Therefore, during this time there was slow cooling and a reduction in solubility of curcumin (through refrigeration) which meant that the nanosuspensions again became supersaturated, although now the level of supersaturation was only great enough to allow for particle growth and not nucleation; therefore diffusible solute (curcumin) migrated to the surface of curcumin nanoparticles which resulted in particle growth. From day 1 to day 7 in the case of all curcumin formulations other than C12, there was either no change, or a reduction in nanoparticle size. The seemingly reduced particle sizes for C1 and C9 over this period can be attributed to a degree of particle sedimentation which was observed visually and naturally caused the largest particles to be removed from the size analysis resulting in a perceived reduction of particle size, however it is most likely that these formulations maintained a similar size to those recorded on day 1 in actuality. For C3, C4, C8, C11 and C14 there were no significant changes in particle size from day 1 to day 7 which exemplifies a key benefit of the MAP technique as the rapid removal of solvent ensured that there was only particle growth following the cooling of nanosuspensions which resulted in their immediate size increase but no significant long-term growth via Ostwald ripening due to the removal of solvent (and hence the removal of diffusible solute). C12 became destabilised after 1 day due to its low solute concentration in the formulation stage which ensured a low degree of supersaturation was attained along with a greater level of particle polydispersity which accelerated the process

of Ostwald ripening and hastened the destabilisation of C12 via growth and sedimentation. After around 15 days all curcumin formulations suffered major sedimentation and were no longer suitable for size analysis. However, the MAP technique clearly increased curcumin particle stability especially when compared to those nanosuspensions in which solvent was not removed (shown previously in Figure 5-3).

Likewise, with all silymarin formulations there was significant growth from day 0 to day 1 following sample refrigeration. Unlike curcumin however, all silymarin samples (other than S1) exhibited continued growth over a 30-day period. This can be attributed to the far greater aqueous solubility of silymarin compared to curcumin which is known to expedite the process of growth via Ostwald ripening (Yamashita et al., 2017).

Both curcumin and silymarin formed relatively stable compound nanoparticles in aqueous suspension whereas preliminary investigations in this study found that other polyphenolic compounds such as quercetin, hesperidin and morin hydrate agglomerated and suffered sedimentation immediately after undergoing the MAP technique; they were highly unstable. The relatively high physical stability of curcumin and silymarin nanoparticles can largely be attributed to their surface-active nature and high zeta potential following nanonisation via the MAP technique as is shown in Table 5-3.

Sample	Surface tension (mN/m)
Water	72.2 ± 0.2
Raw curcumin	72.2 ± 0.4
MAP curcumin (C4)	57.3 ± 0.7
Raw silymarin	60.9 ± 0.6
MAP silymarin (S4)	46.8 ± 0.7

Sample	Zeta potential (mV)
MAP curcumin (C4)	-31.2 ± 0.7
MAP silymarin (S4)	-39.2 ± 1.1

Table 5-3: Surface tension (left) and zeta potential (right) values for curcumin and silymarin compounds in various forms.

Raw curcumin was unable to reduce the surface tension of water and this was attributed to its relatively poor aqueous solubility and large crystal size (~20µm) which promoted flocculation of curcumin crystals and resulted in negligible adsorption of curcumin at the water-air interface. After undergoing the MAP technique however curcumin was able to significantly reduce surface tension. Silymarin even in its raw state significantly reduced surface tension, but its effect was also amplified following nanonisation. Following nanonisation via the MAP technique, the reduced size and crystallinity of both curcumin and silymarin nanosuspensions helps these compounds arrange at the interface (Nayak et al., 2017) between water and air and consequently reduced the surface tension. The surface-active nature of the two compounds following their nanonisation enhanced their colloidal stability in addition to increasing the nucleation rate (as a lower interfacial tension reduces the energy barrier to nucleation) and hence, increased the number of particles. Furthermore, the zeta potentials of both curcumin and silymarin

nanosuspensions following MAP processing are less than -30mv which, as a rule of thumb indicates good colloidal stability (Malvern, 2009) as these dispersed particles are able to effectively repel each other and hence, are resistant to agglomeration and aggregation. The increased reduction of surface tension and more negative zeta potential of silymarin compared to curcumin nanosuspensions was most likely the reason for its enhanced physical stability (stable in suspension for over 30 days) compared to curcumin.

5.4.5 The effect of solvent-antisolvent mixing

The MAP technique consists of two major stages in which particle formation occurs. The first of these occurs during the solvent-antisolvent mixing step, and the second during the solvent removal step via microwave irradiation. The bulk of current research into antisolvent precipitation techniques focuses on optimisation of the solvent-antisolvent mixing step through use of various mixing processes such as simple magnetic stirring (Kakran et al., 2012, Zu et al., 2014), confined impinging jet mixing (Han et al., 2012), sonoprecipitation (Dhumal et al., 2008, Jiang et al., 2012, Liu et al., 2010, Luque de Castro and Priego-Capote, 2007), and the use of supercritical fluids (Zhao et al., 2015). This section serves to investigate the importance of the mixing stage for curcumin and silymarin nanosuspensions and to see if this stage is of far greater importance than the solvent removal step in determining size of formulated nanoparticles. For these experiments, and in contrast to previously performed MAP experiments, solute-laden solvent was added to antisolvent (as described in Section 5.3.4). The flowrate of solvent addition, as well as the speed of stirring were adjusted and the impact of changing these parameters on nanoparticle size both immediately after mixing, and after mixing plus solvent removal (SR) through microwave heating is shown in Table 5-4.

Flow rate (ml/min)	Stirrer speed (RPM)	Curcumin		Silymarin	
		Size after mixing (nm)	Size after mixing + SR (nm)	Size after mixing (nm)	Size after mixing + SR (nm)
2	500	78.6 ± 4.3	183.4 ± 18.9	68.7 ± 1.4	81.7 ± 2.4
10	500	88.4 ± 6.4	195.1 ± 5.2	65.8 ± 4.4	75.7 ± 1.9
25	500	86.7 ± 5.1	181.9 ± 3.8	59.0 ± 2.6	74.9 ± 4.6
25	100	79.4 ± 2.5	191.2 ± 3.2	75.9 ± 1.2	87.1 ± 1.7
25	500	86.7 ± 5.1	181.9 ± 3.8	59.0 ± 2.6	74.9 ± 4.6
25	1500	74.0 ± 13.6	188.5 ± 11	47.7 ± 6.7	68.2 ± 1.2

Table 5-4: Effect of flow rate and mixing rate on the size of formulated curcumin and silymarin nanosuspensions.

In the case of curcumin nanosuspensions, neither adjustment of solvent flowrate from 2-25ml/min nor increased stirrer speed from 100-1500rpm had any significant effect of nanoparticle size measured either immediately after mixing or following mixing plus SR. In contrast, with silymarin nanosuspensions there was an appreciable decrease in particle size both with increasing solvent flowrate and increasing stirrer speed when measured either after mixing or after mixing plus solvent removal. These observations can be understood with reference to the Damkohler number (Da) which is a ratio of the time required for mixing (τ_{mix}) to the time required for precipitation ($\tau_{precipitation}$):

$$Da = \frac{\tau_{mix}}{\tau_{precipitation}} \qquad \textbf{(Equation 5-1)}$$

For values Da > 1, nucleation of particles is controlled by the mixing step (as mixing takes more time than precipitation) whereas for Da < 1 it is controlled by the precipitation

step (Thorat and Dalvi, 2012). With the formation of silymarin nanosuspensions, Da was likely to be greater than one for all investigated parameters because the mixing step impacted greatly upon particle size. Increasing solvent flowrate of silymarin increased the jet velocity and consequently the Reynolds number and shear forces of solvent contacting the antisolvent phase which enhanced mixing efficiency (Kakran et al., 2012). In addition, increased stirrer speed ensured faster mixing of the two phases. Therefore, increasing both these parameters led to the generation of a greater level of supersaturation, which was more uniformly spread throughout the mixture and smaller particles were formed as a result. In comparison to looking at the effect of other process and formulation parameters on the size of silymarin nanosuspensions in Figure 5-5, the impact of mixing appeared to have a relatively large effect. This further reinforces the view that in the case of silymarin nanosuspensions, the size and number of particles generated is dictated almost entirely during the solvent-antisolvent mixing step and not during the solvent removal step.

In the case of curcumin nanosuspensions however $Da < 1$, and therefore the time required for mixing in all cases investigated, was less than that required for precipitation. It is perhaps surprising that the precipitation time for curcumin is greater than for silymarin given the far lower aqueous solubility of curcumin which would be expected to result in higher supersaturation and faster precipitation. However, this was not found to be the case, and the faster precipitation of silymarin could instead be attributed to its ability to reduce the interfacial tension in the solvent antisolvent mixture (as was shown in Table 5-3) which is an important factor in increasing the rate of nucleation.

5.4.6 Dielectric versus thermal heating

The MAP technique makes use of dielectric heating to remove solvent in SAS mixtures. This section focused on a comparison of both initial sizes and stabilities of formulated curcumin nanosuspensions in which either dielectric (microwave) heating was used via the MAP technique, or more conventional thermal (conductive) heating (TH) was used through rotary evaporation to remove ethanol from SAS mixtures. Silymarin nanosuspensions were already confirmed to be unaffected by the rate of solvent removal and therefore this compound was not considered in this particular study.

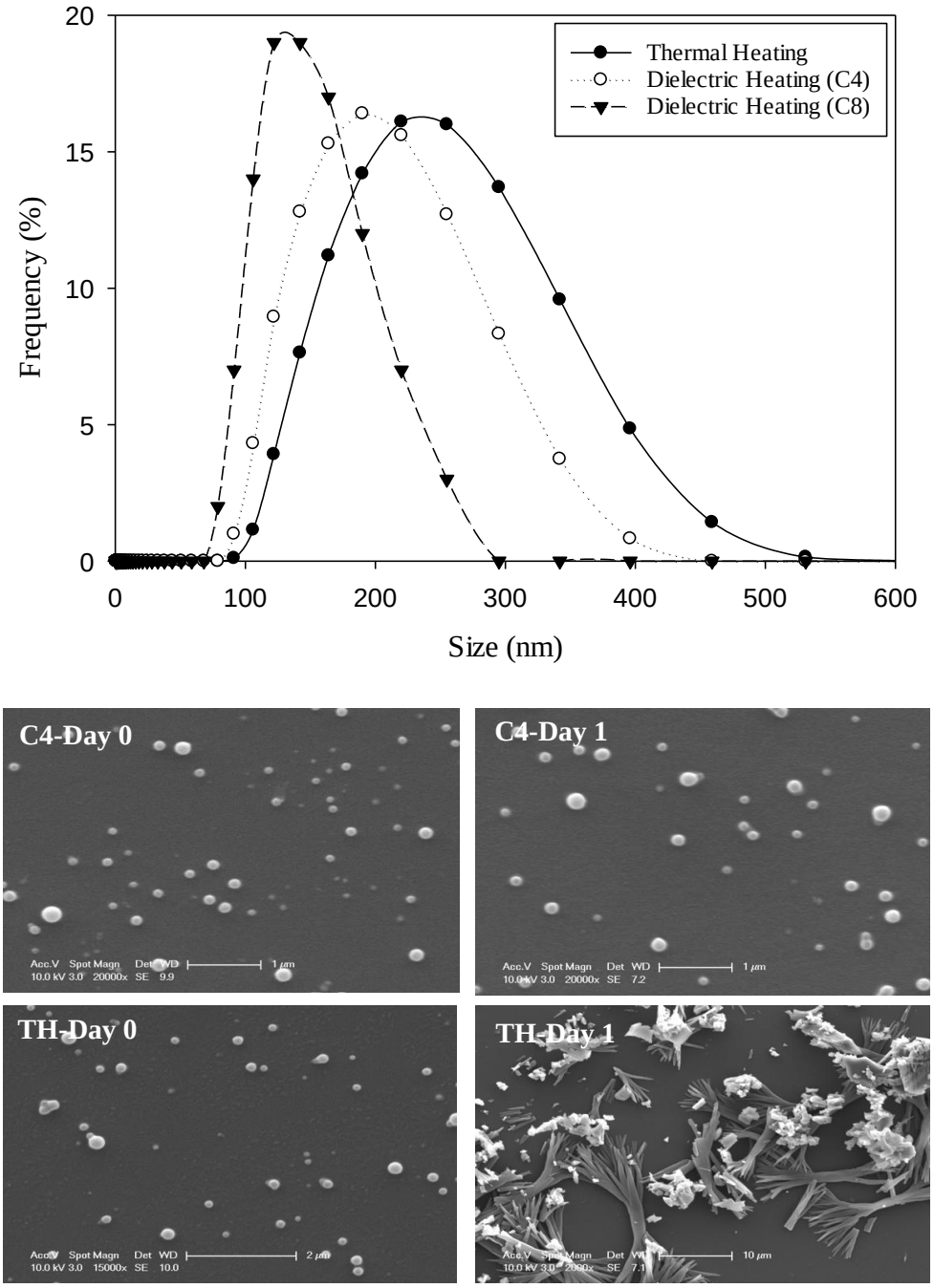

Figure 5-9: Size distributions of curcumin nanosuspensions (top) in which solvent has been removed through dielectric heating (50W, 240s (C4) / 800W, 15s (C8)) or thermal heating (TH) and SEM images (bottom) showing selected formulations on day 0 and day 1.

Previous studies had found that when the mixing step in antisolvent precipitation processes was carried out for long durations, this caused aggregation due to the high

surface energy of nanoparticles (Yadav and Kumar, 2014a) which consequently led to an increase in nanoparticle size. Therefore, it was logical to expect that the speed of rotation during rotary evaporation (thermal heating) could affect particle size. Therefore, preliminary testing was performed which found that the speed of rotation had no significant impact on the initial average sizes of curcumin nanosuspensions in the range of 30-120rpm, therefore, rotary evaporation for thermal heating was carried out at 30rpm.

As shown in Figure 5-9, nanosuspensions produced using the MAP technique for 15 seconds at 800W (C8) were found to be significantly smaller and less polydispersed than those produced through thermal heating for 240 seconds. This shows a key benefit of the MAP technique as dielectric heating allows for ethanol removal in far less time than thermal heating, therefore making it more favourable for commercialisation.

The initial average size distributions of nanosuspensions produced using the MAP technique for 240 seconds at 50W (C4) and thermal heating for 240 seconds were similar, as were their shapes, both of which appeared to be spherical through SEM imaging. The major difference in these nanosuspensions came in their stability; C4 nanoparticles were stable for > 1 day whereas thermally heated nanoparticles displayed multiple signs of instability including aggregation, sedimentation and formation of large crystal structures which was observed in SEM images (TH-Day 1).

This difference in nanosuspension stability can be attributed to the unique properties of dielectric heating which allows ethanol solvent to be rapidly, volumetrically, and even selectively removed due to the favourable dielectric properties of ethanol over water. This ultimately resulted in the faster, more effective solvent removal when dielectric, rather than conventional thermal heating was used. Thermal heating led to reduced ethanol

evaporation which increased particle growth through Ostwald ripening (due to increased curcumin solubility), and this caused greater instability of formed nanoparticles. Furthermore, with less solvent evaporation and, a reduced rate, the degree of supersaturation generated in solvent-antisolvent mixtures was reduced which resulted in less nucleation, and a greater effect of particle growth on particle size in line with the LaMer mechanism (LaMer and Dinegar, 1950) which created additional instability.

5.5 Conclusions

For the first time in this study, the microwave-assisted antisolvent precipitation technique has been investigated for the synthesis of aqueous nanosuspensions. Using this technique, curcumin and silymarin compounds were successfully size reduced from sizes of around 20µm and 10µm to sizes of 0.2µm and 0.1µm respectively. These initially crystalline materials were also transformed to an amorphous morphology after undergoing the MAP technique. Both these changes are known to enhance dissolution velocity and apparent solubility of bioactive compounds and these are important parameters in determining oral bioavailability if these polyphenols are incorporated into food or pharmaceutical products.

The MAP technique was however found to be far more suitable for the synthesis of curcumin rather than silymarin nanosuspensions, and this was primarily attributed to the vastly different aqueous solubilities of the two compounds. The MAP technique essentially consists of two key stages for particle formation, (1) the mixing of solvent and antisolvent phases and (2) the solvent removal stage. In the case of curcumin, the importance of solvent removal was first illustrated with nanosuspensions destabilising far faster when solvent was not removed. Furthermore, dielectric heating immediately

following the mixing of solvent and antisolvent phases allowed for volumetric and selective heating which enabled rapid solvent removal from the solvent-antisolvent mixture. This resulted in the attainment of a high level of supersaturation and consequently the formation of a greater number of (invariably) smaller particles. The physical stability of these samples was found to be highly dependent on process and formulation parameters chosen. The mixing intensity of curcumin solvent with antisolvent was found to be insignificant in determining nanoparticle size, which meant that the mixing time was far less than the precipitation time for curcumin in this study. Although curcumin nanosuspensions prepared via the MAP technique were of similar initial size to those obtained through use of thermal heating, their stability was significantly enhanced and this was attributed to the increased efficiency of solvent removal when dielectric heating was used.

With fabrication of silymarin nanosuspensions however, the solvent removal stage was found to have little impact on the size or stability of formulated nanosuspensions. Moreover, the rate of solvent removal had no bearing on nanoparticle size. This was attributed to the far greater aqueous solubility of silymarin as opposed to curcumin meaning that whether or not solvent was removed, silymarin still possessed relatively high solubility within formulated nanosuspensions. Conversely to curcumin, the intensity of mixing was found to have significant impact on silymarin nanoparticle size, meaning that the Damkohler number for silymarin was greater than one and particle nucleation was mixing controlled as opposed to a Damkohler number of less than one for curcumin in which the nucleation process was precipitation controlled.

This study clearly suggests that the MAP technique is more suitable for compounds which possess lower aqueous solubility's as this effectively increases the importance of the solvent removal step in generating a 'second wave' of supersaturation following the mixing of solvent and antisolvent phases. Although the rate of solvent removal may be unimportant in attaining greater particle formation for some compounds like silymarin, the MAP technique has been shown to impart no detrimental impact on particle size or stability when solvent removal is carried out at greater rates so it allows, even in these cases, for time savings to be made during formulation of nanosuspensions. The MAP technique represents a form of 'green energy' due to its design allowing for both any solvent used to be evaporated, recondensed then reused and the fact that it is a highly energy efficient heating mechanism. This makes the MAP technique highly attractive for more future research and eventual commercialisation.

CHAPTER 6: OVERALL CONCLUSIONS AND RECCOMENDATIONS FOR FUTURE WORK

6.1 Overall conclusions

6.1.1 The efficacy of natural antioxidants at combatting lipid oxidation within different O/W emulsion environments.

One aim of this research was to illustrate how a range of oil-in-water (O/W) emulsion environments impacted on the efficacy of natural antioxidants in combatting lipid oxidation (LO). Results detailed the importance of molecular structure on the antioxidant activity of four natural compounds, namely, quercetin, curcumin, rutin hydrate and ascorbic acid. Antioxidants in possession of a molecular structure which allowed for the greater donation of hydrogen atoms, the greater chelation of prooxidant metals or more effective partitioning within O/W emulsions were found to combat LO more effectively.

The addition of prooxidant ferrous iron to emulsion environments only served to reduce the antioxidant efficacy with all tested compounds and often changed the behaviour of the four 'antioxidant' compounds so that they exhibited a prooxidant effect. Therefore, it is believed that the ability of each compound to chelate ferrous metal ions is far outweighed by the dramatic change in each compounds behaviour in the presence of ferrous iron.

The polarity of different compounds was shown to be paramount in determining their efficacy within different oil-phase volume environments which was due to their altered partitioning behaviour within different emulsion formulations. After investigating combinations of antioxidants in different O/W emulsion environments, synergistic behaviour was found alongside antagonistic and simply additive antioxidant behaviour.

Where synergism was found this was attributed primarily to the different antioxidant mechanisms possessed by each compound which illustrates the importance of using highly dissimilar antioxidants when used in combination.

Overall, this work has shown how changes to emulsion environments can have a profound effect on the efficacy and behaviour of natural antioxidants. Thus, it is imperative to fully understand the environment of any emulsion food formulation prior to the incorporation of natural antioxidants with a view to combatting LO.

6.1.2 Natural antioxidant Pickering particles for O/W emulsion dual-purpose stabilisation.

The novel and dual-purpose use of antioxidant rutin hydrate Pickering particles to provide O/W emulsions with both physical and oxidative stability was assessed. RH antioxidant particles were found to be able to effectively physically stabilise O/W emulsions which was largely due to their polarity allowing them to locate at the oil-water interface. Formulated RH emulsions were physically stable for at least 14 days and provided superior oxidative stability in comparison to conventional emulsifier's polysorbate 20 and sodium dodecyl sulphate and therefore, RH particles were shown to be capable of providing a dual-purpose stabilisation effect to O/W emulsions. However, as an emulsifier RH was found to offer inferior oxidative stability to emulsions compared to whey protein isolate and this was attributed to the fact that RH particles were found to be unable to produce a continuous and effective physical barrier at the oil-water interface and thus were unable to effectively shield oil droplets from oxidative attack. This was hypothesised to be due to the RH Pickering particles themselves which were relatively large, polydispersed, and irregularly shaped due to how they were produced which hindered their effective positioning at the oil-water interface.

The efficacy of RH Pickering emulsions to combat RH was found to be highly dependent on the pH of formulated emulsions, which was attributed to changes in zeta potential values, and hence the surface charge of emulsion droplets under different pH values. Therefore, special consideration must be given to the pH of a food emulsion (which can vary dramatically depending on the food product) before using Pickering particles for antioxidant purposes.

Furthermore, for the first time in this study, the effect of emulsion droplet size on LO was quantified, isolated and subtracted from the levels of primary and secondary oxidation products generated in emulsion samples depending on their average droplet size which allowed other LO factors to be assessed more independently. This work therefore provides a new and novel method for dealing with the many contradictory literature findings concerning the impact of droplet size on oxidative stability.

6.1.3 Development of a scalable nanonisation technique for low-aqueous solubility antioxidant compounds.

The microwave-assisted antisolvent precipitation (MAP) technique was presented as a novel and promising new technique for the production of antioxidant nanoparticles suspended in aqueous media. The MAP technique was shown to be capable of rapidly removing solvent from solvent-antisolvent mixtures (in which an antioxidant solute was dissolved in the solvent phase) to create a ‘second wave’ of supersaturation and particle formation and was thus able to generate stable nanosuspensions. Using MAP, curcumin and silymarin antioxidant compounds were dramatically size-reduced and both materials were transformed from exhibiting crystalline structures before processing to a more amorphous structure post processing. Through using the MAP technique to achieve these changes, it is possible to potentially enhance the bioavailability of poorly soluble

antioxidant compounds. As a relatively simple, rapid, and green-energy process, the MAP technique has shown tremendous potential for being scaled-up and used commercially for both food and pharmaceutical applications.

6.2 Future work recommendations

This section highlights key recommendations for future research, based on the findings of this thesis.

1. Specific examination of the effect of oil phase volume itself on lipid oxidation.

Research in Chapter 3 investigated the efficacy of different antioxidants in O/W emulsions with a range of oil phase volumes. However, during this study it was also found that the oxidative stability of control emulsions in which no antioxidants were added decreased with increasing oil phase volume. This trend contrasted with previously reported findings in the literature but was not further investigated in Chapter 3 as it was not within the scope of this current study. Due to the contrasting findings it is suggested that the specific effect of oil phase volume on LO is investigated.

In chapter 3, the hypothesis with respect to the effect of oil phase volume on LO was that it did not follow the same trend reported in literature due to high quantities of prooxidants harboured within the oil phase of emulsions. It is therefore recommended to test this hypothesis by assessing the oxidative stability of several different oils with respect to oil phase volume. Quantification of key prooxidant species such as iron, copper, hydroperoxides and secondary oxidation products should first be carried out. Assessment of the oxidation of these oils should then be measured and oils which display increased oxidative stability with increased oil phase volumes (a finding reported in the vast majority of previous studies) can then be compared with the sunflower oil used in

this study. These oxidative stability results should then be compared again after the addition of prooxidants (i.e. ferrous iron). Crucially, if it is proven that oils exhibit increased oxidative stability with increasing oil phase volume when no prooxidants are added and then show the opposite trend when subjected to added prooxidants, then the concluding hypothesis stated in Chapter 3 was correct, otherwise it was incorrect.

2. Investigate combinations of natural antioxidants with compounds which possess clear dominant antioxidant mechanisms.

One of the key reasons for current research into the use of natural antioxidants to combat LO in food products is that there is great demand from both consumers and industry to replace synthetic, and often highly effective antioxidants with natural alternatives. Natural antioxidants are typically not as potent or as effective at combatting LO, and furthermore these are often compounds with strong flavours, colours and aromas (i.e. curcumin); therefore it is typically desirable to add as little of these compounds as possible in food products. Therefore, it is crucial to enhance the efficacy of natural antioxidants without increasing their concentration, and the potential to achieve this through utilisation of antioxidant combinations was exemplified in Chapter 3.

Where antioxidant synergy was reported in this study, it was primarily attributed to the use of antioxidants which exhibited antioxidant activity through different antioxidant mechanisms, for example, in the case of ascorbic acid and quercetin. However, antioxidants tested in this study did not possess clear, dominant antioxidant mechanisms, as natural compounds they all possessed a degree of radical scavenging activity, metal chelating ability, oxygen quenching capacity etc. This made it difficult to confidently conclude that use of different antioxidants resulted in synergistic behaviour due to their

array of potent antioxidant mechanisms. Future studies should therefore start by assessing the oxidative stabilities of emulsions in which combinations of natural antioxidants with ethylenediaminetetraaceticacid (EDTA) (a compound with a well-defined dominant antioxidant activity to chelate metal ions) are assessed and compare the oxidative stability they offer with predicted oxidative stabilities if the antioxidant activity was simply additive. This assessment should be conducted in control emulsions containing no added prooxidant metals, as well as under increased prooxidant metal concentrations. It would be especially interesting to see if the addition of a potent metal chelating antioxidant such as EDTA, could prevent prooxidant activity of natural antioxidants such as quercetin, curcumin and rutin hydrate when exposed to higher prooxidant metal concentrations, because otherwise the finding from Chapter 3 that higher metal concentrations switch the behaviour of certain compounds from antioxidant to prooxidant would limit their application to environments with either no or very low amounts of prooxidant metals.

3. Investigate the use of antioxidant nanoparticles formed via the MAP technique as Pickering particles to combat lipid oxidation in O/W emulsions.

The most clear and obvious recommendation from research described in this thesis is to attest a hypothesis formed in Chapter 4. In this chapter it was observed via polarised light microscopy that RH Pickering particles were perhaps hindered in their ability to combat LO in emulsions due to their inability to form a continuous, and effective barrier at the oil-water interface to shield the lipid (oil) phase from oxidative attack. The inability of RH Pickering particles to form an effective barrier was concluded to be due to their large size, polydispersity, and irregular shapes. Due to the promising results displayed within this chapter which found that RH was able to provide dual-purpose functionality to O/W emulsions, at least to some degree, more research is highly warranted into the use of

antioxidant Pickering particles to stabilise O/W emulsions both physically and oxidatively.

Fortunately, research in Chapter 5 illustrated the use of a highly promising MAP technique for the formation of antioxidant nanoparticles. Using the MAP technique, it was possible to produce nanoparticles of a range of sizes by simply adjusting processing/formulation parameters. Once antioxidant nanoparticles are produced via the MAP technique with a defined range of sizes, their efficacy as Pickering emulsifiers should be assessed with particular focus on the impact of particle size on antioxidant efficacy. The effectiveness of antioxidant Pickering particles should also be compared with Pickering particles which harbour no significant conventional antioxidant activity such as silica, solid-lipid or starch nanoparticles. The ability of Pickering particles to locate precisely at the oil-water interface, where the bulk of oxidative reactions are known to occur, is an ability which could be very important indeed if these particles also possess conventional antioxidant activity. After all, many studies have detailed the importance of antioxidant partitioning in determining their efficacy it would therefore be logical to find that the precise placement of antioxidants at the site of LO reactions could greatly enhance their efficacy.

4. **Investigate the capability of the MAP technique to form composite nanoparticles.**

The main purpose of the MAP technique in this thesis was as a method of production for antioxidant and other bioactive nanoparticles in aqueous suspensions. This was predominantly performed to enhance the dissolution velocity and potentially the bioavailability of particular bioactive compounds. However, in order to enhance

bioavailability of many bioactive compounds, nanonisation is only part of the solution and will not automatically result in their bioavailability enhancement upon consumption within a food or pharmaceutical product. This is because bioactive compounds typically suffer limited oral bioavailability for a variety of different reasons. In the case of curcumin for example, this antioxidant compound is known to undergo rapid degradation in the presence of light, oxygen and in alkaline conditions such as those encountered within the gastro-intestinal tract and prior to its absorption into systemic circulation. Curcumin is also believed to be poorly absorbed in the small intestine and into the bloodstream.

Therefore, it is recommended that the MAP technique is assessed for its capacity to produce composite, rather than compound antioxidant nanoparticles which were formed in the current study. These nanoparticles of greater complexity could be designed in a way to overcome all bioavailability issues associated with a particular antioxidant compound. For example, curcumin nanoparticles could be encapsulated in a suitable food grade material to shield it from light and oxygen in storage as well as protect it from the alkaline conditions encountered during its voyage through the alimentary canal and assist in its transport from the small intestine into the bloodstream. The bioavailability enhancement of MAP-formed composite nanoparticles should be compared to that of compound (but otherwise identical) nanoparticles. Bioavailability assessment should be made through investigation of several important facets which are known to hinder bioavailability. In the case of curcumin, the dissolution enhancement could be analysed through use of a standard paddle stirrer to compare dissolution velocities of curcumin before and after processing via MAP. DPPH free radical scavenging and Ferrozine assays should be used to assess any changes in antioxidant activity as a result of MAP processing. Caco-2 cells lines should be used to assess the absorbance of formed

nanoparticles across the intestinal wall and into systemic circulation. This would serve to further illustrate the credentials of MAP as a technique to enhance the bioavailability of a compound rather than solely as a method to nanonise bioactive compounds. Crucially, this research would aid in the future commercialisation of the MAP technique.

CHAPTER 7: REFERENCES

References

1. AANEBY, J. 2012. Iron Catalyzed Lipid Oxidation in Emulsions and the Influence of Antioxidants. Master's thesis. Norwegian institute of Science and Technology.

2. ABENAVOLI, L., CAPASSO, R., MILIC, N. & CAPASSO, F. 2010. Milk thistle in liver diseases: past, present, future. *Phytotherapy Research,* 24**,** 1423-1432.

3. ADITYA, N. P., MILLS, T. & NORTON, I. 2016. Lipid Based Nanosystems for Curcumin: Past, Present and Future. *Current Pharmaceutical Design,* 22**,** 4247-4256.

4. AFTAB, N. & VIEIRA, A. 2010. Antioxidant activities of curcumin and combinations of this curcuminoid with other phytochemicals. *Phytotherapy Research,* 24**,** 500-502.

5. AGUIRRE, L., ARIAS, N., TERESA MACARULLA, M., GRACIA, A. & P PORTILLO, M. 2011. Beneficial effects of quercetin on obesity and diabetes. *The Open Nutraceuticals Journal,* 4.

6. AHMED, M., PICKOVA, J., AHMAD, T., LIAQUAT, M., FARID, A. & JAHANGIR, M. 2016. Oxidation of Lipids in Foods. *Sarhad Journal of Agriculture,* 32**,** 230-238.

7. AKOH, C. & B. MIN, D. 2002. Food Lipids: Chemistry, Nutrition, Biotechnology, New York, Marcel Dekker.

8. ALAMED, J., CHAIYASIT, W., MCCLEMENTS, D. J. & DECKER, E. A. 2009. Relationships between Free Radical Scavenging and Antioxidant Activity in Foods. *Journal of Agricultural and Food Chemistry,* 57**,** 2969-2976.

9. AMIĆ, D., STEPANIĆ, V., LUČIĆ, B., MARKOVIĆ, Z. & DIMITRIĆ MARKOVIĆ, J. M. 2013. PM6 study of free radical scavenging mechanisms of flavonoids: why does O–H bond dissociation enthalpy effectively represent free radical scavenging activity? *Journal of Molecular Modeling,* 19**,** 2593-2603.

10. AMMAR, R. B., BHOURI, W., SGHAIER, M. B., BOUBAKER, J., SKANDRANI, I., NEFFATI, A., BOUHLEL, I., KILANI, S., MARIOTTE, A.-M., CHEKIR-GHEDIRA, L., DIJOUX-FRANCA, M.-G. & GHEDIRA, K. 2009. Antioxidant and free radical-scavenging properties of three flavonoids isolated from the leaves of Rhamnus alaternus L. (Rhamnaceae) : A structure-activity relationship study. *Food Chemistry,* 116**,** 258-264.

11. ANWAR, H., HUSSAIN, G. & MUSTAFA, I. 2018. Antioxidants from Natural Sources. IntechOpen.

12. ARTS, M. J., HAENEN, G. R., WILMS, L. C., BEETSTRA, S. A., HEIJNEN, C. G., VOSS, H. P. & BAST, A. 2002. Interactions between flavonoids and proteins: effect on the total antioxidant capacity. *J Agric Food Chem,* 50**,** 1184-7.

13. BABU, N. J. & NANGIA, A. 2011. Solubility Advantage of Amorphous Drugs and Pharmaceutical Cocrystals. *Crystal Growth & Design,* 11**,** 2662-2679.

14. BAIGRIE, B. D. 2003. TAINTS | Types and Causes. In: CABALLERO, B. (ed.) *Encyclopedia of Food Sciences and Nutrition (Second Edition).* Oxford: Academic Press.

15. BARRIUSO, B., ASTIASARÁN, I. & ANSORENA, D. 2013. A review of analytical methods measuring lipid oxidation status in foods: a challenging task. *European Food Research and Technology,* 236**,** 1-15.

16. BASNIWAL, R. K., KHOSLA, R. & JAIN, N. 2014. Improving the Anticancer Activity of Curcumin Using Nanocurcumin Dispersion in Water. *Nutrition and Cancer,* 66**,** 1015-1022.

17. BENDARY, E., FRANCIS, R. R., ALI, H. M. G., SARWAT, M. I. & EL HADY, S. 2013. Antioxidant and structure–activity relationships (SARs) of some phenolic and anilines compounds. *Annals of Agricultural Sciences,* 58**,** 173-181.

18. BERKER, K., GÜÇLÜ, K., DEMIRATA, B. & APAK, R. 2010. A novel antioxidant assay of ferric reducing capacity measurement using ferrozine as the colour forming complexation reagent. *Anal. Methods,* 2**,** 1770-1778.

19. BERTON-CARABIN, C., ROPERS, M.-H., BERTRAND, D., VIAU, M. & GENOT, C. 2012. Oxidative stability of oil-in-water emulsions stabilised with protein or surfactant emulsifiers in various oxidation conditions. *Food Chemistry - FOOD CHEM,* 131.

20. BERTON-CARABIN, C. C., ROPERS, M.-H. & GENOT, C. 2014. Lipid Oxidation in Oil-in-Water Emulsions: Involvement of the Interfacial Layer. *Comprehensive Reviews in Food Science and Food Safety,* 13**,** 945-977.

21. BEYER, R. E. 1994. The role of ascorbate in antioxidant protection of biomembranes: interaction with vitamin E and coenzyme Q. *Journal of bioenergetics and biomembranes,* 26**,** 349-358.

22. BORS, W., MICHEL, C. & SCHIKORA, S. 1995. Interaction of flavonoids with ascorbate and determination of their univalent redox potentials: A pulse radiolysis study. *Free Radical Biology and Medicine,* 19**,** 45-52.

23. BREVEDAN, M. I. V., CARELLI, A. A. & CRAPISTE, G. H. 2000. Changes in composition and quality of sunflower oils during extraction and degumming. *Grasas y Aceites,* 51**,** 417-423.

24. BROCK, S. L. 2004. Nanostructures and Nanomaterials: Synthesis, Properties and Applications. *Journal of the American Chemical Society,* 126**,** 14679-14679.

25. BROUGH, C. & WILLIAMS, R. O. 2013. Amorphous solid dispersions and nano-crystal technologies for poorly water-soluble drug delivery. *International Journal of Pharmaceutics,* 453**,** 157-166.

26. C. HIDER, R., D. LIU, Z. & KHODR, H. 2001. Metal Chelation of Polyphenols. *Methods in enzymology,* 335**,** 190-203.

27. CALEJA, C., BARROS, L., ANTONIO, A. L., OLIVEIRA, M. B. P. P. & FERREIRA, I. C. F. R. 2017. A comparative study between natural and synthetic antioxidants: Evaluation of their performance after incorporation into biscuits. *Food Chemistry,* 216**,** 342-346.

28. CELIKBILEK ERSUNDU, M., ERSUNDU, A. E. & AYDIN, S. 2012. Crystallization Kinetics of Amorphous Materials.

29. CENGIZ, A., KAHYAOGLU, T., SCHRÖEN, K. & BERTON-CARABIN, C. 2019. Oxidative stability of emulsions fortified with iron: the role of liposomal phospholipids. *Journal of the Science of Food and Agriculture,* 99**,** 2957-2965.

30. CENTRE, P. L. S. 2016. Differential Scanning Calorimetry [Online]. Available: http://pslc.ws/macrog/dsc.htm [Accessed 25/10/2016 2016].

31. CHAN, H.-K. & KWOK, P. C. L. 2011. Production methods for nanodrug particles using the bottom-up approach. *Advanced Drug Delivery Reviews,* 63**,** 406-416.

32. CHAPMAN, R. A. & MACKAY, K. 1949. The estimation of peroxides in fats and oils by the ferric thiocyanate method. *Journal of the American Oil Chemists' Society,* 26**,** 360-363.

33. CHOE, E. & MIN, D. B. 2009. Mechanisms of Antioxidants in the Oxidation of Foods. *Comprehensive Reviews in Food Science and Food Safety,* 8**,** 345-358.

34. CORREDDU, F., NUDDA, A., MANCA, M. G., PULINA, G. & DALSGAARD, T. K. 2015. Light-induced lipid oxidation in sheep milk: effects of dietary grape seed and linseed, alone or in combination, on milk oxidative stability. *J Agric Food Chem,* 63**,** 3980-6.

35. CORY, H., PASSARELLI, S., SZETO, J., TAMEZ, M. & MATTEI, J. 2018. The Role of Polyphenols in Human Health and Food Systems: A Mini-Review. *Frontiers in nutrition,* 5**,** 87-87.

36. DAI, F., CHEN, W.-F. & ZHOU, B. 2008. Antioxidant synergism of green tea polyphenols with α-tocopherol and l-ascorbic acid in SDS micelles. *Biochimie,* 90**,** 1499-1505.

37. DANIEL, S., LIMSON, J. L., DAIRAM, A., WATKINS, G. M. & DAYA, S. 2004. Through metal binding, curcumin protects against lead- and cadmium-induced lipid peroxidation in rat brain homogenates and against lead-induced tissue damage in rat brain. *Journal of Inorganic Biochemistry,* 98**,** 266-275.

38. DASGUPTA, A. & KLEIN, K. 2014. Chapter 2 - Methods for Measuring Oxidative Stress in the Laboratory. *In:* DASGUPTA, A. & KLEIN, K. (eds.) *Antioxidants in Food, Vitamins and Supplements.* San Diego: Elsevier.

39. DE ARAÚJO, M. E. M. B., MOREIRA FRANCO, Y. E., ALBERTO, T. G., SOBREIRO, M. A., CONRADO, M. A., PRIOLLI, D. G., FRANKLAND SAWAYA, A. C. H., RUIZ, A. L. T. G., DE CARVALHO, J. E. & DE OLIVEIRA CARVALHO, P. 2013. Enzymatic de-glycosylation of rutin improves its antioxidant and antiproliferative activities. *Food Chemistry,* 141**,** 266-273.

40. DE FOLTER, J. W. J., VAN RUIJVEN, M. W. M. & VELIKOV, K. P. 2012. Oil-in-water Pickering emulsions stabilized by colloidal particles from the water-insoluble protein zein. *Soft Matter,* 8**,** 6807-6815.

41. DE SOUZA, R. F. & DE GIOVANI, W. F. 2004. Antioxidant properties of complexes of flavonoids with metal ions. *Redox Rep,* 9**,** 97-104.

42. DEYRIEUX, C., VILLENEUVE, P., BARÉA, B., DECKER, E. A., GUILLER, I., MICHEL SALAUN, F. & DURAND, E. 2018. Measurement of Peroxide Values in Oils by Triphenylphosphine/Triphenylphosphine Oxide (TPP/TPPO) Assay Coupled with FTIR-ATR Spectroscopy: Comparison with Iodometric Titration. *European Journal of Lipid Science and Technology,* 120**,** 1800109.

43. DHUMAL, R. S., BIRADAR, S. V., YAMAMURA, S., PARADKAR, A. R. & YORK, P. 2008. Preparation of amorphous cefuroxime axetil nanoparticles by sonoprecipitation for enhancement of bioavailability. *Eur J Pharm Biopharm,* 70**,** 109-15.

44. DICKINSON, E. 2009. 2 - Hydrocolloids and emulsion stability. *In:* PHILLIPS, G. O. & WILLIAMS, P. A. (eds.) *Handbook of Hydrocolloids (Second Edition).* Woodhead Publishing.

45. DINIS, T. C. P., MADEIRA, V. M. C. & ALMEIDA, L. M. 1994. Action of Phenolic Derivatives (Acetaminophen, Salicylate, and 5-Aminosalicylate) as Inhibitors of Membrane Lipid Peroxidation and as Peroxyl Radical Scavengers. *Archives of Biochemistry and Biophysics,* 315**,** 161-169.

46. DOMÍNGUEZ, R., PATEIRO, M., GAGAOUA, M., BARBA, F. J., ZHANG, W. & LORENZO, J. M. 2019. A Comprehensive Review on Lipid Oxidation in Meat and Meat Products. *Antioxidants (Basel, Switzerland),* 8**,** 429.

47. DONNELLY, J. L., DECKER, E. A. & MCCLEMENTS, D. J. 1998. Iron-Catalyzed Oxidation of Menhaden Oil as Affected by Emulsifiers. *Journal of Food Science,* 63**,** 997-1000.

48. DOW, M., MOLINARO, A., COOPER, R. M. & NEWMAN, M.-A. 2010. Chapter 40 - Microbial glycosylated components in plant disease. *In:* HOLST, O.,

BRENNAN, P. J., ITZSTEIN, M. V. & MORAN, A. P. (eds.) *Microbial Glycobiology.* San Diego: Academic Press.

49. EBERT, S., KOO, C. K. W., WEISS, J. & MCCLEMENTS, D. J. 2017. Continuous production of core-shell protein nanoparticles by antisolvent precipitation using dual-channel microfluidization: Caseinate-coated zein nanoparticles. *Food Research International,* 92**,** 48-55.

50. EGHBALIFERIZ, S. & IRANSHAHI, M. 2016. Prooxidant Activity of Polyphenols, Flavonoids, Anthocyanins and Carotenoids: Updated Review of Mechanisms and Catalyzing Metals: Prooxidant Activity of Polyphenols and Carotenoids. *Phytotherapy Research,* 30.

51. FATIMA, K., MASOOD, N. & LUQMAN, S. 2016. Quenching of singlet oxygen by natural and synthetic antioxidants and assessment of electronic UV/Visible absorption spectra for alleviating or enhancing the efficacy of photodynamic therapy. *Biomedical Research and Therapy,* 3.

52. FOUEGUE TAMAFO, A. D., GHOGOMU, J. N., NKUNGLI, N. K. 2017. Quantum Chemical Investigation on the Antioxidant Activity of Neutral and Anionic Forms of Juglone: Metal Chelation and Its Effect on Radical Scavenging Activity. *Journal of Chemistry,* 2017**,** 14.

53. FRANKEL, E. N. 2001. Interfacial Lipid Oxidation and Antioxidation. *Journal of Oleo Science,* 50**,** 387-391.

54. FRANKEL, E. N. 2012. Chapter 7 - Stability methods. *In:* FRANKEL, E. N. (ed.) *Lipid Oxidation (Second Edition).* Woodhead Publishing.

55. FRENCH, D. J., BROWN, A. T., SCHOFIELD, A. B., FOWLER, J., TAYLOR, P. & CLEGG, P. S. 2016. The secret life of Pickering emulsions: particle exchange revealed using two colours of particle. *Scientific Reports,* 6**,** 31401.

56. GANGWAR, M., GAUTAM, M. K., SHARMA, A. K., TRIPATHI, Y. B., GOEL, R. K. & NATH, G. 2014. Antioxidant capacity and radical scavenging effect of polyphenol rich Mallotus philippenensis fruit extract on human erythrocytes: an in vitro study. *ScientificWorldJournal,* 2014**,** 279451.

57. GHNIMI, S., BUDILARTO, E. & KAMAL-ELDIN, A. 2017. The New Paradigm for Lipid Oxidation and Insights to Microencapsulation of Omega-3 Fatty Acids. *Comprehensive Reviews in Food Science and Food Safety,* 16**,** 1206-1218.

58. GHORBANI GORJI, S., CALINGACION, M., SMYTH, H. E. & FITZGERALD, M. 2019. Effect of natural antioxidants on lipid oxidation in mayonnaise compared with BHA, the industry standard. *Metabolomics,* 15**,** 106.

59. GIBBS, J. W. 1873. Graphical Methods in the Thermodynamics of Fluids, Connecticut Academy.

60. GLODDE, F., GÜNAL, M., KINSEL, M. E. & ABUGHAZALEH, A. 2018. Effects of Natural Antioxidants on The Stability of Omega-3 Fatty Acids in Dog Food. *Journal of veterinary research,* 62**,** 103-108.

61. GOHTANI, S., SIRENDI, M., YAMAMOTO, N., KAJIKAWA, K. & YAMANO, Y. 1999. Effect of droplet size on oxidation of docosahexaenoic acid in emulsion system. *Journal of Dispersion Science and Technology,* 20**,** 1319-1325.

62. GRAF, E. & EATON, J. W. 1990. Antioxidant functions of phytic acid. *Free Radical Biology and Medicine,* 8**,** 61-69.

63. GÜELL, C., FERRANDO, M., TRENTIN, A. & SCHROËN, K. 2017. Apparent Interfacial Tension Effects in Protein Stabilized Emulsions Prepared with Microstructured Systems. *Membranes,* 7**,** 19.

64. GUO, Z., ZHANG, M., LI, H., WANG, J. & KOUGOULOS, E. 2005. Effect of ultrasound on anti-solvent crystallization process. *Journal of Crystal Growth,* 273**,** 555-563.

65. HAJIMEHDIPOOR, H., SHAHRESTANI, R. & SHEKARCHI, M. 2014. Investigating the synergistic antioxidant effects of some flavonoid and phenolic compounds. *Research Journal of Pharmacognosy,* 1**,** 35-40.

66. HAN, J., ZHU, Z., QIAN, H., WOHL, A. R., BEAMAN, C. J., HOYE, T. R. & MACOSKO, C. W. 2012. A simple confined impingement jets mixer for flash nanoprecipitation. *Journal of Pharmaceutical Sciences,* 101**,** 4018-4023.

67. HASLER, C. M. 2002. Functional Foods: Benefits, Concerns and Challenges—A Position Paper from the American Council on Science and Health. *The Journal of Nutrition,* 132**,** 3772-3781.

68. HERRERO-MARTÍNEZ, J. M., SANMARTIN, M., ROSÉS, M., BOSCH, E. & RÀFOLS, C. 2005. Determination of dissociation constants of flavonoids by capillary electrophoresis. *ELECTROPHORESIS,* 26**,** 1886-1895.

69. HONG, C., DANG, Y., LIN, G., YAO, Y., LI, G., JI, G., SHEN, H. & XIE, Y. 2014. Effects of stabilizing agents on the development of myricetin nanosuspension and its characterization: An in vitro and in vivo evaluation. *International Journal of Pharmaceutics,* 477**,** 251-260.

70. HU, M., MCCLEMENTS, D. J. & DECKER, E. A. 2003a. Impact of Whey Protein Emulsifiers on the Oxidative Stability of Salmon Oil-in-Water Emulsions. *Journal of Agricultural and Food Chemistry,* 51**,** 1435-1439.

71. HU, M., MCCLEMENTS, D. J. & DECKER, E. A. 2003b. Lipid Oxidation in Corn Oil-in-Water Emulsions Stabilized by Casein, Whey Protein Isolate, and Soy Protein Isolate. *Journal of Agricultural and Food Chemistry,* 51**,** 1696-1700.

72. HUANG, S.-W., FRANKEL, E. N., AESCHBACH, R. & GERMAN, J. B. 1997. Partition of Selected Antioxidants in Corn Oil−Water Model Systems. *Journal of Agricultural and Food Chemistry,* 45**,** 1991-1994.

73. HUANG, S.-W., SATUÉ-GRACIA, M. T., FRANKEL, E. N. & GERMAN, J. B. 1999. Effect of Lactoferrin on Oxidative Stability of Corn Oil Emulsions and Liposomes. *Journal of Agricultural and Food Chemistry,* 47**,** 1356-1361.

74. IM, S., NAM, T. G., LEE, S. G., KIM, Y. J., CHUN, O. K. & KIM, D.-O. 2014. Additive antioxidant capacity of vitamin C and tocopherols in combination. *Food Science and Biotechnology,* 23**,** 693-699.

75. INOUE, N., AKASAKA, K., ARIMOTO, H. & OHRUI, H. 2006. Effect of Ascorbic Acid on the Chemiluminescence of Polyphenols. *Bioscience, Biotechnology, and Biochemistry,* 70**,** 1517-1520.

76. ITO, J., KOMURO, M., PARIDA, I. S., SHIMIZU, N., KATO, S., MEGURO, Y., OGURA, Y., KUWAHARA, S., MIYAZAWA, T. & NAKAGAWA, K. 2019. Evaluation of lipid oxidation mechanisms in beverages and cosmetics via analysis of lipid hydroperoxide isomers. *Scientific Reports,* 9**,** 7387.

77. JACOBSEN, C. 2016. Chapter 8 - Oxidative Stability and Shelf Life of Food Emulsions. *In:* HU, M. & JACOBSEN, C. (eds.) *Oxidative Stability and Shelf Life of Foods Containing Oils and Fats.* AOCS Press.

78. JANOS, F. & GABRIELLA, L. 2012. Silymarin in the Prevention and Treatment of Liver Diseases and Primary Liver Cancer. *Current Pharmaceutical Biotechnology,* 13**,** 210-217.

79. JAVED, S., KOHLI, K. & ALI, M. 2011. Reassessing Bioavailability of Silymarin. *Alternative Medicine Review;,* 16**,** 239-249.

80. JIA, J., WANG, W., GAO, Y. & ZHAO, Y. 2015. Controlled morphology and size of curcumin using ultrasound in supercritical CO2 antisolvent. *Ultrason Sonochem,* 27**,** 389-94.

81. JIANG, T., HAN, N., ZHAO, B., XIE, Y. & WANG, S. 2012. Enhanced dissolution rate and oral bioavailability of simvastatin nanocrystal prepared by sonoprecipitation. *Drug Dev Ind Pharm,* 38**,** 1230-9.

82. JO, S.-H., KA, E. H., LEE, H. S., APOSTOLIDIS, E., JANG, H. D. & KWON, Y. I. 2009. Comparison of Antioxidant Potential and Rat intestinal a-Glucosidases inhibitory Activities of Quercetin, Rutin, and Isoquercetin. *International Journal of Applied Research in Natural Products,* 2.

83. JOHNSON, D. R. & DECKER, E. A. 2015. The Role of Oxygen in Lipid Oxidation Reactions: A Review. *Annual Review of Food Science and Technology,* 6**,** 171-190.

84. JOYE, I. J. & MCCLEMENTS, D. J. 2013. Production of nanoparticles by anti-solvent precipitiation for use in food systems. *Trends in Food Science and Technology***,** 109-123.

85. JURASEKOVA, Z., DOMINGO, C., GARCIA-RAMOS, J. V. & SANCHEZ-CORTES, S. 2014. Effect of pH on the chemical modification of quercetin and structurally related flavonoids characterized by optical (UV-visible and Raman) spectroscopy. *Physical Chemistry Chemical Physics,* 16**,** 12802-12811.

86. JURENKA, J. S. 2009. Anti-inflammatory Properties of Curcumin, a Major Constituent of Curcuma longa: A Review of preclinical and Clinical Research. *Alternative Medicine Review; ,* 14**,** 141-153.

87. KAKRAN, M., SAHOO, N. G., ANTIPINA, M. N. & LI, L. 2013. Modified supercritical antisolvent method with enhanced mass transfer to fabricate drug nanoparticles. *Mater Sci Eng C Mater Biol Appl,* 33**,** 2864-70.

88. KAKRAN, M., SAHOO, N. G., TAN, I.-L. & LI, L. 2012. Preparation of nanoparticles of poorly water-soluble antioxidant curcumin by antisolvent precipitation methods. *Journal of Nanoparticle Research,* 14**,** 757.

89. KAKRAN M, S. G., LI L 2015. Fabrication of Nanoparticles of Silymarin, Hesperetin and Glibenclamide by Evaporative Precipitation of Nanosuspension for Fast Dissolution. *Pharm Anal Acta 6:326,* 6.

90. KALEPU, S. & NEKKANTI, V. 2015. Insoluble drug delivery strategies: review of recent advances and business prospects. *Acta Pharmaceutica Sinica B,* 5**,** 442-453.

91. KARGAR, M., FAYAZMANESH, K., ALAVI, M., SPYROPOULOS, F. & NORTON, I. T. 2012. Investigation into the potential ability of Pickering emulsions (food-grade particles) to enhance the oxidative stability of oil-in-water emulsions. *Journal of Colloid and Interface Science,* 366**,** 209-215.

92. KARGAR, M., SPYROPOULOS, F. & NORTON, I. T. 2011a. The effect of interfacial microstructure on the lipid oxidation stability of oil-in-water emulsions. *Journal of Colloid and Interface Science,* 357**,** 527-533.

93. KARGAR, M., SPYROPOULOS, F. & NORTON, I. T. 2011b. Microstructural design to reduce lipid oxidation in oil-inwater emulsions. *Procedia Food Science,* 1**,** 104-108.

94. KATEPALLI, H. 2014. Formation and stability of emulsions: Effect of surfactant-particle interactions and particle shape. Doctor of Philosophy, University of Rhode Island.

95. KATŌ, K. & KOMORITA, H. 1967. Pyrolysis of Cellulose Part IV. Effect of Crystallinity of Cellulose on the Formation of the Volatile Compounds*. *Agricultural and Biological Chemistry,* 32**,** 21-26.

96. KOSTYUK, V. A., POTAPOVICH, A. I., VLADYKOVSKAYA, E. N., KORKINA, L. G. & AFANAS'EV, I. B. A. 2001. Influence of Metal Ions on Flavonoid Protection against Asbestos-Induced Cell Injury. *Archives of Biochemistry and Biophysics,* 385**,** 129-137.

97. KUMAR, P. & SINGH, C. 2013. A Study on Solubility Enhancement Methods for Poorly Water Soluble Drugs. *American Journal of Pharmacological Sciences,* 1**,** 67-73.

98. LAMER, V. K. & DINEGAR, R. H. 1950. Theory, Production and Mechanism of Formation of Monodispersed Hydrosols. *Journal of the American Chemical Society,* 72**,** 4847-4854.

99. LAMOTHE, S., DESROCHES, V. & BRITTEN, M. 2019. Effect of milk proteins and food-grade surfactants on oxidation of linseed oil-in-water emulsions during in vitro digestion. *Food Chemistry,* 294**,** 130-137.

100. LEE, S. J., CHOI, S. J., LI, Y., DECKER, E. A. & MCCLEMENTS, D. J. 2011. Protein-stabilized nanoemulsions and emulsions: comparison of physicochemical stability, lipid oxidation, and lipase digestibility. *J Agric Food Chem,* 59**,** 415-27.

101. LEOPOLDINI, M., RUSSO, N., CHIODO, S. & TOSCANO, M. 2006. Iron Chelation by the Powerful Antioxidant Flavonoid Quercetin. *Journal of Agricultural and Food Chemistry,* 54**,** 6343-6351.

102. LETHUAUT, L., MÉTRO, F. & GENOT, C. 2002. Effect of droplet size on lipid oxidation rates of oil-in-water emulsions stabilized by protein. *Journal of the American Oil Chemists' Society,* 79**,** 425.

103. LI, H., WANG, J., BAO, Y., GUO, Z. & ZHANG, M. 2003. Rapid sonocrystallization in the salting-out process. *Journal of Crystal Growth,* 247**,** 192-198.

104. LI, X., YUAN, Q., HUANG, Y., ZHOU, Y. & LIU, Y. 2010. Development of Silymarin Self-Microemulsifying Drug Delivery System with Enhanced Oral Bioavailability. *AAPS PharmSciTech,* 11**,** 672-678.

105. LINKE, C. & DRUSCH, S. 2018. Pickering emulsions in foods - opportunities and limitations. *Critical Reviews in Food Science and Nutrition,* 58**,** 1971-1985.

106. LIU, K., LIU, Y. & CHEN, F. 2019. Effect of storage temperature on lipid oxidation and changes in nutrient contents in peanuts. *Food science & nutrition,* 7**,** 2280-2290.

107. LIU, W. & GUO, R. 2006. Interaction between flavonoid, quercetin and surfactant aggregates with different charges. *Journal of Colloid and Interface Science,* 302**,** 625-632.

108. LIU, Y. H., SUN, C. S., HAO, Y. R., JIANG, T. Y., ZHENG, L. & WANG, S. L. 2010. Mechanism of Dissolution Enhancement and Bioavailability of Poorly Water Soluble Celecoxib by Preparing Stable Amorphous Nanoparticles. *Journal of Pharmacy and Pharmaceutical Sciences,* 13**,** 589-606.

109. LÓPEZ-MARTÍNEZ, A. & ROCHA-URIBE, A. 2018. Antioxidant Hydrophobicity and Emulsifier Type Influences the Partitioning of Antioxidants in the Interface Improving Oxidative Stability in O/W Emulsions Rich in n-3 Fatty Acids. *European Journal of Lipid Science and Technology,* 120**,** 1700277.

110. LU, F. S. H., BRUHEIM, I., HAUGSGJERD, B. O. & JACOBSEN, C. 2014. Effect of temperature towards lipid oxidation and non-enzymatic browning reactions in krill oil upon storage. *Food Chemistry,* 157**,** 398-407.

111. LÜ, J.-M., LIN, P. H., YAO, Q. & CHEN, C. 2010. Chemical and molecular mechanisms of antioxidants: experimental approaches and model systems. *Journal of Cellular and Molecular Medicine,* 14**,** 840-860.

112. LU, X., XIAO, J. & HUANG, Q. 2018. Pickering emulsions stabilized by media-milled starch particles. *Food Research International,* 105**,** 140-149.

113. LUO, Z., MURRAY, B. S., ROSS, A.-L., POVEY, M. J. W., MORGAN, M. R. A. & DAY, A. J. 2012. Effects of pH on the ability of flavonoids to act as Pickering emulsion stabilizers. *Colloids and Surfaces B: Biointerfaces,* 92**,** 84-90.

114. LUQUE DE CASTRO, M. D. & PRIEGO-CAPOTE, F. 2007. Ultrasound-assisted crystallization (sonocrystallization). *Ultrasonics Sonochemistry,* 14**,** 717-724.

115. LYNCH, S. R. & STOLTZFUS, R. J. 2003. Iron and Ascorbic Acid: Proposed Fortification Levels and Recommended Iron Compounds. *The Journal of Nutrition,* 133**,** 2978S-2984S.

116. MALVERN, P. 2009. Zetasizer nano user manual. *MAN0317-5.0.* England.

117. MANCUSO, J. R., MCCLEMENTS, D. J. & DECKER, E. A. 1999. Ability of Iron To Promote Surfactant Peroxide Decomposition and Oxidize α-Tocopherol. *Journal of Agricultural and Food Chemistry,* 47**,** 4146-4149.

118. MATTEUCCI, M. E., HOTZE, M. A., JOHNSTON, K. P. & WILLIAMS, R. O. 2006. Drug Nanoparticles by Antisolvent Precipitation: Mixing Energy versus Surfactant Stabilization. *Langmuir,* 22**,** 8951-8959.

119. MCCLEMENTS, D. J. 2004. *Food Emulsions,* Boca Raton, CRC Press.

120. MCCLEMENTS, D. J. & DECKER, E. 2018. Interfacial Antioxidants: A Review of Natural and Synthetic Emulsifiers and Coemulsifiers That Can Inhibit Lipid Oxidation. *Journal of Agricultural and Food Chemistry,* 66**,** 20-35.

121. MCCLEMENTS, D. J. & DECKER, E. A. 2000. Lipid Oxidation in Oil-in-Water Emulsions: Impact of Molecular Environment on Chemical Reactions in Heterogeneous Food Systems. *Journal of Food Science,* 65**,** 1270-1282.

122. MEI, L., MCCLEMENTS, D. J. & DECKER, E. A. 1999. Lipid Oxidation in Emulsions As Affected by Charge Status of Antioxidants and Emulsion Droplets. *Journal of Agricultural and Food Chemistry*, 47**,** 2267-2273.

123. MEI, L., MCCLEMENTS, D. J., WU, J. & DECKER, E. A. 1998. Iron-catalyzed lipid oxidation in emulsion as affected by surfactant, pH and NaCl. *Food Chemistry,* 61**,** 307-312.

124. MERCKMILLIPORE. 2019. *Lipid Hydroperoxide (LPO) Assay Kit* [Online]. Available: http://www.merckmillipore.com/GB/en/product/Lipid-Hydroperoxide-LPO-Assay-Kit,EMD_BIO-437639?ReferrerURL=https%3A%2F%2Fwww.google.com%2F#anchor_REF [Accessed 08/12/2019 2019].

125. MIHALJEVIĆ, B., KATUŠIN-RAŽEM, B. & RAŽEM, D. 1996. The reevaluation of the ferric thiocyanate assay for lipid hydroperoxides with special considerations of the mechanistic aspects of the response. *Free Radical Biology and Medicine,* 21**,** 53-63.

126. MIN, D. B. & BOFF, J. M. 2002. Chemistry and Reaction of Singlet Oxygen in Foods. *Comprehensive Reviews in Food Science and Food Safety,* 1**,** 58-72.

127. MISTRY, B. S. & MIN, D. B. 1987. Effects of Fatty Acids on the Oxidative Stability of Soybean Oil. *Journal of Food Science,* 52**,** 831-832.

128. MIYASHITA, K., AZUMA, G. & OTA, T. 1995. Oxidative stability of geometric and positional isomers of unsaturated fatty acids in aqueous solution. *Yukagaku,* 44**,** 425-430.

129. MODASIYA, M. K. & PATEL, V. M. 2012. Studies on solubility of curcumin. *INTERNATIONAL JOURNAL OF PHARMACY & LIFE SCIENCES,* 3**,** 1490-1497.

130. MOSHARRAF, M. & NYSTROM, C. 2003. Apparent solubility of drugs in partially crystalline systems. *Drug Dev Ind Pharm,* 29**,** 603-22.

131. MOZURAITYTE, R., KRISTINOVA, V., STANDAL, I. B., CARVAJAL, A. K. & AURSAND, M. 2016. Chapter 5 - Oxidative Stability and Shelf Life of Fish Oil. *In:* HU, M. & JACOBSEN, C. (eds.) *Oxidative Stability and Shelf Life of Foods Containing Oils and Fats.* AOCS Press.

132. MURDANDE, S. B., SHAH, D. A. & DAVE, R. H. 2015. Impact of Nanosizing on Solubility and Dissolution Rate of Poorly Soluble Pharmaceuticals. *Journal of Pharmaceutical Sciences,* 104**,** 2094-2102.

133. NAYAK, A., HAMILTON, I. & NORTON, I. 2017. Amorphous nano-curcumin stabilized oil in water emulsion: Physico chemical characterization. *Food Chemistry*, 224, 191-200.

134. NGAI, T. & BON, S. 2015. Particle-Stabilized Emulsions and Colloids: Formation and Applications. *Royal Society of Chemistry*.

135. NIELSEN, N. S., HORN, A. F. & JACOBSEN, C. 2013. Effect of emulsifier type, pH and iron on oxidative stability of 5% fish oil-in-water emulsions. *European Journal of Lipid Science and Technology,* 115**,** 874-889.

136. NNOROM, I. C. & EWUZIE, U. 2015. Comparative study of trace metal (Cd, Cr, Cu, Fe, K, Mg, Na, and Zn) contents of local and imported vegetable oil brands consumed in Nigeria *Asian Journal of Plant Science and Research,* 5**,** 22-29.

137. NOYES, A. A. & WHITNEY, W. R. 1897. THE RATE OF SOLUTION OF SOLID SUBSTANCES IN THEIR OWN SOLUTIONS. *Journal of the American Chemical Society,* 19**,** 930-934.

138. NUCHI, C., GUARDIOLA, F., BOU, R., BONDIOLI, P., DELLA BELLA, L. & CODONY, R. 2009. Assessment of the Levels of Degradation in Fat Co- and Byproducts for Feed Uses and Their Relationships with Some Lipid Composition Parameters. *Journal of Agricultural and Food Chemistry,* 57**,** 1952-1959.

139. NUCHI, C. D., MCCLEMENTS, D. J. & DECKER, E. A. 2001. Impact of Tween 20 Hydroperoxides and Iron on the Oxidation of Methyl Linoleate and Salmon Oil Dispersions. *Journal of Agricultural and Food Chemistry,* 49**,** 4912-4916.

140. O'DWYER, S. P., O'BEIRNE, D., EIDHIN, D. N. & O'KENNEDY, B. T. 2013. Effects of emulsification and microencapsulation on the oxidative stability of camelina and sunflower oils. *Journal of Microencapsulation,* 30**,** 451-459.

141. OEHLKE, K., ADAMIUK, M., BEHSNILIAN, D., GRAF, V., MAYER-MIEBACH, E., WALZ, E. & GREINER, R. 2014. Potential bioavailability enhancement of bioactive compounds using food-grade engineered nanomaterials: a review of the existing evidence. *Food Funct,* 5**,** 1341-59.

142. OJHA, H., SHARMA, K., KALLEPALLI, S., RAINA, S. & AGRAWALA, P. K. 2016. In-vitro evaluation of rutin and rutin hydrate as potential radiation countermeasure agents.

143. OLUGBAMI, J. O., GBADEGESIN, M. A. & ODUNOLA, O. A. 2015. In vitro free radical scavenging and antioxidant properties of ethanol extract of Terminalia glaucescens. *Pharmacognosy research,* 7**,** 49-56.

144. OSBORN, H. T. & AKOH, C. C. 2003. Effects of natural antioxidants on iron-catalyzed lipid oxidation of structured lipid-based emulsions. *Journal of the American Oil Chemists' Society,* 80**,** 847-852.

145. OSBORN, H. T. & AKOH, C. C. 2004. Effect of emulsifier type, droplet size, and oil concentration on lipid oxidation in structured lipid-based oil-in-water emulsions. *Food Chemistry,* 84**,** 451-456.

146. OSTWALD, W. 1900. Über die vermeintliche Isomerie des roten und gelben Quecksilberoxyds und die Oberflächenspannung fester Körper. *Zeitschrift für Physikalische Chemie,* 34U**,** 495-503.

147. OSTWALD, W. 1901. Blocking of Ostwald ripening allowing long-term stabilization. *Phys. Chem,* 37**,** 385.

148. OTTO, D. P. & DE VILLIERS, M. M. 2009. Physicochemical Principles of Nanosized Drug Delivery Systems. *In:* DE VILLIERS, M. M., ARAMWIT, P. & KWON, G. S. (eds.) *Nanotechnology in Drug Delivery.* New York, NY: Springer New York.

149. P, A., ALAGARSAMY, S., SIVANANDHAM, K. & S.SATISHKUMARAN 2014. NATURAL ANTIOXIDANTS AND ITS BENEFITS. *International Journal of Food and Nutritional Sciences,* 3**,** 226-232.

150. PATEL, A. A. L. A. S. R. 2013. Antisolvent Crystallization of Poorly Water Soluble Drugs. *International Journal of Chemical Engineering and Applications,* 4**,** 337-341.

151. PATEL, A. R. & VELIKOV, K. P. 2011. Colloidal delivery systems in foods: A general comparison with oral drug delivery. *LWT - Food Science and Technology,* 44**,** 1958-1964.

152. PAWAR, A. B., CAGGIONI, M., ERGUN, R., HARTEL, R. W. & SPICER, P. T. 2011. Arrested coalescence in Pickering emulsions. *Soft Matter,* 7**,** 7710-7716.

153. PAZOS, M., GALLARDO, J. M., TORRES, J. L. & MEDINA, I. 2005. Activity of grape polyphenols as inhibitors of the oxidation of fish lipids and frozen fish muscle. *Food Chemistry,* 92**,** 547-557.

154. PEKKARINEN, S. S., STÖCKMANN, H., SCHWARZ, K., HEINONEN, I. M. & HOPIA, A. I. 1999. Antioxidant Activity and Partitioning of Phenolic Acids in Bulk and Emulsified Methyl Linoleate. *Journal of Agricultural and Food Chemistry,* 47**,** 3036-3043.

155. PICHOT, R. 2010. Stability and Characterisation of Emulsions in the presence of Colloidal Particles and Surfactants. Doctor of Philosophy, University of Birmingham.

156. PICHOT, R., SPYROPOULOS, F. & NORTON, I. T. 2010. O/W emulsions stabilised by both low molecular weight surfactants and colloidal particles: The effect of surfactant type and concentration. *Journal of Colloid and Interface Science,* 352**,** 128-135.

157. PICKERING, S. U. 1907. CXCVI.—Emulsions. *Journal of the Chemical Society, Transactions,* 91**,** 2001-2021.

158. PRASAD, N., SIDDARAMAIAH, B. & BANU, M. 2015. Effect of antioxidant tertiary butyl hydroquinone on the thermal and oxidative stability of sesame oil (sesamum indicum) by ultrasonic studies. *Journal of food science and technology,* 52**,** 2238-2246.

159. PRAYOG, E. 2017. What is Nanotechnology it's Features and Applications? [Online]. Available: https://www.engineeringprayog.com/what-is-nanotechnology-applications/ [Accessed 09/04/2018 2018].

160. PRICE, A. 2020. Attitutes towards healthy eating UK, February 2020. Mintel.

161. QIU, C., ZHAO, M., DECKER, E. A. & MCCLEMENTS, D. J. 2015. Influence of anionic dietary fibers (xanthan gum and pectin) on oxidative stability and lipid digestibility of wheat protein-stabilized fish oil-in-water emulsion. *Food Research International,* 74**,** 131-139.

162. RAHIM, N. A., ZAKARIA, N., DZULKARNAIN, S. M. H., AZAHAR, N. M. Z. M. & ABDULLA, M. A. 2017. Antioxidant activity of alstonia Angustifolia ethanolic leaf extract. *AIP Conference Proceedings,* 1891**,** 020012.

163. RAMEL, F., BIRTIC, S., CUINÉ, S., TRIANTAPHYLIDÈS, C., RAVANAT, J.-L. & HAVAUX, M. 2012. Chemical quenching of singlet oxygen by carotenoids in plants. *Plant physiology,* 158**,** 1267-1278.

164. RAMSDEN, W. & GOTCH, F. 1904. Separation of solids in the surface-layers of solutions and suspensions (observations on surface-membranes, bubbles, emulsions, and mechanical coagulation). Preliminary account. *Proceedings of the Royal Society of London,* 72**,** 156-164.

165. REGE, S., MOMIN, S. & BHOWMICK, D. 2015. Effect of Ascorbic Acid on the Oxidative Stability of Water-In-Oil Emulsion in the Presence of Lipophilic Antioxidants. *International Journal of Food Properties,* 18**,** 259-265.

166. REGE, S., MOMIN, S., WADEKAR, S., PRATAP, A. & BHOWMICK, D. 2012. Effect of Demethoxycurcumin and Bisdemethoxycurcumin on Antioxidant Activity of Curcumin in Refined Sunflower Oil.

167. REVERCHON, E. 1999. Supercritical antisolvent precipitation of micro- and nano-particles. *The Journal of Supercritical Fluids,* 15**,** 1-21.

168. RIETJENS, I. M. C. M., BOERSMA, M. G., HAAN, L. D., SPENKELINK, B., AWAD, H. M., CNUBBEN, N. H. P., VAN ZANDEN, J. J., WOUDE, H. V. D., ALINK, G. M. & KOEMAN, J. H. 2002. The pro-oxidant chemistry of the natural antioxidants vitamin C, vitamin E, carotenoids and flavonoids. *Environmental Toxicology and Pharmacology,* 11**,** 321-333.

169. ROOZEN, J. P., FRANKEL, E. N. & KINSELLA, J. E. 1994. Enzymic and autoxidation of lipids in low fat foods: model of linoleic acid in emulsified hexadecane. *Food Chemistry,* 50**,** 33-38.

170. SAIFULLAH, M., AHSAN, A. & SHISHIR, M. R. I. 2016. 12 - Production, stability and application of micro- and nanoemulsion in food production and the food processing industry. *In:* GRUMEZESCU, A. M. (ed.) *Emulsions.* Academic Press.

171. SCHAICH, K. M. 2016. Chapter 1 - Analysis of Lipid and Protein Oxidation in Fats, Oils, and Foods. *In:* HU, M. & JACOBSEN, C. (eds.) *Oxidative Stability and Shelf Life of Foods Containing Oils and Fats.* AOCS Press.

172. SCHRÖDER, A., SPRAKEL, J., BOERKAMP, W., SCHROËN, K. & BERTON-CARABIN, C. C. 2019. Can we prevent lipid oxidation in emulsions by using fat-based Pickering particles? *Food Research International,* 120**,** 352-363.

173. SCHUBERT, H., ENGEL, R. & KEMPA, L. 2009. CHAPTER 1 - Principles of Structured Food Emulsions: Novel Formulations and Trends. *In:* BARBOSA-CÁNOVAS, G., MORTIMER, A., LINEBACK, D., SPIESS, W., BUCKLE, K. & COLONNA, P. (eds.) *Global Issues in Food Science and Technology.* San Diego: Academic Press.

174. SEMB, T. N. 2012. Analytical methods for determination of the oxidative status in oils. Institutt for bioteknologi.

175. SHAHIDI, F. 2000. Antioxidants in food and food antioxidants. *Food / Nahrung,* 44**,** 158-163.

176. SHAHIDI, F. 2015. 1 - Antioxidants: Principles and applications. *In:* SHAHIDI, F. (ed.) *Handbook of Antioxidants for Food Preservation.* Woodhead Publishing.

177. SHAHIDI, F. & ZHONG, Y. 2010. Lipid oxidation and improving the oxidative stability. *Chemical Society Reviews,* 39**,** 4067-4079.

178. SHAHIDI, F. & ZHONG, Y. 2011. Revisiting the Polar Paradox Theory: A Critical Overview. *Journal of Agricultural and Food Chemistry,* 59**,** 3499-3504.

179. SHAHIDI, F. & ZHONG, Y. 2015. Lipid Oxidation: Measurement Methods. *Bailey's Industrial Oil and Fat Products.*

180. SHANTHA, N. & DECKER, E. A. 1994. Rapid, sensitive, iron-based spectrophotometric methods for determination of peroxide values of food lipids.

181. SHARIARE, M. H., SHARMIN, S., JAHAN, I., REZA, H. M. & MOHSIN, K. 2018. The impact of process parameters on carrier free paracetamol nanosuspension prepared using different stabilizers by antisolvent precipitation method. *Journal of Drug Delivery Science and Technology,* 43**,** 122-128.

182. SHEKUNOV, B., CHATTOPADHYAY, P. & SEITZINGER, J. 2004. Method and apparatus for producing particles via supercritical fluid processing. Google Patents.

183. SHIMADA, K., MUTA, H., NAKAMURA, Y., OKADA, H., MATSUO, K., YOSHIOKA, S., MATSUDAIRA, T. & NAKAMURA, T. 1994. Iron-binding property and antioxidative activity of xanthan on the autoxidation of soybean oil in emulsion. *Journal of Agricultural and Food Chemistry,* 42**,** 1607-1611.

184. SHIN, G. H., LI, J., CHO, J. H., KIM, J. T. & PARK, H. J. 2016. Enhancement of Curcumin Solubility by Phase Change from Crystalline to Amorphous in Cur-TPGS Nanosuspension. *Journal of Food Science,* 81**,** N494-N501.

185. SIBUEA, P., RAHARJO, S., PANDIANGAN, M. & PANJAITAN, D. The role of tocopherol on photooxidation reactions palm oil emulsion in water. IOP Conference Series: Earth and Environmental Science, 2018. IOP Publishing, 012038.

186. SILVA, E. L. D., ABDALLA, D. S. P. & TERAO, J. 2000. Inhibitory Effect of Flavonoids on Low-Density Lipoprotein Peroxidation Catalyzed by Mammalian 15-Lipoxygenase. *IUBMB Life,* 49**,** 289-295.

187. SINGH, M. K., POOJA, D., RAVURI, H. G., GUNUKULA, A., KULHARI, H. & SISTLA, R. 2018. Fabrication of surfactant-stabilized nanosuspension of naringenin to surpass its poor physiochemical properties and low oral bioavailability. *Phytomedicine,* 40**,** 48-54.

188. SINHA, B., MULLER, R. H. & MOSCHWITZER, J. P. 2013. Bottom-up approaches for preparing drug nanocrystals: Formulations and factors affecting particle size. *International Journal of Pharmaceuticals***,** 126-141.

189. SKAPER, S. D., FABRIS, M., FERRARI, V., DALLE CARBONARE, M. & LEON, A. 1997. Quercetin Protects Cutaneous Tissue-Associated Cell Types Including Sensory Neurons From Oxidative Stress Induced By Glutathione Depletion: Cooperative Effects of Ascorbic Acid. *Free Radical Biology and Medicine,* 22**,** 669-678.

190. SON, W.-S., YOON, T. J., PARK, H. J., KIM, M., ADSCHIRI, T. & LEE, Y.-W. 2019. A novel sample preparation method on CeO2 nanoparticles with

TEM grid embedded liquid CO2 displacement and supercritical CO2 drying for microscopic analysis. *The Journal of Supercritical Fluids,* 152**,** 104559.

191. SONAM, K. & GULERIA, S. 2017. Synergistic antioxidant activity of natural products. *Annal. Pharmacol. Pharm. 2017; 2: 1,* 6.

192. SUN, C. & GUNASEKARAN, S. 2009. Effects of protein concentration and oil-phase volume fraction on the stability and rheology of menhaden oil-in-water emulsions stabilized by whey protein isolate with xanthan gum. *Food Hydrocolloids,* 23**,** 165-174.

193. SUN, C., GUNASEKARAN, S. & RICHARDS, M. P. 2007. Effect of xanthan gum on physicochemical properties of whey protein isolate stabilized oil-in-water emulsions. *Food Hydrocolloids,* 21**,** 555-564.

194. SUN, J., WANG, F., SUI, Y., SHE, Z., ZHAI, W., WANG, C. & DENG, Y. 2012. Effect of particle size on solubility, dissolution rate, and oral bioavailability: evaluation using coenzyme Q_{10} as naked nanocrystals. *International journal of nanomedicine,* 7**,** 5733-5744.

195. SUN, Y.-P. 2002. Supercritical Fluid Technology in Materials Science and Engineering: Syntheses: Properties, and Applications, CRC Press.

196. SVAGAN, A. J., MÜLLERTZ, A. & LÖBMANN, K. 2017. Floating solid cellulose nanofibre nanofoams for sustained release of the poorly soluble model drug furosemide. *Journal of Pharmacy and Pharmacology,* 69**,** 1477-1484.

197. SYMONOWICZ, M. & KOLANEK, M. 2012. Flavonoids and their properties to form chelate complexes. *Biotechnology and Food Science,* 76, 35-41.

198. SZYCZEWSKI, P., FRANKOWSKI, M., ZIOLA-FRANKOWSKA, A., SIEPAK, J., SZYCZEWSKI, T. & PIOTROWSKI, P. 2016. A comparative study of the content of heavy metals in oils: Linseed oil, rapeseed oil and soybean oil in technological production processes. *Archives of Environmental Protection,* 42.

199. TATAR, B. C., SUMNU, G. & SAHIN, S. 2017. Chapter 17 - Rheology of Emulsions. *In:* AHMED, J., PTASZEK, P. & BASU, S. (eds.) *Advances in Food Rheology and Its Applications.* Woodhead Publishing.

200. TERAO, J., MINAMI, Y. & BANDO, N. 2011. Singlet molecular oxygen-quenching activity of carotenoids: relevance to protection of the skin from photoaging. *Journal of clinical biochemistry and nutrition,* 48**,** 57-62.

201. THOMSON, W. 1871. LX. On the equilibrium of vapour at a curved surface of liquid. *The London, Edinburgh, and Dublin Philosophical Magazine and Journal of Science,* 42**,** 448-452.

202. THORAT, A. A. & DALVI, S. V. 2012. Liquid antisolvent precipitation and stabilization of nanoparticles of poorly water soluble drugs in aqueous

suspensions: Recent developments and future perspective. *Chemical Engineering Journal,* 181**,** 1-34.

203. VAN ACKER, S. A. B. E., VAN BALEN, G. P., VAN DEN BERG, D. J., BAST, A. & VAN DER VIJGH, W. J. F. 1998. Influence of iron chelation on the antioxidant activity of flavonoids. *Biochemical Pharmacology,* 56**,** 935-943.

204. VAN HECKE, T., VAN CAMP, J. & DE SMET, S. 2017. Oxidation during digestion of meat: interactions with the diet and helicobacter pylori gastritis, and implications on human health. *Comprehensive Reviews in Food Science and Food Safety,* 16**,** 214-233.

205. VIEIRA, S. A., MCCLEMENTS, D. J. & DECKER, E. A. 2015. Challenges of Utilizing Healthy Fats in Foods. *Advances in Nutrition,* 6**,** 309S-317S.

206. VILLIÈRE, A., VIAU, M., BRONNEC, I., MOREAU, N. & GENOT, C. 2005. Oxidative Stability of Bovine Serum Albumin- and Sodium Caseinate-Stabilized Emulsions Depends on Metal Availability.

207. WANG, Y., BAMDAD, F. & CHEN, L. 2014. New Technologies in the Processing of Functional and Nutraceutical Cereals and Extruded Products. *Nutraceutical and Functional Food Processing Technology.* John Wiley & Sons, Ltd.

208. WARAHO, T., MCCLEMENTS, D. J. & DECKER, E. A. 2011. Mechanisms of lipid oxidation in food dispersions. *Trends in Food Science & Technology,* 22**,** 3-13.

209. WILDE, P. J., HUSBAND, F. A., COOPER, D., RIDOUT, M. J., MULLER, R. E. & MILLS, E. N. C. 2003. Destabilization of Beer Foam by Lipids: Structural and Interfacial Effects. *Journal of the American Society of Brewing Chemists,* 61**,** 196-202.

210. WINTERBOURN, C. C. 1995. Toxicity of iron and hydrogen peroxide: the Fenton reaction. *Toxicology Letters,* 82-83**,** 969-974.

211. WU, M., FENG, Z., DENG, Y., ZHONG, C., LIU, Y., LIU, J., ZHAO, X. & FU, Y. 2019. Liquid antisolvent precipitation: an effective method for ocular targeting of lutein esters. *International journal of nanomedicine,* 14**,** 2667.

212. WUNSCH, N.-G. 2019. Health and wellness food trends in Europe - Statistics and Facts. Statista.

213. XIA, W. & BUDGE, S. M. 2017. Techniques for the Analysis of Minor Lipid Oxidation Products Derived from Triacylglycerols: Epoxides, Alcohols, and Ketones. *Comprehensive Reviews in Food Science and Food Safety,* 16**,** 735-758.

214. XU, D. P., LI, Y., MENG, X., ZHOU, T., ZHOU, Y., ZHENG, J., ZHANG, J. J. & LI, H. B. 2017. Natural Antioxidants in Foods and Medicinal Plants: Extraction, Assessment and Resources. *Int J Mol Sci,* 18.

215. YADAV, D. & KUMAR, N. 2014. Nanonization of curcumin by antisolvent precipitation: Process development, characterization, freeze drying and stability performance. *International Journal of Pharmaceutics,* 477**,** 564-577.

216. YAMASHITA, Y., MIYAHARA, R. & SAKAMOTO, K. 2017. Chapter 28 - Emulsion and Emulsification Technology. *In:* SAKAMOTO, K., LOCHHEAD, R. Y., MAIBACH, H. I. & YAMASHITA, Y. (eds.) *Cosmetic Science and Technology.* Amsterdam: Elsevier.

217. YANG, D., WANG, X.-Y. & LEE, J. H. 2015. Effects of flavonoids on physical and oxidative stability of soybean oil O/W emulsions. *Food Science and Biotechnology,* 24**,** 851-858.

218. YANG, X. & BOYLE, R. A. 2016. Chapter 3 - Sensory Evaluation of Oils/Fats and Oil/Fat–Based Foods. *In:* HU, M. & JACOBSEN, C. (eds.) *Oxidative Stability and Shelf Life of Foods Containing Oils and Fats.* AOCS Press.

219. YANG, Y., FANG, Z., CHEN, X., ZHANG, W., XIE, Y., CHEN, Y., LIU, Z. & YUAN, W. 2017a. An Overview of Pickering Emulsions: Solid-Particle Materials, Classification, Morphology, and Applications. *Frontiers in pharmacology,* 8**,** 287-287.

220. YANG, Y., FANG, Z., CHEN, X., ZHANG, W., XIE, Y., CHEN, Y., LIU, Z. & YUAN, W. 2017b. An Overview of Pickering Emulsions: Solid-Particle Materials, Classification, Morphology, and Applications. *Frontiers in Pharmacology,* 8.

221. YI, B., KA, H., KWON, Y., CHOI, H., KIM, S., KIM, J., KIM, M.-J. & LEE, J. 2017. Oxidative Stability in Oil-in-Water Emulsions with Quercetin or Rutin Under Iron Catalysis or Riboflavin Photosensitization. *Journal of Food Science,* 82**,** 890-896.

222. YI, B., KIM, M.-J. & LEE, J. 2016. Effects of emulsifier charges on the oxidative stability in oil-in-water emulsions under riboflavin photosensitization. *Food Science and Biotechnology,* 25**,** 1003-1009.

223. YOUNG, T. 1805. III. An essay on the cohesion of fluids. *Philosophical Transactions of the Royal Society of London,* 95**,** 65-87.

224. ZAFEIRI, I., NORTON, J. E., SMITH, P., NORTON, I. T. & SPYROPOULOS, F. 2017. The role of surface active species in the fabrication and functionality of edible solid lipid particles. *Journal of Colloid and Interface Science,* 500**,** 228-240.

225. ZAFEIRI, I., SMITH, P., NORTON, I. T. & SPYROPOULOS, F. 2020. O/W emulsions stabilised by solid lipid particles: Understanding how the particles' Pickering functionality can be retained post their dehydration and subsequent rehydration. *Colloids and Surfaces A: Physicochemical and Engineering Aspects,* 599**,** 124916.

226. ZAHID, A., SEO, J.-K., PARK, J.-Y., JEONG, J.-Y., JIN, S.-K., PARK, T.-S. & YANG, H.-S. 2018. The Effects of Natural Antioxidants on Protein Oxidation, Lipid Oxidation, Color, and Sensory Attributes of Beef Patties during Cold Storage at 4°C. *Korean journal for food science of animal resources,* 38**,** 1029-1042.

227. ZHANG, W., SUN, X., FAN, X., LI, M. & HE, G. 2018. Pickering emulsions stabilized by hydrophobically modified alginate nanoparticles: Preparation and pH-responsive performance in vitro. *Journal of Dispersion Science and Technology,* 39**,** 367-374.

228. ZHAO, H., WANG, J., ZHANG, H., SHEN, Z., YUN, J. & CHEN, J. 2009. Facile Preparation of Danazol Nanoparticles by High-Gravity Anti-solvent Precipitation (HGAP) Method. *Chinese Journal of Chemical Engineering,* 17**,** 318-323.

229. ZHAO, Z., XIE, M., LI, Y., CHEN, A., LI, G., ZHANG, J., HU, H., WANG, X. & LI, S. 2015. Formation of curcumin nanoparticles via solution-enhanced dispersion by supercritical CO(2). *International Journal of Nanomedicine,* 10**,** 3171-3181.

230. ZHOU, L. 2012. Elucidation of pro-oxidant mechanisms of the bioactive polyphenol,(-)-epigallocatechin gallate, in food emulsions, Doctor of Philosophy, Pennsylvania State University.

231. ZHOU, L. & ELIAS, R. J. 2012. Factors Influencing the Antioxidant and Pro-Oxidant Activity of Polyphenols in Oil-in-Water Emulsions. *Journal of Agricultural and Food Chemistry,* 60**,** 2906-2915.

232. ZHOU, L. & ELIAS, R. J. 2013. Antioxidant and pro-oxidant activity of (−)-epigallocatechin-3-gallate in food emulsions: Influence of pH and phenolic concentration. *Food Chemistry,* 138**,** 1503-1509.

233. ZHU, Z., ZHAO, C., YI, J., LIU, N., CAO, Y., DECKER, E. A. & MCCLEMENTS, D. J. 2018. Impact of Interfacial Composition on Lipid and Protein Co-Oxidation in Oil-in-Water Emulsions Containing Mixed Emulisifers. *Journal of Agricultural and Food Chemistry,* 66**,** 4458-4468.

234. ZU, Y., WU, W., ZHAO, X., LI, Y., WANG, W., ZHONG, C., ZHANG, Y. & ZHAO, X. 2014. Enhancement of solubility, antioxidant ability and bioavailability of taxifolin nanoparticles by liquid antisolvent precipitation technique. *Int J Pharm,* 471**,** 366-76.

235. ZUNINO, M. P. & ZYGADLO, J. A. 2004. Effect of monoterpenes on lipid oxidation in maize. *Planta,* 219**,** 303-309.